ON THE NONLINEAR OSCILLATION OF FLUIDS IN A RIGID CONTAINER WITH APPLICATION TO VIBRATION REDUCTION

A THESIS

Presented to

The Faculty of the Graduate Division

by

Pei-Ying Chen

In Partial Fulfillment

of the Requirements for the Degree

Doctor of Philosophy

in the School of Engineering Science and Mechanics

Georgia Institute of Technology

May, 1970

In presenting the dissertation as a partial fulfillment of the requirements for an advanced degree from the Georgia Institute of Technology, I agree that the Library of the Institute shall make it available for inspection and circulation in accordance with its regulations governing materials of this type. I agree that permission to copy from, or to publish from, this dissertation may be granted by the professor under whose direction it was written, or, in his absence, by the Dean of the Graduate Division when such copying or publication is solely for scholarly purposes and does not involve potential financial gain. It is understood that any copying from, or publication of, this dissertation which involves potential financial gain will not be allowed without written permission.

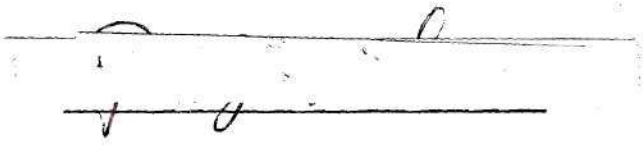

7/25/68

ON THE NONLINEAR OSCILLATION OF FLUIDS IN A RIGID CONTAINER WITH APPLICATION TO VIBRATION REDUCTION

Approved: _____

_____

_____

_____

Date approved by Chairman: 5/14/70

ACKNOWLEDGMENTS

I wish to express my deepest appreciation to Professor Edward R. Wood, my adviscr and friend, for his encouragement, ideas, guidance, and personal advice. Particular thanks are due to Dr. Helmut F. Bauer for his interest, valuable comments, and suggestions in the preparation of this thesis. I also wish to thank Dr. J. R. Baumgarten, Dr. D. V. Ho, and Dr. A. W. Marris for their interest and cooperation, and all the above for reading my thesis.

Furthermore, I am indebted to Dr. Milton E. Raville, Director of the School of Engineering Science and Mechanics, for his encouragement, assistance, and arranging for financial support during the years of my study at the Georgia Institute of Technology.

I am also grateful to Mr. John W. Shipley and Mr. M. G. Turner for their assistance on the experimental apparatus, and to the staff of the Rich Electronic Computer Center for their cooperation.

I also wish to thank Dr. James T. S. Wang for his encouragement and cooperation throughout my graduate studies here at the Georgia Institute of Technology.

To My Wife

Diana Hung Chen

whose love, patience, and understanding have made

this work possible.

TABLE OF CONTENTS

TABLE OF CONTENTS (Concluded)

LIST OF TABLES

LIST OF ILLUSTRATIONS

LIST OF ILLUSTRATIONS (Concluded)

LIST OF PRINCIPAL SYMBOLS

a	outer radius of the tank
A	amplitude of the linear free surface displacement
$A_{mn}(t)$	generalized coordinates of the (m,n) mode for the velocity potential Φ
b	inner radius of the tank
c	length of the rectangular tank (parallel to the direction of excitation)
c_{ij}	constants defined in Appendix I(B)
$C_{\nu_m}(\xi_{mn}\frac{r}{a})$	eigenfunction corresponding to the (m,n) mode
d	diameter of the tank
$D(r,\theta,z,t)$	an analytic function describing the dynamic condition of the free surface
e_{mn}, f_{mn}	coupled nonlinear terms as defined by Eqs. (III-14a) and (III-15b), respectively
E_{ij}, F_{ij}	constants defined in Appendix I(A)
$F_x^{(T)}$	total force response in x direction
$F_x^{(1)}$	harmonic component of force in x direction
$F_x^{(3)}$	triple harmonic component of force in x direction
F_x, F_y, F_z	liquid forces
$\vec{g}$	gravity vector
H_{ch}	characteristic depth
h	undisturbed liquid height
k	ratio of inner to outer tank radius, $\frac{b}{a}$
k_1, k_2, k_e	spring constants

$K(r,\theta,z,t)$	an analytic function describing the kinematic condition of the free surface
K_j, $j=1,2,\ldots7$	constants defined in Appendix I(C)
$J_{\nu_m}(\xi_{mn}\frac{r}{a})$	ν_n^{th} order Bessel function of the first kind
ℓ	length of the cables
m	absorber mass
m_o	nonsloshing mass
m_1	sloshing mass corresponding to the fundamental (1,1) mode
m_T	total liquid mass
M	mass of the main system
M_x, M_y, M_z	liquid moments
$O(A)$	order of magnitude A
p	pressure
p_{ij}	constants defined in Appendix I(B)
r,θ,z	container-fixed polar coordinates
x,y,z	container-fixed rectangular Cartesian coordinates
$X(t)$	translatory excitation function of the container
x_{mn}	defined by Eq. (III-15a)
$\overline{Y}_o$	average amplitude of the free surface displacement as defined by Eq. (V-2)
$Y_{\nu_m}(\xi_{mn}\frac{r}{a})$	ν_m^{th} order Bessel function of the second kind
$2\pi\alpha$	sector angle of the tank cross section, where $0 < \alpha < 1$
$\alpha_{mn}(t)$	generalized coordinates of the (m,n) mode for the surface displacement η
ρ	liquid mass density
ϵ	amplitude of the excitation
$\eta(r,\theta,t)$	free surface displacement

$\Phi(r,\theta,z,t)$	velocity potential
ξ_{mn}	eigenvalue corresponding to the (m,n) mode
λ_{mn}	$\frac{\xi_{mn}}{a}$
ν_{mn}	$\frac{m}{2\alpha}$ with m an integer
ω	excitation frequency or the free surface response frequency
ω_a	natural frequency of the vibration absorber
ω_{mn}	linear natural frequency of the (m,n) mode
Ω_n	natural frequency of the main system
Ω^2	frequency parameter, $\frac{\omega^2}{\omega_{11}^2}$
r_{01}^2	frequency parameter, $\frac{\omega_{11}^2}{\omega_{01}^2}$
r_{21}^2	frequency parameter, $\frac{\omega_{11}^2}{\omega_{21}^2}$
τ	dimensionless time, ωt
δ_i, i=1,2,...8	defined in Appendix I(D)
μ	ratio of absorber mass to mass of the main system, $\frac{m}{M}$
$( )'$	$\frac{\partial}{\partial\tau}( )$
$(\dot{})$	$\frac{\partial}{\partial t}( )$

SUMMARY

A theoretical and experimental study has been made of finite-amplitude free and forced oscillations of a perfect fluid in a cylindrical container with an annular sector cross section, which can be regenerated to various annular or various sector containers. The first antisymmetric mode gravity wave responses to a lateral harmonic excitation are investigated by a third order theory approximating the nonlinear coupling of the free surface waves. It is shown that the character of nonlinear behavior of the liquid can be described by a generalized Duffing-type equation.

The characteristic depth, H_{ch}, at which the liquid exhibits linear vibration motion, is found for a semicircular tank, a quarter sector tank, a 45° sector tank, and an annular semicircular tank with radius ratio of 0.3. A surprising result, which has been confirmed by the experiments, is that more than one characteristic depth exists for certain tank configurations. For a liquid height $h \neq H_{ch}$, the liquid system would behave as either a nonlinear soft spring or as a nonlinear hard spring.

The expressions of free surface elevation, pressure distributions, liquid forces, and moments are derived. Numerical examples are given to compare with whatever theoretical and experimental data are available.

Additional experiments were performed to find the characteristic

depth for a rectangular tank.

Applying the concept of a characteristic depth, a theoretical and experimental investigation on the application of liquid lateral response as a dynamic vibration absorber has also been conducted. The experiments have confirmed that the liquid oscillating at the first antisymmetric mode can be developed as a device for vibration reduction.

A motion picture showing the experimental procedures and demonstrating the liquid behavior has been made to supplement this dissertation.

CHAPTER I

INTRODUCTION

The problem of liquid oscillations has been an interesting and important subject for scientists and engineers in the past 150 years. It is of academic interest as well as of practical importance. In the early years, seismologists and civil engineers were concerned about the effects of earthquakes on the oscillations of water in lakes, harbors, oil tanks, and water reservoirs. Later, the effect of liquid fuel sloshing in wing fuel tanks on the flutter characteristics of the airplane wing, and the overall effect of fuel sloshing on airplane dynamic stability constituted a significant problem in the aircraft industry. Recently, with the advent of the space age, for the appearance of the large liquid propelled rocket and supersonic transport, in which a large portion (sometimes about 90 percent) of the takeoff gross weight may be in liquid fuel, the fuel sloshing problem could be of governing importance to many aspects of the design.

The problem of liquid oscillation in a rigid container has been investigated very thoroughly in the past based on an approximate theory which results when the amplitude of the surface waves is considered to be small. This hypothesis leads to a linear theory and to boundary value problems more or less of classical type. The equations of motion of a perfect liquid were found by Euler in 1755 [1] in terms of the velocity components. In 1781, Lagrange introduced the idea of a single-

valued function called a "velocity-potential." It was Cauchy who presented the first rigorous demonstration in terms of the velocity potential in 1827. The fluid wave motion in a rectangular container studied by Merian in 1828 [24] is among the earliest to have been thoroughly treated with linear theory. The problem of the liquid oscillations in a circular basin of any uniform depth was treated by Poisson in 1828, but the results were not interpreted for the reason that the theory of Bessel functions had not at that time been worked out [1, §191]. It was not until 1876 that the full solution of the problem, with numerical details, was given by Rayleigh [2]. From then on, especially in the years of the 1950's, extensive investigations of the liquid sloshing based on the linear theory for various tank configurations, both stationary and moving containers, were subsequently reported. The review of these literatures can be found in [3,4]. For design engineers and research scientists, a design handbook and a monograph were prepared [5,27].

Although the linearized theory of the small oscillations of a free surface in rigid containers is well established, nonlinearities in the amplitude-frequency response of liquids in containers of various geometries, nevertheless, have long been noted [4,6,16]. Moreover, the liquid sloshing, resulting from the external forces, has been shown experimentally to be most critical when the excitation frequency is in the neighborhood of a natural frequency of lower mode liquid oscillations. For such a resonance case, the linearized theory fails to predict the liquid motion. Hence, in recent developments, attention has

been concentrated upon investigation of the finite-amplitude liquid motion.

Quite a few theoretical and experimental studies of the finite-amplitude liquid motions were made. In fact, the nonlinear phenomenon of the rotation or shifting of a nodal diameter in a circular cylindrical trough was first reported by Guthrie [6] early in 1875. However, no reason was given and this nonlinear phenomenon was considered to be an experimental fault (this was clarified later by Hutton [21]). One of the earliest and most complete theoretical investigations on standing gravity waves of finite amplitude (designed to assist in the engineering design of harbors for the Normandy invasion) was carried out during World War II and was later published by Penney and Price [16] in 1952, who were concerned with the free oscillation of two dimensional standing waves in a rectangular tank of infinite depth. In 1958, employing a perturbation method and characteristic functions, Moiseyev [15] investigated the nonlinear vibrations of a liquid in an arbitrary tank. The perturbation method was also used by Verma and Keller in 1952 [7], by Tadjbaksh and Keller in 1959 [18], and by DiMaggio and Rehm in 1965 [23]. Through the use of Dini expansions and the iterative procedure, Mack [22] studied the finite-amplitude axisymmetric gravity waves in a circular cylindrical container. Extending the basic Penney and Price theory, Lin and Howard [8] in 1960, Bauer [20] in 1964 treated the forced oscillations of a liquid in a rectangular tank. In 1963, Hutton [21] developed a theory for the investigation of resonant, nonlinear non-planar free surface oscillation of a fluid in a circular cylindrical tank and thus clarified the doubt of Guthrie [6] about the

nonlinear resonant phenomenon of the rotation of a nodal diameter. Another topic concerning the nonlinear free oscillation of a liquid in a cylindrical sector container was presented by Baird [20] who analyzed the problem by using the Krylov-Bogoliubov method. Some experimental work concerning the nonlinear surface waves was studied by Taylor [17], Fultz [19], and Abramson, et al. [14]. A closely related topic is the study of the liquid surface oscillations in longitudinally excited rigid cylindrical containers by Dodge, et al. [9].

In this dissertation, studies are made in two phases. In the first phase a nonlinear analysis is performed for the lateral oscillations of an inviscid, incompressible fluid of arbitrary depth with irrotational flow in an annular circular rigid cylindrical sector container, which can be regenerated to various sector or various annular containers. The analysis is carried out for a standing gravity wave motion corresponding to the lowest antisymmetric mode coupled with the other surface waves. Both free oscillations and forced oscillations due to lateral harmonic excitation are studied. Analytical expressions for liquid surface elevation, liquid forces and moments are derived. The theoretical results obtained from present studies are compared with the available theoretical and experimental data obtained by the other investigators. In the second phase, the result of the free oscillation analysis in the first phase is examined experimentally and is applied to investigate, both theoretically and experimentally, the dynamic coupling of the fluid system with other dynamic systems employing the principle of the vibration absorber.

CHAPTER II

FORMULATION OF THE BOUNDARY VALUE PROBLEM

The problem under consideration is the motion of a perfect fluid of irrotational flow in an annular circular cylindrical sector container, which is filled with the liquid of density ρ to a height h. The walls and the bottom of the container are assumed to be rigid. The inner radius is denoted by b, the outer radius by a, and the sector angle by $2\pi\alpha$, where $0 < \alpha < 1$.

A container-fixed Cartesian coordinate system, $Oxyz$, is introduced such that the xy plane coincides with the undisturbed free surface and is perpendicular to the gravity vector $\vec{g}$, and the z-axis is directed positive upward (Figure 1). In a polar coordinate system, r, θ, and z are the corresponding container-fixed coordinates. Then the displacement of the liquid free surface from the $r\theta$-plane is denoted by $z = \eta(r,\theta,t)$, which is due to the perturbations induced by some initial disturbance (free oscillation) or due to a translatory excitation $X(t)$ (forced oscillation). In the solution of forced oscillation and the numerical examples, a harmonic translational excitation of the container will be applied, i.e., $X(t) = \varepsilon \cos \omega t$.

Since the liquid is assumed to be nonviscous and incompressible, and the flow is irrotational, i.e., in a conservative velocity field, there exists a single-valued velocity potential function Φ in a simply-connected region such that

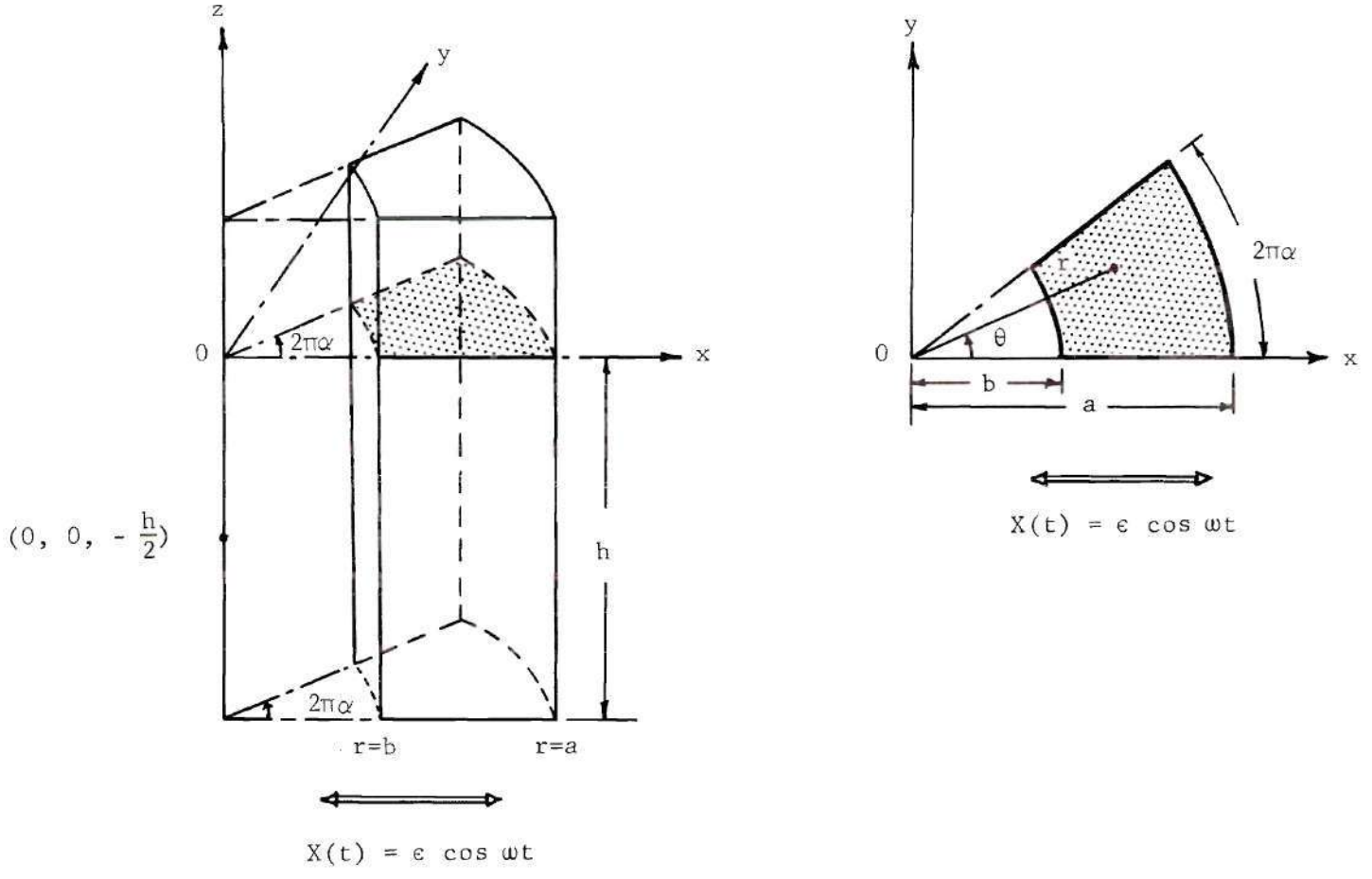

Figure 1. Coordinate System

$$\nabla^2 \Phi = 0 \qquad \text{(II-1)}$$

which follows from the continuity equation. This means that the velocity potential of the liquid must satisfy Laplace's equation, where

$$\nabla^2 \equiv \frac{\partial^2}{\partial r^2} + \frac{1}{r}\frac{\partial}{\partial r} + \frac{1}{r^2}\frac{\partial^2}{\partial \theta^2} + \frac{\partial^2}{\partial z^2}$$

in polar cylindrical coordinates. The boundary conditions at the rigid walls and bottom are:

$$\frac{\partial \Phi}{\partial r} = 0 \qquad r = a, b \qquad \text{(II-2a,b)}$$

$$\frac{1}{r}\frac{\partial \Phi}{\partial \theta} = 0 \qquad \theta = 0, 2\pi\alpha \qquad \text{(II-3a,b)}$$

$$\frac{\partial \Phi}{\partial z} = 0 \qquad z = -h \qquad \text{(II-4)}$$

The remaining boundary condition is the liquid free surface condition which can be obtained by considering the following two facts: (a) the normal velocity of the liquid free surface is equal to the normal velocity of the liquid particles at the free surface, which is called the kinematic condition, and (b) the pressure at the free surface must be equal to the ullage pressure, which is called the dynamic condition.

If the equation of the free surface elevation is expressed as

$$S \equiv z - \eta(r, \theta, t) = 0$$

then the kinematic condition is

$$\frac{DS}{Dt} \equiv \left(\frac{\partial}{\partial t} + \nabla\Phi \cdot \nabla \right) S = 0 \qquad \text{at } z = \eta$$

which gives

$$\frac{\partial \eta}{\partial t} + \frac{\partial \Phi}{\partial r}\frac{\partial \eta}{\partial r} + \frac{1}{r^2}\frac{\partial \Phi}{\partial \theta}\frac{\partial \eta}{\partial \theta} - \frac{\partial \Phi}{\partial z} = 0 \qquad \text{at } z = \eta \qquad \text{(II-5)}$$

Assuming that the external force $\vec{F}$ (including gravity force) is derivable from a potential function P such that

$$\vec{F} = -\nabla P = -\nabla \left\{ x\, \ddot{X}(t) + z g \right\}$$

then the unsteady Bernoulli equation gives

$$\frac{\partial \Phi}{\partial t} + \frac{1}{2}\left[\nabla\Phi \cdot \nabla\Phi \right] + gz + x\, \ddot{X}(t) = -\frac{p}{\rho} \qquad \text{at } z = \eta$$

Thus the dynamical condition at the free surface ($p=0$ at $z=\eta$) yields

$$\frac{\partial \Phi}{\partial t} + \frac{1}{2}\left[\nabla\Phi \cdot \nabla\Phi \right] + gz + x\, \ddot{X}(t) = 0 \qquad \text{at } z = \eta \qquad \text{(II-6)}$$

Hence, the system to be investigated is the following boundary value problem:

$$\begin{aligned}
\nabla^2\Phi &= 0 && \text{for } 0 < \theta < 2\pi\alpha,\ b < r < a,\ -h < z < \eta \\
\Phi_r &= 0 && \text{at } r = a \text{ and } r = b \\
\tfrac{1}{r}\Phi_\theta &= 0 && \text{at } \theta = 0 \text{ and } \theta = 2\pi\alpha \\
\Phi_z &= 0 && \text{at } z = -h
\end{aligned} \qquad \text{(II-7)}$$

$$\eta_t - \bar{\Phi}_r \eta_r + \frac{1}{r^2} \bar{\Phi}_\theta \eta_\theta - \bar{\Phi}_z = 0 \qquad \text{at } z = \eta(r,\theta,t)$$

$$\bar{\Phi}_t - gz + \frac{1}{2}\left(\bar{\Phi}_r^2 + \frac{1}{r^2} \bar{\Phi}_\theta^2 + \bar{\Phi}_z^2 \right) = -r\cos\theta\, \ddot{\bar{X}}(t) \quad \text{at } z = \eta(r,\theta,t) \tag{II-8}$$

where the indicated subscripts denote partial differentiation with respect to the independent variable.

CHAPTER III

SOLUTION OF THE BOUNDARY VALUE PROBLEM

Approximation of Free Surface Conditions

From Equations (II-7) and (II-8) of the preceding chapter, we see that the problem to be solved here is a linear partial differential equation (Laplace's equation) with several homogeneous boundary conditions and two nonlinear boundary conditions. One of the difficulties in this problem is that these two nonlinear boundary conditions hold on the unknown free surface $z = \eta(r,\theta,t)$. This difficulty can be avoided by approximation.

Let the kinematic condition and dynamic condition at the free surface be expressed by the functions $K(r,\theta,z,t)$ and $D(r,\theta,z,t)$, respectively, as follows:

$$K(r,\theta,z,t) \equiv \eta_t + \Phi_r \eta_r + \frac{1}{r^2}\Phi_\theta \eta_\theta - \Phi_z = 0 \qquad \text{at } z = \eta \qquad \text{(III-1)}$$

$$D(r,\theta,z,t) \equiv \Phi_t + gz + \ddot{X}(t)\, r\cos\theta + \frac{1}{2}\left(\Phi_r^2 + \frac{1}{r^2}\Phi_\theta^2 + \Phi_z^2\right) = 0 \qquad \text{at } z = \eta \qquad \text{(III-2)}$$

Assume that $K(r,\theta,z,t)$ and $D(r,\theta,z,t)$ are analytic in the neighborhood of $z=0$ and are equal to zero at $z=\eta$, then it is possible to expand these functions into Taylor series about $z=0$ to be evaluated at $z=\eta$, thus we obtain

$$\left[K\right]_{z=0} + \left[\frac{\partial K}{\partial z}\right]_{z=0}\eta + \left[\frac{\partial^2 K}{\partial z^2}\right]_{z=0}\frac{\eta^2}{2!} + \left[\frac{\partial^3 K}{\partial z^3}\right]_{z=0}\frac{\eta^3}{3!} \qquad \text{(III-3)}$$

$$+ \cdots\cdots + \left[\frac{\partial^n K}{\partial z^n}\right]_{z=0}\frac{\eta^n}{n!} + \cdots\cdots = 0$$

$$\left[D\right]_{z=0} + \left[\frac{\partial D}{\partial z}\right]_{z=0}\eta + \left[\frac{\partial^2 D}{\partial z^2}\right]_{z=0}\frac{\eta^2}{2!} + \left[\frac{\partial^3 D}{\partial z^3}\right]_{z=0}\frac{\eta^3}{3!} \qquad \text{(III-4)}$$

$$+ \cdots\cdots + \left[\frac{\partial^n D}{\partial z^n}\right]_{z=0}\frac{\eta^n}{n!} + \cdots\cdots = 0$$

where

$$\left[K\right]_{z=0} = \left[\eta_t + \Phi_r\eta_r + \frac{1}{r^2}\Phi_\theta\eta_\theta - \Phi_z\right]_{z=0} \qquad \text{(III-5)}$$

$$\left[\frac{\partial K}{\partial z}\right]_{z=0} = \left[\Phi_{rz}\eta_r + \frac{1}{r^2}\Phi_{\theta z}\eta_\theta - \Phi_{zz}\right]_{z=0}$$

$$\left[\frac{\partial^2 K}{\partial z^2}\right]_{z=0} = \left[\Phi_{rzz}\eta_r + \frac{1}{r^2}\Phi_{\theta zz}\eta_\theta - \Phi_{zzz}\right]_{z=0}$$

. . . . . .

$$\left[D\right]_{z=0} = \left[\Phi_t + \ddot{X}(t)\,r\cos\theta + \frac{1}{2}\left(\Phi_r^2 + \frac{1}{r^2}\Phi_\theta^2 + \Phi_z^2\right)\right]_{z=0}$$

$$\left[\frac{\partial D}{\partial z}\right]_{z=0} = \left[\Phi_{tz} + g + \Phi_r\Phi_{rz} + \frac{1}{r^2}\Phi_\theta\Phi_{\theta z} + \Phi_z\Phi_{zz}\right]_{z=0}$$

$$\left[\frac{\partial^2 D}{\partial z^2}\right]_{z=0} = \left[\Phi_{tzz} + \Phi_{rz} + \Phi_r\Phi_{rzz} + \frac{1}{r^2}\Phi_{\theta z}^2 + \frac{1}{r^2}\Phi_\theta\Phi_{\theta zz} + \Phi_{zz}^2 + \Phi_z\Phi_{zzz}\right]_{z=0}$$

. . . . . .

Since the nonlinear free surface boundary conditions cannot be satisfied exactly, an approximation method shall be employed, the j^{th} order approximate solution corresponding to the (p,q) mode is that in

which terms up to the order of A^j are retained while terms of the order of A^{j+1} or higher are neglected, and where A is the amplitude of the linear free surface displacement corresponding to the (p,q) mode. A third order nonlinear analysis will be adopted for this problem.

To provide a guide for the approximation procedure, the nonlinear free surface conditions can be expressed in terms of A. For the order of magnitude consideration, it is evident that the velocity potential Φ has the same order as the wave height η. This can be seen by neglecting the nonlinear terms for free oscillations in Eq. (III-2), i.e.,

$$\eta \doteq -\frac{1}{g}\Phi_t$$

Thus $$\Phi = O(\eta) = O(A)$$

for the first approximation.

Letting $\Phi = \phi A$, $\eta = \bar{\eta} A$, and using Eq. (III-5), we obtain from Eqs. (III-3) and (III-4)

$$\left[\bar{\eta}_t - \phi_z\right]_{z=0} A + \left[\phi_r \bar{\eta}_r + \frac{1}{r^2}\phi_\theta \bar{\eta}_\theta - \phi_{zz}\bar{\eta}\right]_{z=0} A^2 \qquad \text{(III-6)}$$

$$+\left[\phi_{rz}\bar{\eta}_r\bar{\eta} + \frac{1}{r^2}\phi_{\theta z}\bar{\eta}_\theta\bar{\eta} - \frac{\bar{\eta}^2}{2!}\phi_{zzz}\right]_{z=0} A^3 + O(A^4) = 0$$

$$\ddot{X}(t) r\cos\theta + \left[\phi_t + g\bar{\eta}\right]_{z=0} A + \left[\frac{1}{2}\left(\phi_r^2 + \frac{1}{r^2}\phi_\theta^2 + \phi_z^2\right) + \phi_{tz}\bar{\eta}\right]_{z=0} A^2 \qquad \text{(III-7)}$$

$$+\left[\phi_r\phi_{rz}\bar{\eta} + \frac{1}{r^2}\phi_\theta\phi_{\theta z}\bar{\eta} + \phi_z\phi_{zz}\bar{\eta} + \frac{1}{2!}\phi_{tzz}\bar{\eta}^2\right]_{z=0} A^3 + O(A^4) = 0$$

Thus, up to the third order approximation, the free surface conditions become

$$\eta_t - \Phi_z + \Phi_r \eta_r + \frac{1}{r^2}\Phi_\theta \eta_\theta - \Phi_{zz}\eta + \Phi_{rz}\eta_r \eta \qquad \text{(III-8)}$$

$$+ \frac{1}{r^2}\Phi_{\theta z}\eta_\theta \eta - \frac{\eta^2}{2}\Phi_{zzz} = 0 \quad \text{at } z = 0$$

$$\Phi_t + g\eta + \frac{1}{2}\left(\Phi_r^2 + \frac{1}{r^2}\Phi_\theta^2 + \Phi_z^2\right) + \Phi_{tz}\eta + \Phi_r \Phi_{rz}\eta \qquad \text{(III-9)}$$

$$+ \frac{1}{r^2}\Phi_\theta \Phi_{\theta z}\eta + \Phi_z \Phi_{zz}\eta + \frac{1}{2}\Phi_{tzz}\eta^2 = -\ddot{X}(t) r\cos\theta \quad \text{at } z = 0$$

Equation (II-7) together with free surface conditions, Eqs. (III-8) and (III-9), constitute our boundary value problem.

Method of Solution

Boundary Galerkin Method [28]

By the method of separation of variables, a function which is the sum of a set of eigenfunctions (normal sloshing modes) satisfying Eqs. (II-7) is found to be

$$\Phi(r,\theta,z,t) = A_{00}(t) + \sum_{m=0}^{\infty}\sum_{n=1}^{\infty} A_{mn}(t)\cos\left(\frac{m}{2\alpha}\theta\right) \qquad \text{(III-10)}$$

$$\cdot \frac{\cosh\left[\xi_{mn}\left(\frac{z+h}{a}\right)\right]}{\cosh\left[\xi_{mn}\frac{h}{a}\right]} C_{\frac{m}{2\alpha}}\left(\xi_{mn}\frac{r}{a}\right)$$

where $C_{m/2\alpha}(\xi_{mn}\frac{r}{a})$ represents the cylinder function, with $k = \frac{b}{a}$,

$$C_{\frac{m}{2\alpha}}\left(\xi_{mn}\frac{r}{a}\right) = J_{\frac{m}{2\alpha}}\left(\xi_{mn}\frac{r}{a}\right) - \frac{Y_{\frac{m}{2\alpha}}\left(\xi_{mn}\frac{r}{a}\right) J'_{\frac{m}{2\alpha}}(k\xi_{mn})}{Y'_{\frac{m}{2\alpha}}(k\xi_{mn})}$$

and ξ_{mn} are the n^{th} roots of the following equation, for each m,

$$\Delta_{\frac{m}{2\alpha}} = \frac{d}{dr}\left[C_{\frac{m}{2\alpha}}\left(\xi_{mn}\frac{r}{a}\right)\right]\Bigg|_{r=a}$$

$$= \frac{\xi_{mn}}{a}\left[J'_{\frac{m}{2\alpha}}(\xi_{mn}) - \frac{Y'_{\frac{m}{2\alpha}}(\xi_{mn})\, J'_{\frac{m}{2\alpha}}(k\xi_{mn})}{Y'_{\frac{m}{2\alpha}}(k\xi_{mn})}\right] = 0$$

where prime means the differentiation with respect to the argument. The roots ξ_{mn} corresponding to each α are given in reference [20]. Those for $\alpha=\frac{1}{4}, \frac{1}{2}, \frac{1}{8}$ are given in Table 1. It is to be noted that $A_{oo}(t)$ is the eigenfunction corresponding to the eigenvalue $\xi_{oo} = 0$ and is needed for the calculation of the pressure distributions. If k approaches to zero, then

$$C_{\frac{m}{2\alpha}}\left(\xi_{mn}\frac{r}{a}\right) \longrightarrow J_{\frac{m}{2\alpha}}\left(\epsilon_{mn}\frac{r}{a}\right) \; ; \quad \xi_{mn} \longrightarrow \epsilon_{mn}$$

$$\Delta_{\frac{m}{2\alpha}} = 0 \longrightarrow J'_{\frac{m}{2\alpha}}(\epsilon_{mn}) = 0$$

The unknown functions $A_{mn}(t)$ are time dependent functions and are called the generalized coordinates of the (m,n) mode for the velocity potential Φ.

Now the sets of functions $\{1, \cos(\frac{m}{2\alpha}\theta)\}$ and $\{C_{m/2\alpha}(\xi_m \frac{r}{a})\}$ are complete in Hilbert space because their individual ordinary differential equation system is self-adjoint. Thus, by a well-known theorem [11], the set of eigenfunctions $\{1, \cos(\frac{m}{2\alpha}\theta)\, C_{m/2\alpha}(\xi_{mn}\frac{r}{a})\}$ is complete. Therefore we can expand the surface displacement η in terms of the eigenfunctions, i.e.,

Table 1 [Reference 26]

$$\text{The Roots of } \Delta_{\frac{m}{2\alpha}} = \frac{d}{dr}\left[C_{\frac{m}{2\alpha}}(\xi_{mn}\frac{r}{a})\right]_{r=a} = \frac{\xi_{mn}}{a}\left[J'_{\frac{m}{2\alpha}}(\xi_{mn}) - \frac{Y'_{\frac{m}{2\alpha}}(\xi_{mn})J'_{\frac{m}{2\alpha}}(k\xi_{mn})}{Y'_{\frac{m}{2\alpha}}(k\xi_{mn})}\right] = 0$$

$$k = \frac{b}{a}$$

$\alpha = \frac{1}{2}$										
ξ_{mn} \ k	0	0.1	0.2	0.3	0.4	0.5	0.6	0.7	0.8	0.9
ξ_{01}	3.83171	3.94094	4.23575	4.70577	5.39118	6.39316	7.93008	10.52203	15.73755	31.42923
ξ_{11}	1.84118	1.80347	1.70512	1.58207	1.46178	1.35467	1.26208	1.18237	1.11337	1.05314
ξ_{21}	3.05425	3.05294	3.03472	2.96850	2.84240	2.68120	2.51595	2.36285	2.22646	2.10622
$\alpha = \frac{1}{4}$										
ξ_{01}	3.83171	3.94094	4.23575	4.70577	5.39118	6.39316	7.93008	10.52203	15.73775	31.42923
ξ_{11}	3.05425	3.05294	3.03472	2.96850	2.84240	2.68120	2.51595	2.36285	2.22646	2.10622
ξ_{21}	5.31757	5.31756	5.31735	5.31298	5.28210	5.17523	4.96965	4.71085	4.45074	4.21234

Table 1. (Concluded)

$\alpha = \frac{1}{8}$

ξ_{mn} \ k	0	0.1	0.2	0.3	0.4	0.5	0.6	0.7	0.8	0.9
ξ_{01}	3.83171	3.94094	4.23575	4.70577	5.39118	6.39316	7.93008	10.52203	15.73755	31.42923
ξ_{11}	5.31757	5.31756	5.31735	5.31298	5.28210	5.17523	4.96965	4.71085	4.45074	4.21234
ξ_{21}	9.59581	9.59581	9.59581	9.59581	9.59543	9.58985	9.52458	9.26081	8.87557	8.42639

$$\eta(r,\theta,t) = \alpha_{oo}(t) + \sum_{m=0}^{\infty}\sum_{n=1}^{\infty} \alpha_{mn}(t)\cos\left(\frac{m}{2\alpha}\theta\right) C_{\frac{m}{2\alpha}}\left(\frac{\zeta_{mn}}{a}r\right)$$

In the present case, $\alpha_{oo}(t) \equiv 0$ with our choice of axes such that the mean water level is zero at z=0, i.e., $\int_0^{2\pi\alpha}\int_b^a \eta(r,\theta)\, r dr d\theta = 0$. Thus

$$\eta(r,\theta,t) = \sum_{m=0}^{\infty}\sum_{n=1}^{\infty} \alpha_{mn}(t)\cos\left(\frac{m}{2\alpha}\theta\right) C_{\frac{m}{2\alpha}}\left(\frac{\zeta_{mn}}{a}r\right) \qquad \text{(III-11)}$$

where the unknown functions $\alpha_{mn}(t)$ are the generalized coordinates of the (m,n) mode for the surface displacement η.

Substituting Eqs. (III-10) and (III-11) into (III-8) and (III-9) and letting

$$\lambda_{mn} = \frac{\zeta_{mn}}{a} \quad , \quad \nu_m = \frac{m}{2\alpha} \quad , \quad \frac{\omega_{mn}^2}{g} = \frac{\zeta_{mn}}{a}\tanh\left(\zeta_{mn}\frac{h}{a}\right)$$

where ω_{mn} is the linear natural frequency corresponding to the (m,n) mode, we obtain

$$\sum_{m=0}^{\infty}\sum_{n=1}^{\infty}\left[\dot{\alpha}_{mn} - \frac{\omega_{mn}}{g}A_{mn}\right]\cos\nu_m\theta\, C_{\nu_m}(\lambda_{mn}r) \qquad \text{(III-12)}$$

$$+\sum_{m=0}^{\infty}\sum_{n=1}^{\infty}\sum_{i=0}^{\infty}\sum_{j=1}^{\infty} A_{mn}\alpha_{ij}\Big[\lambda_{mn}\lambda_{ij}\cos\nu_m\theta\cos\nu_i\theta\, C'_{\nu_m}(\lambda_{mn}r)C'_{\nu_i}(\lambda_{ij}r)$$

$$+\left(\frac{1}{r^2}\nu_m\nu_i\sin\nu_m\theta\sin\nu_i\theta - \lambda_{mn}^2\cos\nu_m\theta\cos\nu_i\theta\right)C_{\nu_m}(\lambda_{mn}r)C_{\nu_i}(\lambda_{ij}r)\Big]$$

$$+\sum_{m=0}^{\infty}\sum_{n=1}^{\infty}\sum_{i=0}^{\infty}\sum_{j=1}^{\infty}\sum_{k=0}^{\infty}\sum_{l=1}^{\infty} A_{mn}\alpha_{ij}\alpha_{kl}\left[\frac{\omega_{mn}^2\lambda_{mn}\lambda_{ij}}{g}\cos\nu_m\theta\cos\nu_i\theta\cos\nu_k\theta\, C'_{\nu_m}(\lambda_{mn}r)C'_{\nu_i}(\lambda_{ij}r)C_{\nu_k}(\lambda_{kl}r)\right.$$

$$+\left(\frac{1}{r^2}\frac{\omega_{mn}^2 \nu_m \nu_i}{g}\sin\nu_m\theta\,\sin\nu_i\theta\cos\nu_k\theta - \frac{1}{2}\frac{\omega_{mn}^2\lambda_{mn}^2}{g}\cos\nu_m\theta\cos\nu_i\theta\cos\nu_k\theta\right)$$

$$\cdot\, C_{\nu_m}(\lambda_{mn}r)\, C_{\nu_i}(\lambda_{ij}r)\, C_{\nu_k}(\lambda_{kx}r)\Big] = 0.$$

$$\dot{A}_{00}(t) + \sum_{m=0}^{\infty}\sum_{n=1}^{\infty}\left[\dot{A}_{mn} + g\alpha_{mn}\right]\cos\nu_m\theta\, C_{\nu_m}(\lambda_{mn}r) \qquad \text{(III-13)}$$

$$+\sum_{m=0}^{\infty}\sum_{n=1}^{\infty}\sum_{i=0}^{\infty}\sum_{j=1}^{\infty}\left\{\frac{1}{2}A_{mn}A_{ij}\left[\lambda_{mn}\lambda_{ij}\cos\nu_m\theta\cos\nu_i\theta\, C'_{\nu_m}(\lambda_{mn}r)\, C'_{\nu_i}(\lambda_{ij}r)\right.\right.$$

$$\left.+\left(\frac{1}{r^2}\nu_m\nu_i\sin\nu_m\theta\sin\nu_i\theta + \frac{\omega_{mn}^2\omega_{ij}^2}{g}\cos\nu_m\theta\cos\nu_i\theta\right) C_{\nu_m}(\lambda_{mn}r)\, C_{\nu_i}(\lambda_{ij}r)\right]$$

$$\left.+\,\dot{A}_{mn}\alpha_{ij}\frac{\omega_{mn}^2}{g}\cos\nu_m\theta\cos\nu_i\theta\, C_{\nu_m}(\lambda_{mn}r)\, C_{\nu_i}(\lambda_{ij}r)\right\} + \sum_{m=0}^{\infty}\sum_{n=1}^{\infty}\sum_{i=0}^{\infty}\sum_{j=1}^{\infty}\sum_{k=0}^{\infty}\sum_{l=1}^{\infty}$$

$$\cdot\left\{A_{mn}A_{ij}\alpha_{kl}\left[\frac{\lambda_{mn}\lambda_{ij}\omega_{ij}^2}{g}\cos\nu_m\theta\cos\nu_i\theta\cos\nu_k\theta\, C'_{\nu_m}(\lambda_{mn}r)\, C'_{\nu_i}(\lambda_{ij}r)\, C_{\nu_k}(\lambda_{kl}r)\right.\right.$$

$$+\left(\frac{1}{r^2}\frac{\nu_m\nu_i\omega_{ij}^2}{g}\sin\nu_m\theta\sin\nu_i\theta\cos\nu_k\theta + \frac{\omega_{mn}^2\lambda_{ij}^2}{g^2}\cos\nu_m\theta\cos\nu_i\theta\cos\nu_k\theta\right)$$

$$\left.\cdot\, C_{\nu_m}(\lambda_{mn}r)\, C_{\nu_i}(\lambda_{ij}r)\, C_{\nu_k}(\lambda_{kl}r)\right] + \frac{1}{2}\dot{A}_{mn}\alpha_{ij}\alpha_{kl}\lambda_{mn}^2\cos\nu_m\theta\cos\nu_i\theta\cos\nu_k\theta$$

$$\left.\cdot\, C_{\nu_m}(\lambda_{mn}r)\, C_{\nu_i}(\lambda_{ij}r)\, C_{\nu_k}(\lambda_{kl}r)\right\} = -\ddot{\overset{\circ}{X}}(t)\, r\cos\theta$$

Employing the boundary Galerkin method and utilizing the orthogonal properties of the eigenfunctions, we multiply both sides of Eq.

(III-12) by $r \cos\nu_m\theta \, C_{\nu_m}(\lambda_{mn} r)$ and integrate it over the free surface to obtain

$$\dot{\alpha}_{mn} - \frac{\omega_{mn}^2}{g} A_{mn} + e_{mn} = 0 \qquad \begin{matrix} m=0,1,2,\ldots. \\ n=1,2,\ldots. \end{matrix} \qquad \text{(III-14)}$$

where

$$e_{mn} = \frac{\int_b^a \int_0^{2\pi\alpha} E\, r \cos\nu_m\theta \, C_{\nu_m}(\lambda_{mn} r)\, d\theta\, dr}{\int_b^a \int_0^{2\pi\alpha} r \cos^2\nu_m\theta \; C_{\nu_m}^2(\lambda_{mn} r)\, d\theta\, dr} \qquad \text{(III-14a)}$$

$$E = \sum_{m=0}^{\infty} \sum_{n=1}^{\infty} \sum_{i=0}^{\infty} \sum_{j=1}^{\infty} A_{mn} \alpha_{ij} \Big[\lambda_{mn}\lambda_{ij} \cos\nu_m\theta \cos\nu_i\theta \, C'_{\nu_m}(\lambda_{mn} r) C'_{\nu_i}(\lambda_{ij} r) \qquad \text{(III-14b)}$$

$$+ \left(\frac{1}{r^2} \nu_m \nu_i \sin\nu_m\theta \sin\nu_i\theta - \lambda_{mn}^2 \cos\nu_m\theta \cos\nu_i\theta \right) C_{\nu_m}(\lambda_{mn} r) C_{\nu_i}(\lambda_{ij} r) \Big] +$$

$$+ \sum_{m=0}^{\infty} \sum_{n=1}^{\infty} \sum_{i=0}^{\infty} \sum_{j=1}^{\infty} \sum_{k=0}^{\infty} \sum_{l=1}^{\infty} A_{mn} \alpha_{ij} \alpha_{kl}$$

$$\cdot \left[\frac{\omega_{mn}^2 \lambda_{mn} \lambda_{ij}}{g} \cos\nu_m\theta \cos\nu_i\theta \cos\nu_k\theta \, C'_{\nu_m}(\lambda_{mn} r) C'_{\nu_i}(\lambda_{ij} r) C_{\nu_k}(\lambda_{kl} r) \right]$$

A similar procedure for Eq. (III-13) leads to

$$\dot{A}_{mn} + g\alpha_{mn} + f_{mn} = -x_{mn} \ddot{X}(t) \qquad \begin{matrix} m=0,1,2,\ldots. \\ n=1,2,\ldots. \end{matrix} \qquad \text{(III-15)}$$

where

$$x_{mn} = \frac{\int_b^a \int_0^{2\pi\alpha} r^2 \cos\theta \cos\nu_m\theta \, C_{\nu_m}(\lambda_{mn} r)\, d\theta\, dr}{\int_b^a \int_0^{2\pi\alpha} r \cos^2\nu_m\theta \; C_{\nu_m}^2(\lambda_{mn} r)\, d\theta\, dr} \qquad \text{(III-15a)}$$

$$f_{mn} = \frac{\int_b^a \int_0^{2\pi\alpha} F\, r \cos\nu_m\theta \, C_{\nu_m}(\lambda_{mn} r)\, d\theta\, dr}{\int_b^a \int_0^{2\pi\alpha} r \cos^2\nu_m\theta \; C_{\nu_m}^2(\lambda_{mn} r)\, d\theta\, dr} \qquad \text{(III-15b)}$$

$$F = \sum_{m=0}^{\infty}\sum_{n=1}^{\infty}\sum_{i=0}^{\infty}\sum_{j=1}^{\infty}\Bigg\{\frac{1}{2}A_{mn}A_{ij}\Big[\lambda_{mn}\lambda_{ij}\cos\nu_m\theta\cos\nu_i\theta\,C'_{\nu_m}(\lambda_{mn}r)\,C'_{\nu_i}(\lambda_{ij}r) \qquad \text{(III-15c)}$$

$$+\Big(\frac{1}{r^2}\nu_m\nu_i\sin\nu_m\theta\sin\nu_i\theta+\frac{\omega_{mn}^2\omega_{ij}^2}{g^2}\cos\nu_m\theta\cos\nu_i\theta\Big)C_{\nu_m}(\lambda_{mn}r)\,C_{\nu_i}(\lambda_{ij}r)\Big]$$

$$+\dot{A}_{mn}\alpha_{ij}\frac{\omega_{mn}^2}{g}\cos\nu_m\theta\cos\nu_i\theta\,C_{\nu_m}(\lambda_{mn}r)\,C_{\nu_i}(\lambda_{ij}r)\Bigg\}$$

$$+\sum_{m=0}^{\infty}\sum_{n=1}^{\infty}\sum_{i=0}^{\infty}\sum_{j=1}^{\infty}\sum_{k=0}^{\infty}\sum_{l=1}^{\infty}\Bigg\{A_{mn}A_{ij}\alpha_{kl}$$

$$\cdot\Big[\frac{\lambda_{mn}\lambda_{ij}\omega_{ij}^2}{g}\cos\nu_m\theta\cos\nu_i\theta\cos\nu_k\theta\;C'_{\nu_m}(\lambda_{mn}r)\,C'_{\nu_i}(\lambda_{ij}r)\,C_{\nu_k}(\lambda_{kl}r)$$

$$+\Big(\frac{1}{r^2}\frac{\nu_m\nu_i\omega_{ij}^2}{g}\sin\nu_m\theta\sin\nu_i\theta\cos\nu_k\theta+\frac{\omega_{mn}^2\lambda_{ij}^2}{g}\cos\nu_m\theta\cos\nu_i\theta\cos\nu_k\theta\Big)$$

$$\cdot C_{\nu_m}(\lambda_{mn}r)\,C_{\nu_i}(\lambda_{ij}r)\,C_{\nu_k}(\lambda_{kl}r)\Big]+\frac{1}{2}\dot{A}_{mn}\alpha_{ij}\alpha_{kl}\lambda_{mn}^2\cos\nu_m\theta\cos\nu_i\theta\cos\nu_k\theta$$

$$\cdot C_{\nu_m}(\lambda_{mn}r)\,C_{\nu_i}(\lambda_{ij}r)\,C_{\nu_k}(\lambda_{kl}r)\Bigg\}$$

For $A_{oo}(t)$, we multiply Eq. (III-13) by r and integrate it over the free surface. Again, the orthogonality of eigenfunctions leads to

$$\dot{A}_{oo}(t)=\frac{-1}{\pi\alpha^2(a^2-b^2)}\Big[\int_b^a\int_0^{2\pi\alpha}F\,r\,d\theta\,dr+\ddot{\bar{X}}(t)\int_b^a\int_0^{2\pi\alpha}r^2\cos\theta\,d\theta\,dr\Big] \qquad \text{(III-16)}$$

It is to be noted that e_{mn} in Eq. (III-14) and f_{mn} in Eq. (III-15) are nonlinear terms involving A_{ij}, α_{ij}, $\dot{A}_{ij}$, $\dot{\alpha}_{ij}$, and their products. If $e_{mn} = f_{mn} = 0$, we have equations of motion corresponding to linear theory [25].

From Eqs. (III-14) and (III-15), it can be seen that there are doubly infinitely many sets of nonlinear differential equations describing the fluid motion. To obtain an approximate solution, we take only a finite number of equations. From the linear theory and experimental evidence, it is a well known fact that the fluid motion corresponding to the lowest natural frequency (n=1) of the m=1 mode exhibits the most important effects in the case of transverse oscillations (e.g. producing the largest force and moment). The previous nonlinear analyses and the experimental results [21,8,14] together with the present experimental observation show that the fundamental mode always coupled with some other small amplitude waves. Therefore, it is the purpose of this investigation to study the liquid motion corresponding to the fundamental antisymmetric mode (α_{11}, A_{11}) coupled with the first symmetric mode (α_{01}, A_{01}) and the first cos 2θ-mode (α_{21},A_{21}). Then the corresponding generalized coordinates α_{11}, A_{11} dominate the other generalized coordinates and are assumed to have the order of magnitude O(A), i.e.,

$$\alpha_{11} = O(A)$$

$$A_{11} = O(A)$$

The corresponding generalized coordinates for the coupled modes (α_{01},A_{01},α_{21},A_{21}) produce secondary effects and are assumed to have the order of magnitude $O(A^2)$, i.e.,

$$\alpha_{01} = O(A^2)$$

$$A_{01} = O(A^2)$$

$$\alpha_{21} = O(A^2)$$

$$A_{21} = O(A^2)$$

Based on the above hypothesis, the nonlinear differential equations describing the kinematic free surface condition are obtained from (III-14); they are

$$\dot{\alpha}_{11} - \frac{\omega_{11}^2}{g} A_{11} + e_{11} = 0 \qquad \text{(III-17)}$$

$$\dot{\alpha}_{01} - \frac{\omega_{01}^2}{g} A_{01} + e_{01} = 0$$

$$\dot{\alpha}_{21} - \frac{\omega_{21}^2}{g} A_{21} + e_{21} = 0$$

where

$$e_{11} = E_{11} A_{01} \alpha_{11} + E_{12} A_{11} \alpha_{01} + E_{13} A_{11} \alpha_{21} + E_{14} A_{21} \alpha_{11} + E_{15} \frac{\omega_{11}^2}{g} A_{11} \alpha_{11}^2$$

$$e_{01} = E_{01} A_{11} \alpha_{11}$$

$$e_{21} = E_{21} A_{11} \alpha_{11}$$

in which E_{ij}'s are constants depending only upon the tank geometry and are given in Appendix I(A).

Similarly, the nonlinear differential equations describing the dynamic free surface condition are obtained from (III-15); they are

$$\dot{A}_{11} + g\alpha_{11} + f_{11} = -x_{11} \ddot{X} \qquad \text{(III-18)}$$

$$\dot{A}_{01} + g\alpha_{01} + f_{01} = -x_{01} \ddot{X}$$

$$\dot{A}_{21} + g\alpha_{21} + f_{21} = -x_{21} \ddot{X}$$

where

$$f_{11} = \left(F_{11} + \frac{\omega_{11}^2\omega_{01}^2}{g^2}F_{12}\right)A_{01}A_{11} + F_{12}\frac{\omega_{01}^2}{g}\dot{A}_{01}\alpha_{11} + F_{12}\frac{\omega_{11}^2}{g}\dot{A}_{11}\alpha_{01}$$

$$+ \left(F_{13} + \frac{\omega_{21}^2\omega_{11}^2}{g^2}F_{14}\right)A_{11}A_{21} + F_{14}\frac{\omega_{11}^2}{g}\dot{A}_{11}\alpha_{21} + F_{14}\frac{\omega_{21}^2}{g}\dot{A}_{21}\alpha_{11}$$

$$+ F_{15}\dot{A}_{11}\alpha_{11}^2 + F_{16}\frac{\omega_{11}^2}{g}A_{11}^2\alpha_{11}$$

$$f_{01} = F_{01}\frac{\omega_{11}^2}{g}\dot{A}_{11}\alpha_{11} + \left(F_{02} + F_{03}\frac{\omega_{11}^4}{g}\right)A_{11}^2$$

$$f_{21} = F_{21}\frac{\omega_{11}^2}{g}\dot{A}_{11}\alpha_{11} + \left(F_{22} + F_{23}\frac{\omega_{11}^4}{g}\right)A_{11}^2$$

again, F_{ij}'s and x_{ij}'s are constants depending only upon the tank geometry and are given in Appendix I(A).

By the same manner, Eq. (III-16) becomes

$$\dot{A}_{oc}(t) = -\frac{2}{a^2-b^2}\left\{\frac{A_{11}^2}{4}\left[\lambda_{11}^2\int_b^a r\,C_{\nu_1}'^2(\lambda_{11}r)\,dr\right.\right. \qquad \text{(III-19)}$$

$$+\nu_1^2\left(\int_b^a \frac{1}{r}C_{\nu_1}^2(\lambda_{11}r)\,dr\right) + \frac{\omega_{11}^4}{g}\left(\int_b^a r\,C_{\nu_1}^2(\lambda_{11}r)\,dr\right)\Bigg]$$

$$\left.+\frac{\omega_{11}^2}{2g}\dot{A}_{11}\alpha_{11}\left(\int_b^a r\,C_{\nu_1}^2(\lambda_{11}r)\,dr\right) + \frac{\sin 2\pi\alpha}{2\pi\alpha}\frac{(a^3-b^3)}{3}\ddot{\chi}(t)\right\}$$

Equations (III-17) and (III-18) can be combined by retaining terms up to the third order to form a set of three second-order ordinary differential equations describing the boundary condition of the liquid at the free surface in terms of the generalized coordinates (amplitudes) of the surface displacement. The results are

$$D_3[\alpha_{11}, \alpha_{21}, \tau] \equiv \Omega^2 \gamma_{21}^2 \alpha_{21}'' + \alpha_{21} + C_{21} \Omega^2 \gamma_{21}^2 \alpha_{11}'' \alpha_{11}$$

$$+ C_{22} \Omega^2 \gamma_{21}^2 \alpha_{11}'^2 \mp \epsilon \Omega^2 \gamma_{21}^2 P_{21} \cos\tau = 0$$

where

$$(\,)' \equiv \frac{d}{d\tau}(\,) \quad , \quad \Omega^2 = \frac{\omega^2}{\omega_{11}^2} \quad , \quad \gamma_{01}^2 = \frac{\omega_{11}^2}{\omega_{01}^2} \quad , \quad \gamma_{21}^2 = \frac{\omega_{11}^2}{\omega_{21}^2}$$

We assume a solution of the form as follows (the form of solution is suggested by the observation of experimental surface waves and the solution of free oscillations in a sector cylindrical tank [10]),

$$\alpha_{11} = a_{11} \cos\tau + a_{13} \cos 3\tau \qquad \text{(III-22)}$$

$$\alpha_{01} = a_{00} + a_{01} \cos 2\tau$$

$$\alpha_{21} = a_{20} + a_{21} \cos 2\tau$$

where the order of magnitude of a_{11} is of $O(A)$, that of a_{13} is of $O(A^3)$, and that of a_{00}, a_{01}, a_{20}, a_{21} is of $O(A^2)$.

The Ritz conditions are then

$$\int_0^{2\pi} D_1[\alpha_{11}, \alpha_{01}, \alpha_{21}, \tau] \cos\tau \, d\tau = 0 \qquad \text{(III-23)}$$

$$\int_0^{2\pi} D_1[\alpha_{11}, \alpha_{01}, \alpha_{21}, \tau] \cos 3\tau \, d\tau = 0$$

$$\int_0^{2\pi} D_2[\alpha_{11}, \alpha_{01}, \tau]\, d\tau = 0$$

$$\int_0^{2\pi} D_2[\alpha_{11}, \alpha_{01}, \tau] \cos 2\tau\, d\tau = 0$$

$$\int_0^{2\pi} D_3[\alpha_{11}, \alpha_{21}, \tau]\, d\tau = 0$$

$$\int_0^{2\pi} D_3[\alpha_{11}, \alpha_{21}, \tau] \cos 2\tau\, d\tau = 0$$

which yield, after the substitution of Eqs. (III-22) into Eqs. (III-21), for the third-order theory,

$$(1-\Omega^2)a_{11} + \frac{1}{4}(c_{11} - 3c_{12})\Omega^2 a_{11}^3 - c_{13}\Omega^2 a_{00} a_{11} \qquad \text{(III-24)}$$

$$- c_{14}\Omega^2 a_{20} a_{11} - \left(\frac{c_{13}}{2} - c_{15} + 2c_{16}\right)\Omega^2 a_{01} a_{11}$$

$$- \left(\frac{c_{14}}{2} - c_{17} + 2c_{18}\right)\Omega^2 a_{21} a_{11} \mp \epsilon\Omega^2 P_{11} = 0$$

$$(1-9\Omega^2)a_{13} - \frac{1}{4}(c_{11} + c_{12})\Omega^2 a_{11}^3 - \left(\frac{c_{13}}{2} + c_{15} + 2c_{16}\right)\Omega^2 a_{01} a_{11} \qquad \text{(III-25)}$$

$$- \left(\frac{c_{14}}{2} + c_{17} + 2c_{18}\right)\Omega^2 a_{21} a_{11} = 0$$

$$a_{00} = \frac{1}{2}(c_{01} - c_{02})\Omega^2 r_{01}^2 a_{11}^2 \qquad \text{(III-26)}$$

$$a_{20} = \frac{1}{2}(c_{21} - c_{22})\Omega^2 r_{21}^2 a_{11}^2$$

$$a_{01} = \frac{(c_{01} + c_{02})\,\Omega^2 r_{01}^2}{2(1 - 4\Omega^2 r_{01}^2)}\, a_{11}^2$$

$$a_{21} = \frac{(c_{21} + c_{22})\,\Omega^2 r_{21}^2}{2(1 - 4\Omega^2 r_{21}^2)}\, a_{11}^2$$

Substituting Eqs. (III-26) into Eqs. (III-24) and (III-25) and simplifying, we obtain

$$a_{11}^3 (K_1 \Omega^2 + K_2 \Omega^4 + K_3 \Omega^6 + K_4 \Omega^8) + a_{11}(1 - \Omega^2)(1 - 4\Omega^2 r_{01}^2) \qquad \text{(III-27)}$$

$$\cdot (1 - 4\Omega^2 r_{21}^2) \mp \epsilon p_{11} \Omega^2 (1 - 4\Omega^2 r_{01}^2)(1 - 4\Omega^2 r_{21}^2) = 0$$

$$a_{13} = \frac{(K_5 \Omega^2 + K_6 \Omega^4 + K_7 \Omega^6)\; a_{11}^3}{(1 - 9\Omega^2)(1 - 4\Omega^2 r_{01}^2)(1 - 4\Omega^2 r_{21}^2)} \qquad \text{(III-28)}$$

where K_1, K_2, K_3, K_4, K_5, K_6, K_7 are constants given in Appendix I(C).

It is to be noted here that Eq. (III-27) is the amplitude-frequency relationship of the harmonic response. It is an algebraic equation representing a form of solution corresponding to a generalized Duffing's equation. Depending upon the liquid height $\frac{h}{a}$, the nonlinear system will exhibit a softening effect or a hardening effect according to this equation. The liquid system will behave like a linear system at a liquid height H_{ch} which is called the characteristic depth and can be obtained from free oscillation analysis.

As can be seen from Eqs. (III-26), (III-27), and (III-28), once a_{11} is solved by Eq. (III-27), the rest of the generalized coordinates of free surface displacement can be determined.

Free Surface Displacement and Velocity Potential

If we let

$$\beta_1 = \frac{(K_5\Omega^2 + K_6\Omega^4 + K_7\Omega^6)}{(1-9\Omega^2)(1-4\Omega^2 r_{01}^2)(1-4\Omega^2 r_{21}^2)} \quad ; \quad \beta_2 = \frac{1}{2}(C_{01} - C_{02}) r_{01}^2 \Omega^2$$

$$\beta_3 = \frac{(C_{01} + C_{02}) r_{01}^2 \Omega^2}{2(1 - 4\Omega^2 r_{01}^2)} \quad ; \quad \beta_4 = \frac{1}{2}(C_{21} - C_{22}) r_{21}^2 \Omega^2$$

$$\beta_5 = \frac{(C_{21} + C_{22}) r_{21}^2 \Omega^2}{2(1 - 4\Omega^2 r_{21}^2)}$$

then from Eqs. (III-26) and (III-28), we have

$$a_{13} = \beta_1 a_{11}^3 \quad ; \quad a_{00} = \beta_2 a_{11}^2 \quad ; \quad a_{01} = \beta_3 a_{11}^2$$

$$a_{20} = \beta_4 a_{11}^2 \quad ; \quad a_{21} = \beta_5 a_{11}^2$$

Therefore, the free surface displacement can be written as

$$\eta(r,\theta,t) = \underline{(a_{11}\cos\omega t + \beta_1 a_{11}^3 \cos 3\omega t)\cos\nu_1\theta\, C_{\nu_1}(\lambda_{11} r)} \qquad \text{(III-29)}$$

$$+ (\beta_2 + \beta_3 \cos 2\omega t) a_{11}^2 C_0(\lambda_{01} r) + (\beta_4 + \beta_5 \cos 2\omega t) a_{11}^2 \cos\nu_2\theta\, C_{\nu_2}(\lambda_{21} r)$$

where the underlined term represents the linearized solution, in which a_{11} is obtained from Eq. (III-27) by omitting the a_{11}^3 term.

Knowing α_{11}, α_{01}, and α_{21}, the expressions for the generalized coordinates of the velocity potential can be obtained, again based on

third order theory, from Eqs. (III-17). The results are

$$A_{11} = (\delta_1 a_{11} + \delta_2 a_{11}^3) \sin \omega t + \delta_3 a_{11}^3 \sin 3\omega t$$

$$A_{01} = \delta_4 a_{11}^2 \sin 2\omega t$$

$$A_{21} = \delta_5 a_{11}^2 \sin 2\omega t$$

From Eq. (III-19) and the above results, we obtain

$$\dot{A}_{00} = \frac{\delta_6 + \delta_7}{2} a_{11}^2 + \delta_8 \epsilon \cos \omega t + \frac{\delta_7 - \delta_6}{2} a_{11}^2 \cos 2\omega t$$

where $\delta_1, \delta_2, \ldots \delta_8$ are given in Appendix I(D)

Therefore the expression for the velocity potential is

$$\Phi = A_{00} + A_{01} \frac{\cosh[\lambda_{01}(z+h)]}{\cosh(\lambda_{01} h)} C_0(\lambda_{01} r) \qquad \text{(III-30)}$$

$$+ A_{11} \cos \nu_1 \theta \frac{\cosh[\lambda_{11}(z+h)]}{\cosh(\lambda_{11} h)} C_{\nu_1}(\lambda_{11} r) + A_{21} \cos \nu_2 \theta \frac{\cosh[\lambda_{21}(z+h)]}{\cosh(\lambda_{21} h)} C_{\nu_2}(\lambda_{21} r)$$

which can be rewritten as

$$\Phi = A_{00} + \cos \nu_1 \theta \frac{\cosh[\lambda_{11}(z+h)]}{\cosh(\lambda_{11} h)} C_{\nu_1}(\lambda_{11} r) \Big[\delta_1 a_{11} \sin \omega t \qquad \text{(III-31)}$$

$$+ \delta_2 a_{11}^3 \sin \omega t + \delta_3 a_{11}^3 \sin 3\omega t \Big] + A_{01} \frac{\cosh[\lambda_{01}(z+h)]}{\cosh(\lambda_{01} h)} C_0(\lambda_{01} r)$$

$$+ A_{21} \cos \nu_2 \theta \frac{\cosh[\lambda_{21}(z+h)]}{\cosh(\lambda_{21} h)} C_{\nu_2}(\lambda_{21} r)$$

where the underlined term together with the harmonic part of the integrated value of $\dot{A}_{oo}$ represent the part of the linearized solution, in which a_{11} is obtained from Eq. (III-27) by ignoring the a_{11}^{3} term.

CHAPTER IV

FLUID FORCES AND MOMENTS

The pressure exerting on the tank due to the fluid oscillation can be obtained from the unsteady Bernoulli equation in terms of the disturbance velocity potential:

$$p = -\rho\left\{\Phi_t + gz - \epsilon\omega^2 r\cos\theta\cos\omega t + \frac{1}{2}\left(\Phi_r^2 + \frac{1}{r^2}\Phi_\theta^2 + \Phi_z^2\right)\right\} \qquad \text{(IV-1)}$$

In order to be consistent with the third order theory, the pressure, forces, and moments will be obtained up to the third order terms. Thus, by Eqs. (III-30) with the abbreviations: $C_0 \equiv C_0(\lambda_{01} r)$; $C_{\nu_1} = C_{\nu_1}(\lambda_{11} r)$; $C_{\nu_2} = C_{\nu_2}(\lambda_{21} r)$, the expression for the pressure distribution is:

$$p(r,\theta,z,t) = -\rho\left\{ p_0 + p_1\cos\omega t + p_2\cos 2\omega t + p_3\cos 3\omega t\right\} \qquad \text{(IV-2)}$$

where

$$p_0 = \frac{1}{2}(\delta_6 + \delta_7)a_{11}^2 + gz + \frac{\lambda_{11}^2}{4}\delta_1^2 a_{11}^2\cos^2\nu_1\theta\left[\frac{\cosh[\lambda_{11}(z+h)]}{\cosh(\lambda_{11}h)}\right]^2 C_{\nu_1}'^2$$

$$+ \frac{\delta_1^2 a_{11}^2}{16\alpha^2 r^2}\sin^2\nu_1\theta\left[\frac{\cosh[\lambda_{11}(z+h)]}{\cosh(\lambda_{11}h)}\right]^2 C_{\nu_1}^2 + \frac{\lambda_{11}^2}{4}\delta_1^2 a_{11}^2\cos\nu_1\theta\left[\frac{\sinh[\lambda_{11}(z+h)]}{\cosh(\lambda_{11}h)}\right]^2 C_{\nu_1}'^2$$

$$\phi_1 = \epsilon\delta_8 - \epsilon\omega^2 r\cos\theta + (\delta_1 a_{11} + \delta_2 a_{11}^3)\,\omega\cos\nu_1\theta\,\frac{\cosh[\lambda_{11}(z+h)]}{\cosh(\lambda_{11}h)}\,C_{\nu_1}$$

$$+\frac{1}{2}\delta_1\delta_4\lambda_{01}\lambda_{11}a_{11}^3\,\frac{\cosh[\lambda_{01}(z+h)]\cosh[\lambda_{11}(z+h)]}{\cosh(\lambda_{01}h)\cosh(\lambda_{11}h)}\cos\nu_1\theta\,C_0'\,C_{\nu_1}'$$

$$+\frac{1}{2}\delta_1\delta_5\lambda_{21}\lambda_{11}a_{11}^3\,\frac{\cosh[\lambda_{21}(z+h)]\cosh[\lambda_{11}(z+h)]}{\cosh(\lambda_{21}h)\cosh(\lambda_{11}h)}\cos\nu_1\theta\cos\nu_2\theta\,C_{\nu_1}'\,C_{\nu_2}'$$

$$+\frac{\delta_1\delta_5}{4\alpha^2r^2}\,a_{11}^3\,\frac{\cosh[\lambda_{21}(z+h)]\cosh[\lambda_{11}(z+h)]}{\cosh(\lambda_{21}h)\cosh(\lambda_{11}h)}\sin\nu_1\theta\sin\nu_2\theta\,C_{\nu_1}C_{\nu_2}$$

$$+\frac{1}{2}\delta_1\delta_4\lambda_{01}\lambda_{11}a_{11}^3\,\frac{\sinh[\lambda_{01}(z+h)]\sinh[\lambda_{11}(z+h)]}{\cosh(\lambda_{01}h)\cosh(\lambda_{11}h)}\cos\nu_1\theta\,C_0\,C_{\nu_1}$$

$$+\frac{1}{2}\delta_1\delta_5\lambda_{21}\lambda_{11}a_{11}^3\,\frac{\sinh[\lambda_{21}(z+h)]\sinh[\lambda_{11}(z+h)]}{\cosh(\lambda_{21}h)\cosh(\lambda_{11}h)}\cos\nu_1\theta\cos\nu_2\theta\,C_{\nu_1}C_{\nu_2}$$

$$\phi_2 = \frac{1}{2}(\delta_7-\delta_6)a_{11}^2 + 2\omega\delta_4 a_{11}^2\,\frac{\cosh[\lambda_{01}(z+h)]}{\cosh(\lambda_{01}h)}\,C_0$$

$$+2\omega\delta_5 a_{11}^2\,\frac{\cosh[\lambda_{21}(z+h)]}{\cosh(\lambda_{21}h)}\cos\nu_2\theta\,C_{\nu_2}$$

$$-\frac{\lambda_{11}^2}{4}\delta_1^2 a_{11}^2\left[\frac{\cosh[\lambda_{11}(z+h)]}{\cosh(\lambda_{11}h)}\right]^2\cos^2\nu_1\theta\,C_{\nu_1}'^2$$

$$-\frac{\delta_1^2 a_{11}^2}{16\alpha^2r^2}\left[\frac{\cosh[\lambda_{11}(z+h)]}{\cosh(\lambda_{11}h)}\right]^2\sin^2\nu_1\theta\,C_{\nu_1}^2$$

$$-\frac{\lambda_{11}^2}{4}\delta_1^2 a_{11}^2\left[\frac{\sinh[\lambda_{11}(z+h)]}{\cosh(\lambda_{11}h)}\right]^2\cos^2\nu_1\theta\,C_{\nu_1}^2$$

$$\phi_3 = 3\omega\delta_3 a_{11}^3\,\frac{\cosh[\lambda_{11}(z+h)]}{\cosh(\lambda_{11}h)}\cos\nu_1\theta\,C_{\nu_1}$$

$$-\frac{1}{2}\delta_1\delta_4\lambda_{01}\lambda_{11}a_{11}^3\,\frac{\cosh[\lambda_{01}(z+h)]\cosh[\lambda_{11}(z+h)]}{\cosh(\lambda_{01}h)\cosh(\lambda_{11}h)}\cos\nu_1\theta\,C_0'\,C_{\nu_1}'$$

$$-\frac{1}{2}\delta_1\delta_5\lambda_{21}\lambda_{11}a_{11}^3\,\frac{\cosh[\lambda_{21}(z+h)]\cosh[\lambda_{11}(z+h)]}{\cosh(\lambda_{21}h)\cosh(\lambda_{11}h)}\cos\nu_1\theta\cos\nu_2\theta\,C'_{\nu_1}C'_{\nu_2}$$

$$-\frac{\delta_1\delta_5}{4\alpha^2r^2}a_{11}^3\,\frac{\cosh[\lambda_{21}(z+h)]\cosh[\lambda_{11}(z+h)]}{\cosh(\lambda_{21}h)\cosh(\lambda_{11}h)}\sin\nu_1\theta\sin\nu_2\theta\,C_{\nu_1}C_{\nu_2}$$

$$-\frac{1}{2}\delta_1\delta_4\lambda_{01}\lambda_{11}a_{11}^3\,\frac{\sinh[\lambda_{01}(z+h)]\sinh[\lambda_{11}(z+h)]}{\cosh(\lambda_{01}h)\cosh(\lambda_{11}h)}\cos\nu_1\theta\,C_0C_{\nu_1}$$

$$-\frac{1}{2}\delta_1\delta_5\lambda_{21}\lambda_{11}a_{11}^3\,\frac{\sinh[\lambda_{21}(z+h)]\sinh[\lambda_{11}(z+h)]}{\cosh(\lambda_{21}h)\cosh(\lambda_{11}h)}\cos\nu_1\theta\cos\nu_2\theta\,C_{\nu_1}C_{\nu_2}$$

With appropriate pressure distributions, the total force in any direction can be calculated by integrating the components of the pressure distributions over the wetted surface. Thus the total force on the tank in x-direction due to the liquid oscillation is

$$F_x=\int_0^{2\pi\alpha}\int_{-h}^{[\eta]_{r=a}}[p]_{r=a}\,a\cos\theta\,dz\,d\theta-\int_0^{2\pi\alpha}\int_{-h}^{[\eta]_{r=b}}[p]_{r=b}\,b\cos\theta\,dz\,d\theta \qquad \text{(IV-3)}$$

$$-\int_b^a\int_{-h}^{[\eta]_{\theta=2\pi\alpha}}[p]_{\theta=2\pi\alpha}\sin 2\pi\alpha\,dz\,dr$$

The first two terms represent the force contributions from the pressure distributions at the circular cylindrical segments and the last term represents that from the pressure at the sector wall $\theta = 2\pi\alpha$.

The total forces in the y- and z-directions are, respectively,

$$F_y=\int_0^{2\pi\alpha}\int_{-h}^{[\eta]_{r=a}}[p]_{r=a}\,a\sin\theta\,dz\,d\theta-\int_0^{2\pi\alpha}\int_{-h}^{[\eta]_{r=b}}[p]_{r=b}\,b\sin\theta\,dz\,d\theta \qquad \text{(IV-4)}$$

$$+\int_b^a\int_{-h}^{[\eta]_{\theta=2\pi\alpha}}[p]_{\theta=2\pi\alpha}\cos 2\pi\alpha\,dz\,dr-\int_b^a\int_{-h}^{[\eta]_{\theta=0}}[p]_{\theta=0}\,dz\,dr$$

$$F_z = -\int_0^{2\pi\alpha}\int_b^a [p]_{z=-h}\, r\,dr\,d\theta \qquad \text{(IV-5)}$$

The moments about the axes passing through the point (0,0,-h/2) and parallel to the x, y, and z axes due to the liquid motion can be obtained by the following formulas:

$$M_x = -\int_0^{2\pi\alpha}\int_{-h}^{[\eta]_{r=a}} [p]_{r=a}\left(\frac{h}{2}+z\right) a \sin\theta\, dz\, d\theta \qquad \text{(IV-6)}$$
$$+\int_0^{2\pi\alpha}\int_{-h}^{[\eta]_{r=b}} [p]_{r=b}\left(\frac{h}{2}+z\right) b \sin\theta\, dz\, d\theta - \int_0^{2\pi\alpha}\int_b^a [p]_{z=-h} r^2 \sin\theta\, dr\, d\theta$$
$$-\int_b^a\int_{-h}^{[\eta]_{\theta=2\pi\alpha}} [p]_{\theta=2\pi\alpha}\left(\frac{h}{2}+z\right)\cos 2\pi\alpha\, dz\, dr + \int_b^a\int_{-h}^{[\eta]_{\theta=0}} [p]_{\theta=0}\left(\frac{h}{2}+z\right) dz\, dr$$

$$M_y = \int_0^{2\pi\alpha}\int_{-h}^{[\eta]_{r=a}} [p]_{r=a}\left(\frac{h}{2}+z\right) a\cos\theta\, dz\, d\theta + \int_0^{2\pi\alpha}\int_b^a [p]_{z=-h} r^2\cos\theta\, dr\, d\theta \qquad \text{(IV-7)}$$
$$-\int_0^{2\pi\alpha}\int_{-h}^{[\eta]_{r=b}} [p]_{r=b}\left(\frac{h}{2}+z\right) b\cos\theta\, dz\, d\theta - \int_b^a\int_{-h}^{[\eta]_{\theta=2\pi\alpha}} [p]_{\theta=2\pi\alpha}\left(\frac{h}{2}+z\right)\sin 2\pi\alpha\, dz\, dr$$

$$M_z = \int_b^a\int_{-h}^{[\eta]_{\theta=2\pi\alpha}} [p]_{\theta=2\pi\alpha} r\, dr\, dz - \int_b^a\int_{-h}^{[\eta]_{\theta=0}} [p]_{\theta=0}\, r\, dr\, dz \qquad \text{(IV-8)}$$

The first two terms in M_x represent the moment contributions from the pressure distributions at the circular cylindrical segments and the third term represents that from the bottom and the last two terms are those from the sector walls. Since the reference axes do not pass through the center of gravity of the undisturbed liquid, the evaluated expressions for moments will include the static moments of the fluid with respect to the reference axes.

As can be seen from the above expressions for forces and moments, the upper limit of integrations with respect to z is a moving boundary, i.e., the integrated expressions have to be evaluated at $z = \eta(r,\theta,t)$ (Eq. (III-29)). Therefore, for the purpose of evaluation, we expand the pressure $p(r,\theta,z,t)$ into Taylor series about $z = 0$. This is possible because p is analytic at $z = 0$. In order to be consistent with the third order solution, we need to keep only up to the second order terms in the expression for pressure. Thus we have

$$p(r,\theta,z,t) = p(r,\theta,0,t) + p_z(r,\theta,0,t) + O(A^3)$$

then

$$\int_0^\eta p\, dz = \eta\, p(r,\theta,0,t) + \frac{\eta^2}{2} p_z(r,\theta,0,t) + O(\eta^4) \qquad \text{(IV-9)}$$

From Eq. (IV-1) we have

$$p(r,\theta,0,t) = -\rho\left\{\left[\Phi_t + \frac{1}{2}\left(\Phi_r^2 + \frac{1}{r^2}\Phi_\theta^2 + \Phi_z\right)\right]_{z=0} - \epsilon\omega^2 r\cos\theta\cos\omega t\right\} \qquad \text{(IV-10)}$$

and for p_z we need only terms up to the first order, thus

$$p_z(r,\theta,0,t) = -\rho\left\{g + \cos\omega t\left[\delta_1 a_{11}\omega\lambda_{11}\tanh(\lambda_{11}h) C_{\nu_1}(\lambda_{11}r)\cos\nu\theta\right]\right\} \qquad \text{(IV-11)}$$

Therefore, take F_x as an example, we have

$$F_x = \int_0^{2\pi\alpha}\cos\theta\int_{-h}^{0}\left[a\,p(a,\theta,z,t) - b\,p(b,\theta,z,t)\right] dz\, d\theta \qquad \text{(IV-12)}$$

$$+\int_0^{2\pi\alpha}\cos\theta\left\{\left[a\int_0^{\eta}p\,dz\right]_{r=a}-\left[b\int_0^{\eta}p\,dz\right]_{r=b}\right\}d\theta-\sin 2\pi\alpha\int_b^a\int_{-h}^{0}p(r,2\pi\alpha,z,t)\,dz\,dr$$

$$-\sin 2\pi\alpha\int_b^a\left[\int_0^{\eta}p\,dz\right]_{\theta=2\pi\alpha}dr$$

The second and fourth integrals in Eq. (IV-12) can be rewritten, respectively, as

$$\int_0^{2\pi\alpha}\cos\theta\left\{\left[a\int_0^{\eta}p\,dz\right]_{r=a}-\left[b\int_0^{\eta}p\,dz\right]_{r=b}\right\}d\theta \tag{IV-13}$$

$$=\int_0^{2\pi\alpha}\cos\theta\left\{a[\eta]_{r=a}p(a,\theta,0,t)-b[\eta]_{r=b}p(b,\theta,0,t)\right.$$

$$\left.+\frac{1}{2}\left[a[\eta^2]_{r=a}p_z(a,\theta,0,t)-b[\eta^2]_{r=b}p_z(b,\theta,0,t)\right]\right\}d\theta$$

and

$$\sin 2\pi\alpha\int_b^a\left[\int_0^{\eta}p\,dz\right]_{\theta=2\pi\alpha}dr \tag{IV-14}$$

$$=\sin 2\pi\alpha\int_b^a\left[\eta\,p(r,2\pi\alpha,0,t)+\frac{\eta^2}{2}p_z(r,2\pi\alpha,0,t)\right]_{\theta=2\pi\alpha}dr$$

A more detailed evaluation of forces and moments can be found in Appendix II. Again, it is to be remarked here that all the forces and moments are expressed in terms of a_{11}. Thus once a_{11} is solved by Eq. (III-27), the values of forces and moments can be obtained immediately.

CHAPTER V

NUMERICAL EXAMPLES

Free Oscillations

The results for nonlinear free oscillation can be obtained by setting $X(t) \equiv 0$ in the expression of general solution in Chapter III. The relationship between the natural frequency and the liquid amplitude, the so-called "backbone curve," can be determined from Eq. (III-27) by setting $\epsilon \equiv 0$. It becomes

$$a_{11}^2 (K_1 \Omega^2 + K_2 \Omega^4 + K_3 \Omega^6 + K_4 \Omega^8) + (1 - \Omega^2)(1 - 4\Omega^2 r_{01}^2)(1 - 4\Omega^2 r_{21}^2) = 0 \qquad \text{(V-1)}$$

where K_1, K_2, K_3, and K_4 are functions of liquid height and tank geometry. For a given tank configuration, backbone curves are obtained from Eq. (V-1) for various liquid heights. From these backbone curves a characteristic depth H_{ch} could be found for each container such that, at that liquid height, the liquid system would exhibit linear vibration characteristics. For a liquid height $\frac{h}{a} \neq H_{ch}/a$, the liquid system acts as either a nonlinear soft spring or a nonlinear hard spring. These are illustrated in the figures which follow.

Figure 2 shows the backbone curves for a semicircular tank ($k = \frac{b}{a} = 0$, $\alpha = 0.5$). It is to be noted here that the solution for a semicircular tank in the present analysis should correspond to the planar mode solution for a complete circular cylindrical tank, since the eigen-

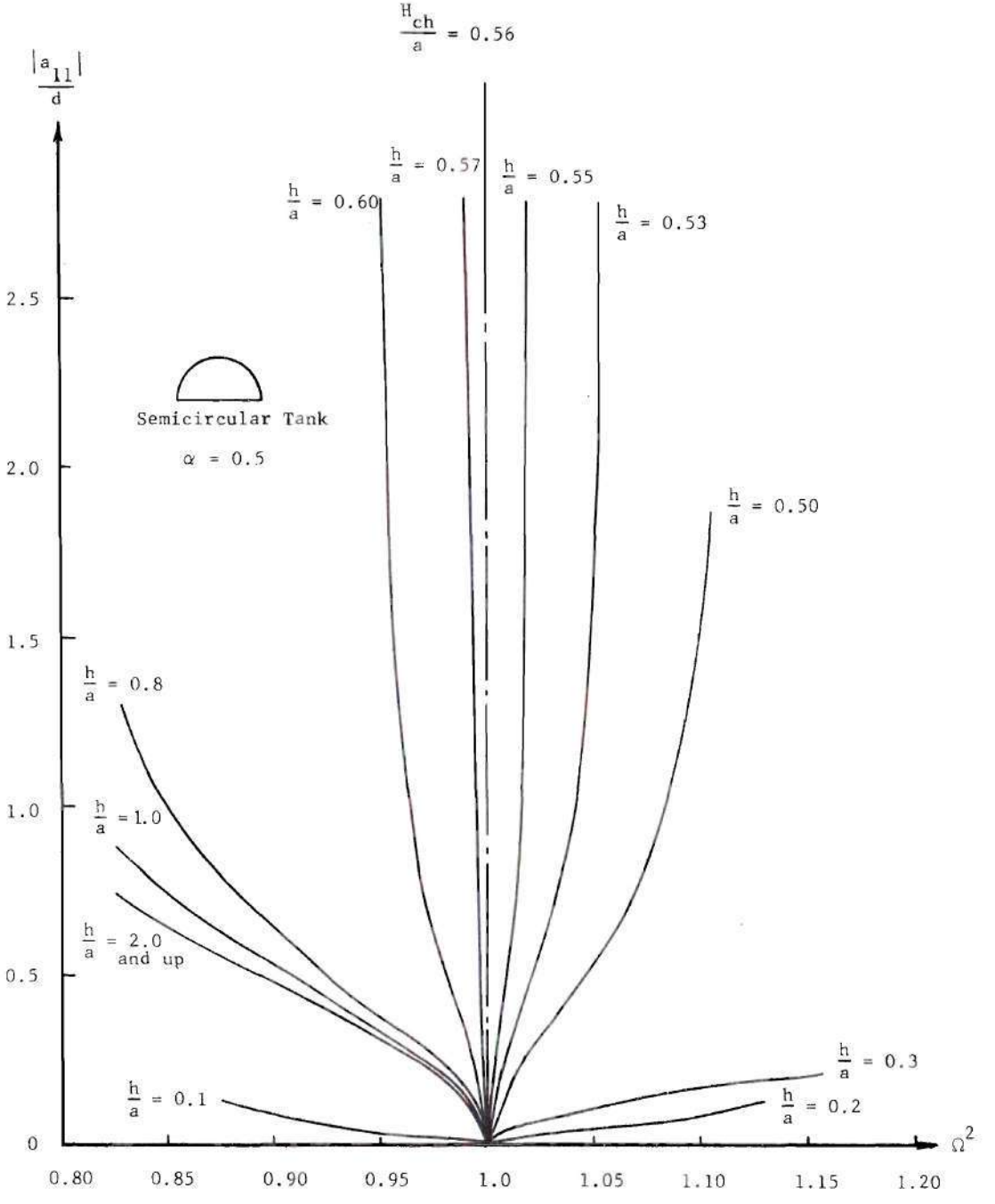

Figure 2. Semicircular Tank: Backbone Curves Corresponding to Various Liquid Heights

values and eigenfunction are the same. From this figure, the characteristic depth for a semicircular tank is found to be $H_{ch}/a = 0.56$, which is in good agreement with the result ($H_{ch} = 0.5$) obtained by DiMaggio and Rehm [23] using the perturbation method.

Backbone curves for a quarter sector tank ($k = 0$, $\alpha = 0.25$) and a 45° sector tank ($k = 0$, $\alpha = 0.125$) are shown in Figures 3 and 4, respectively. A similar pattern of backbone curves exists in these two containers. The characteristic depth for a quarter sector tank is found to be $H_{ch}/a = 0.27$, which is in good agreement with the result ($H_{ch}/a = 0.29$) obtained by Baird [10] using the Krylov-Bogoliubov method. For a 45° sector tank, we see that $H_{ch}/a = 0.17$. This means that a sector tank with decreasing apex angle results in a lower characteristic depth; consequently, the liquid exhibits a nonlinear softening characteristic in a wider range of liquid heights.

A surprising result of the nonlinear free oscillations is that more than one characteristics depth exists for certain tank configurations. For example, there are two characteristic depths for an annular semicircular tank with $k = 0.3$; one is $H_{ch}/a = 0.38$ and the other is $H_{ch}/a = 1.12$ as shown in Figure 5. Experiments (using an annular semicircular tank of $k = 0.306$) confirm that there are two characteristic depths for the annular semicircular tank.

Another striking feature demonstrated in Figure 5 is that there is a sudden reversal of the nonlinear character of the liquid at a certain liquid height without passing through a characteristic depth. For this particular annular semicircular tank the value is $\frac{h}{a} = 0.6$. This is believed to be due to the effects of the secondary mode resonance (i.e.,

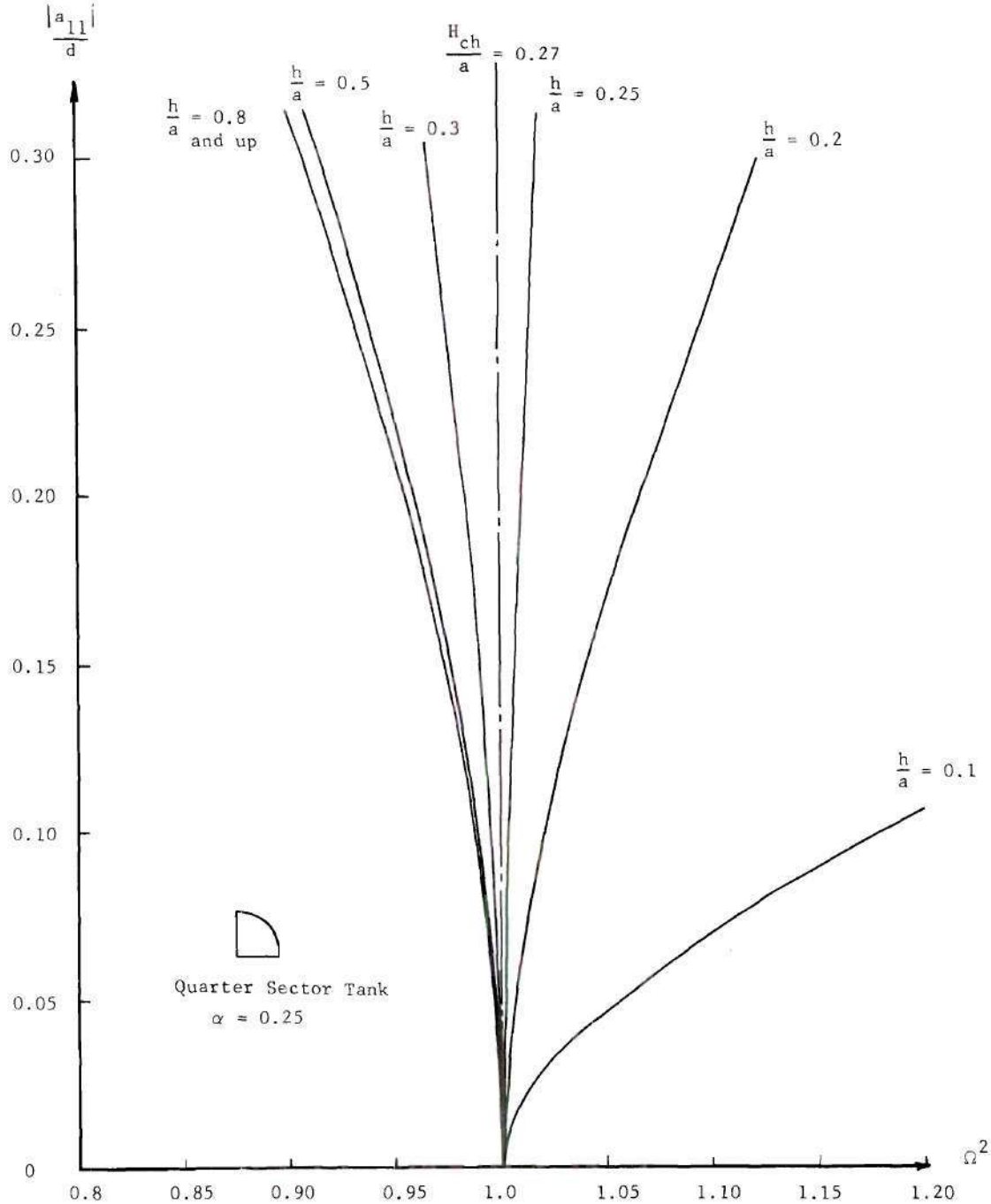

Figure 3. Quarter Sector Tank: Backbone Curves Corresponding to Various Liquid Heights

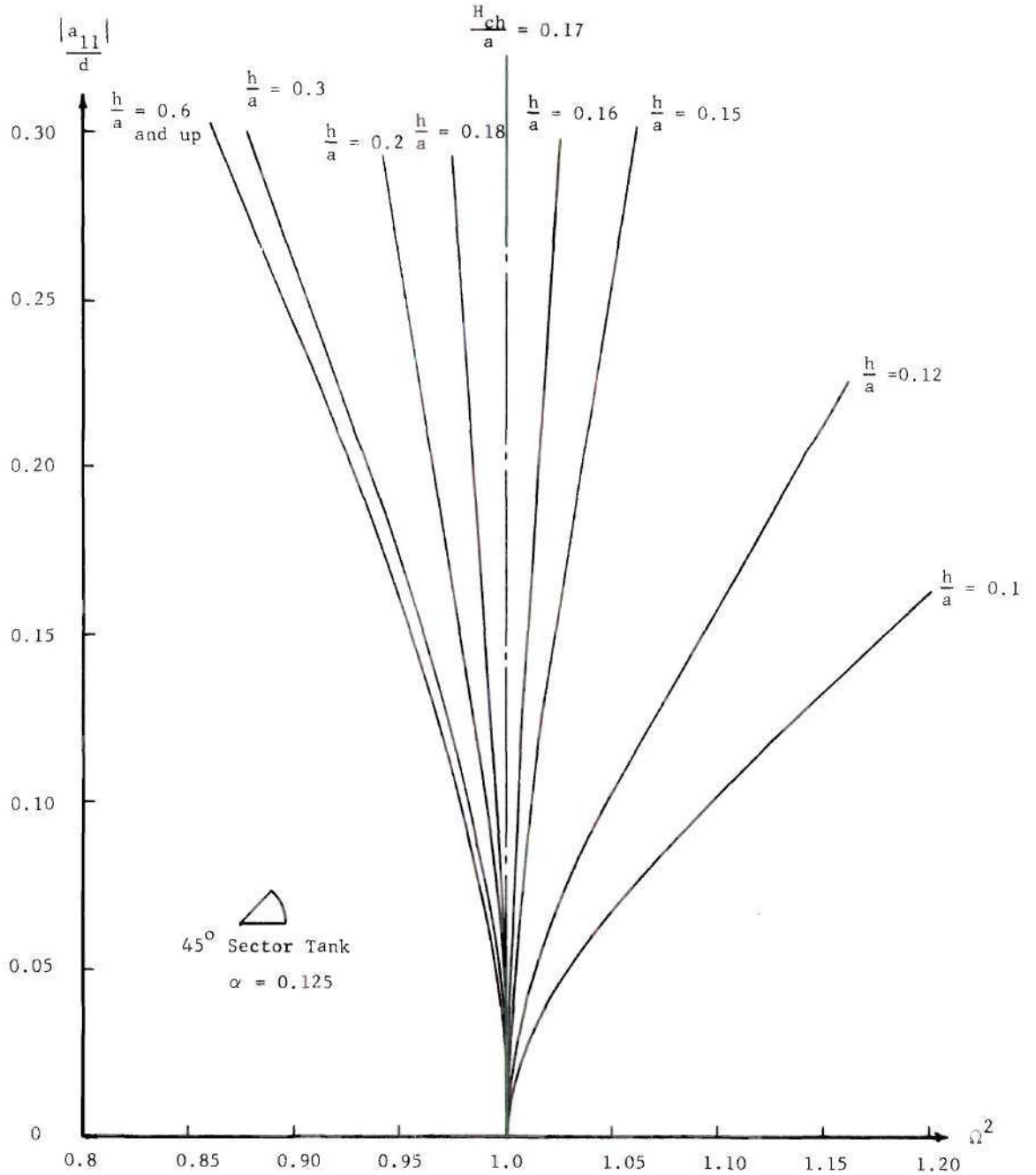

Figure 4. 45° Sector Tank: Backbone Curves Corresponding to Various Liquid Heights

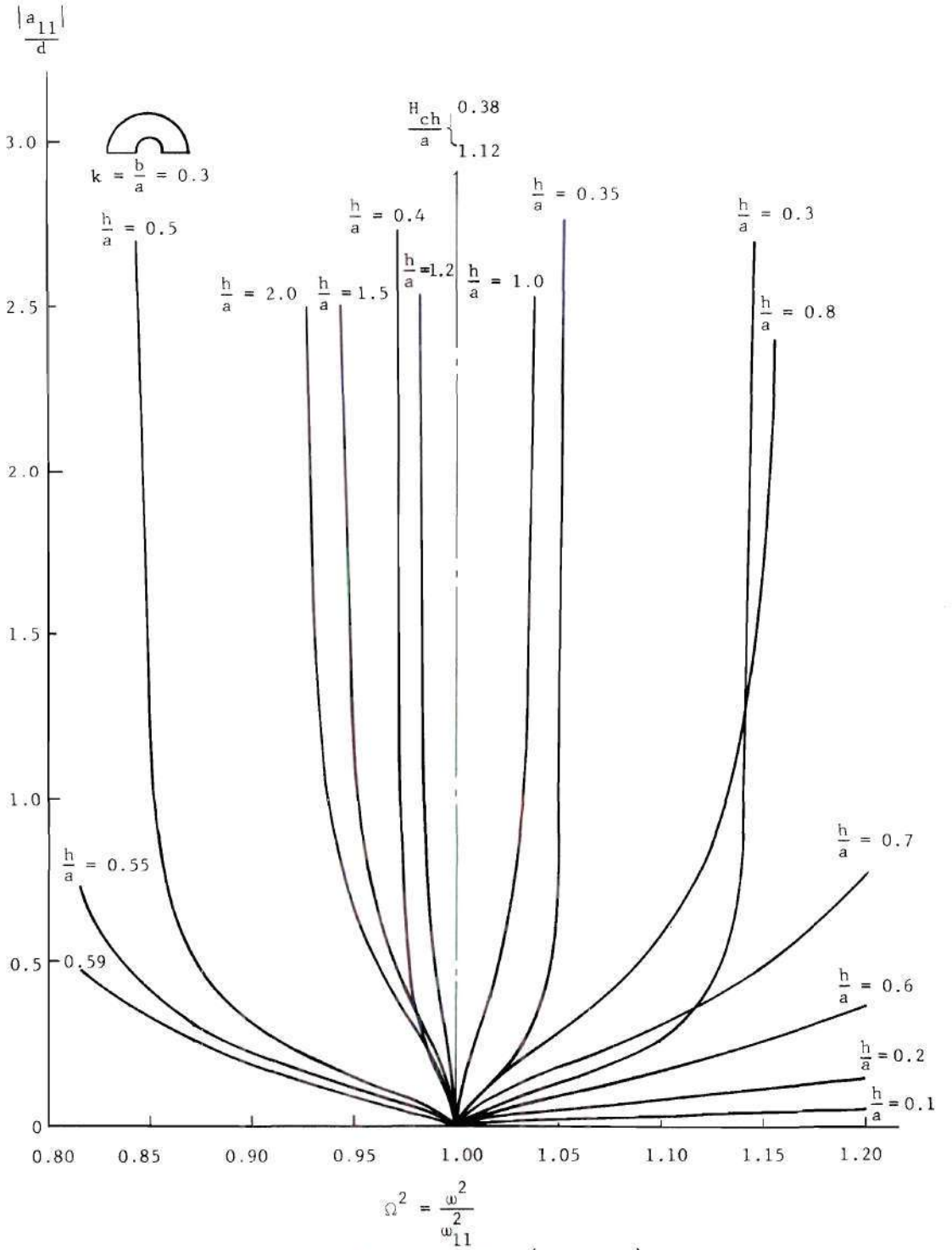

Figure 5. Annular Semicircular Tank (k = 0.3): Backbone Curves Corresponding to Various Liquid Heights

superharmonic resonance of the first symmetric mode having the opposite nonlinear effect to the first antisymmetric mode) as shown in Figure 6. The experiments also indicate the existence of this "sudden reversal" phenomenon. The same result is found theoretically for the semicircular tank (Fig. 2) at $\frac{h}{a} = 0.154$.

A common feature of the results of nonlinear free oscillations for various tank configurations is that, beyond a certain liquid height, the backbone curve remains almost the same, i.e., further increase in liquid height will hardly alter the nonlinear free response; it is $\frac{h}{a} \geq 2.0$ for a semicircular tank (Fig. 2), $\frac{h}{a} \geq 0.8$ for a quarter sector tank (Fig. 3), $\frac{h}{a} \geq 0.6$ for a 45° sector tank (Fig. 4), and $\frac{h}{a} \geq 2.0$ for an annular semicircular tank with $k = 0.3$ (Fig. 5).

Forced Oscillations

To compare with available experimental data for a semicircular tank [14], numerical examples based on the present analysis were carried out and are presented in Figures 7a and 7b for different excitation amplitudes. The excitation is a lateral harmonic motion of the container, i.e., $X(t) = \varepsilon \cos\omega t$. The liquid height in both cases is $\frac{h}{d} = 1.0$ ($\frac{h}{a} = 2.0$); thus, the liquid system should exhibit a nonlinear softening characteristic according to the results of free oscillation analysis. In each of these two figures, four nondimensional quantities are shown; namely the average liquid surface displacement amplitude, $|\overline{Y_o}|/d$, the total force response in x-direction, $F_x^{(T)}$, the harmonic component of force in x-direction, $F_x^{(1)}$, and the triple harmonic component of force in x-direction, $F_x^{(3)}$, all against the frequency parameter $\frac{\omega^2 d}{g}$.

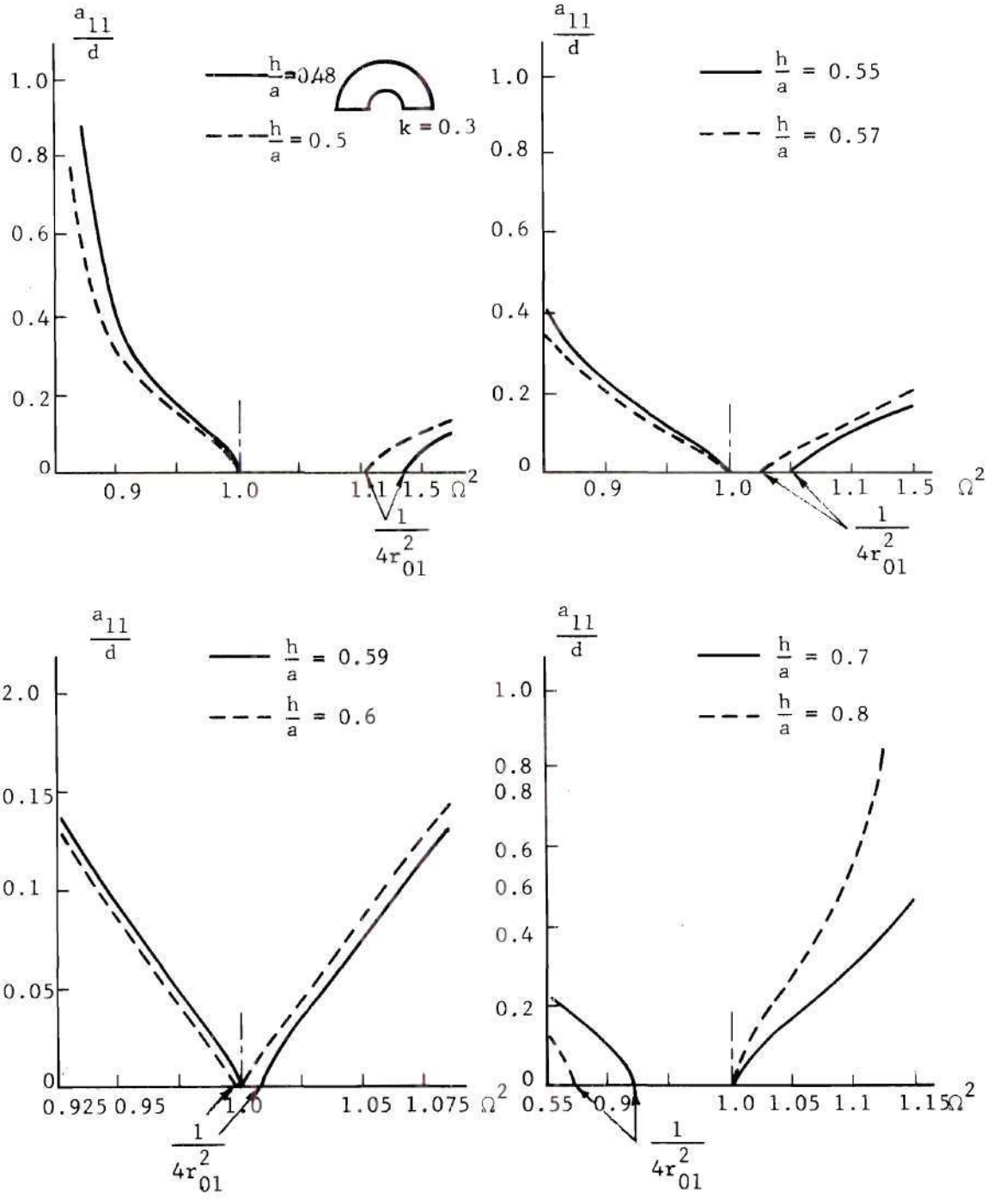

Figure 6. Annular Semicircular Tank (k = 0.3): Backbone Curves Showing Effect of Superharmonic Response

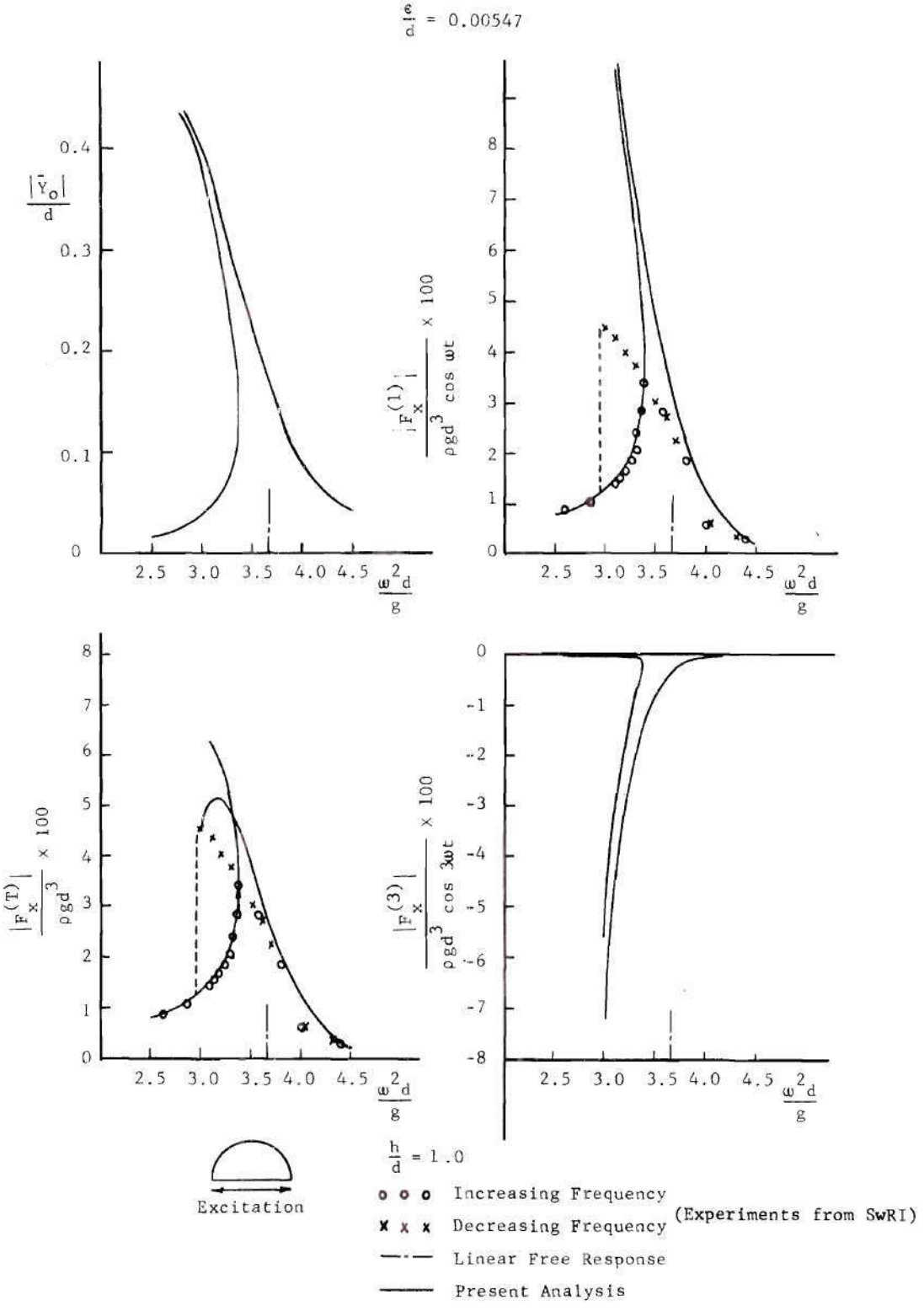

Figure 7a. Semicircular Tank: Liquid Force and Surface Displacement Response Curves (Excitation Amplitude $\epsilon/d = 0.00547$)

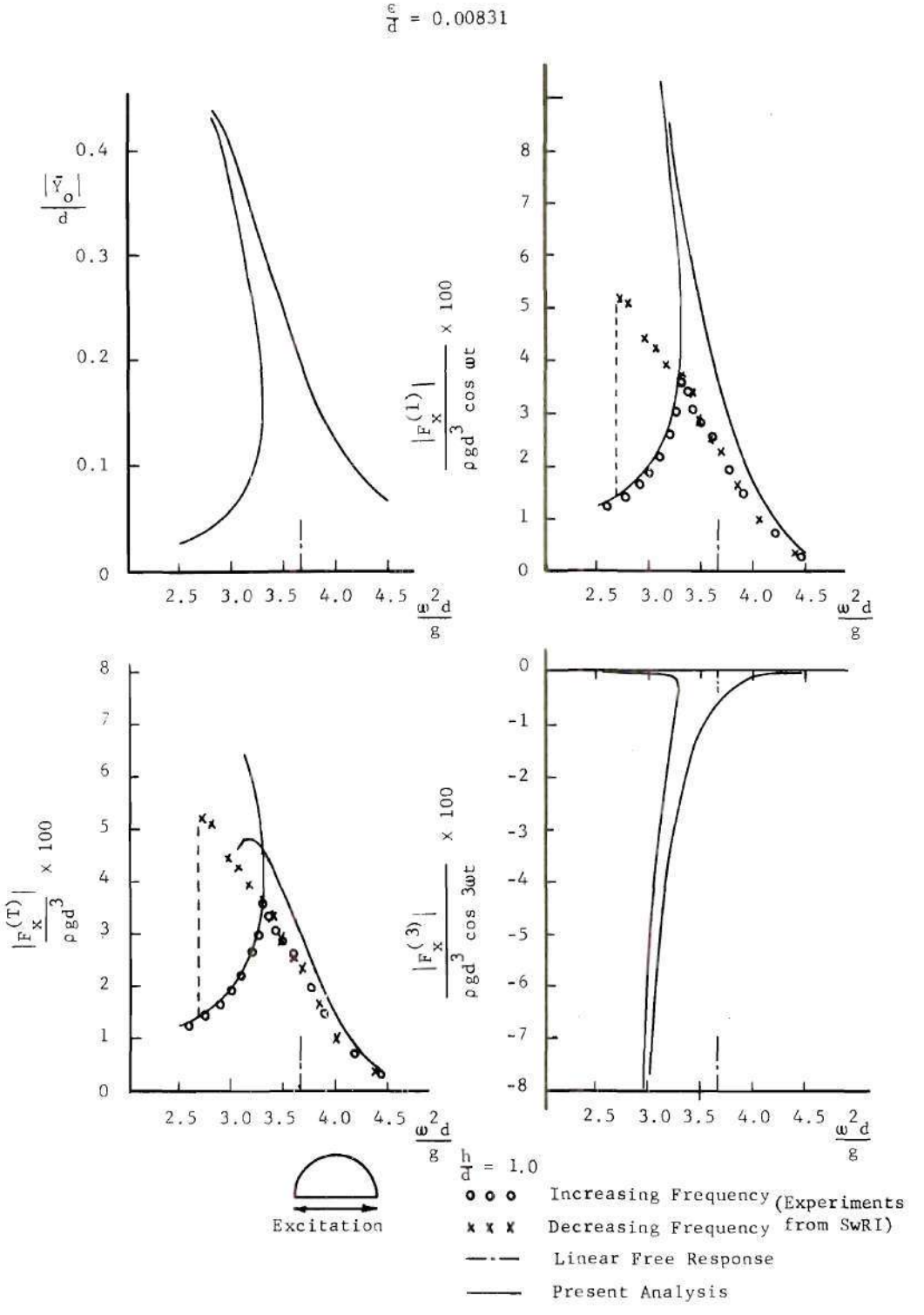

Figure 7b. Semicircular Tank: Liquid Force and Surface Displacement Response Curves (Excitation Amplitude $\epsilon/d = 0.00831$)

Here the average amplitude and the total force have the same meanings as defined in Reference [14], i.e.,

$$\bar{Y}_0 = \frac{1}{2}\left\{ \eta(r=a,\ \theta=0, \omega t=0) - \eta(r=a, \theta=0, \omega t=\pi)\right\} \qquad \text{(V-2)}$$

where $\eta(r,\theta,t)$ is given by Eq. (III-29) and

$$|\bar{F}_x^{(\tau)}| = \frac{1}{2}\left\{ [|F_x|]_{\omega t=0} - [|F_x|]_{\omega t=\pi}\right\} \qquad \text{(V-3)}$$

where F_x is given by (IV-3) or (APII-1).

The experimental points are shown on the graphs of both total force response and the harmonic component of force in the x-direction to demonstrate the importance of the inclusion of the triple harmonic component in calculating total force response. The results are good for engineering applications.

Figures 8 and 9 show the force in the y-direction on a semicircular tank due to liquid sloshing for excitation amplitudes ϵ/d = 0.0026, 0.00574, 0.00831, and 0.0106. It is to be noted that there is no harmonic component of force response in the y-direction for a semicircular tank subjected to harmonic excitation in the x-direction.

Figure 10 shows, similar to Figures 7a and 7b, average displacement amplitude and force response in the x-direction for a quarter sector tank with liquid height $\frac{h}{d}$ = 1.0. These response curves are similar in form to those of the semicircular tank except, in this case, the crossing of the in-phase and out-of-phase response curves happened also in the harmonic component of force in the x-direction in addition to that in the total force responses.

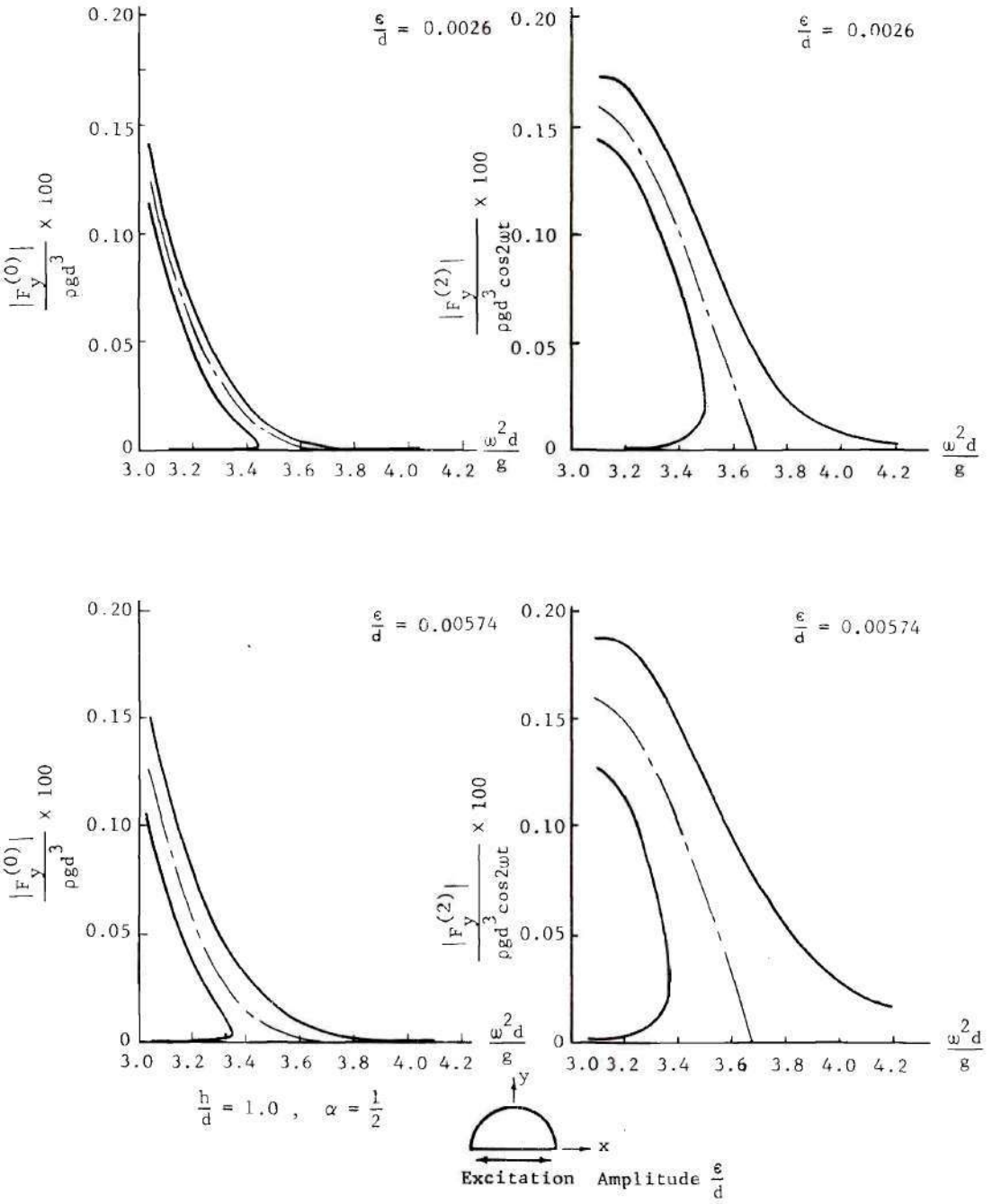

Figure 8. Semicircular Tank: Calculated Response Curves for Components of Crosswise Liquid Force (y-direction), I

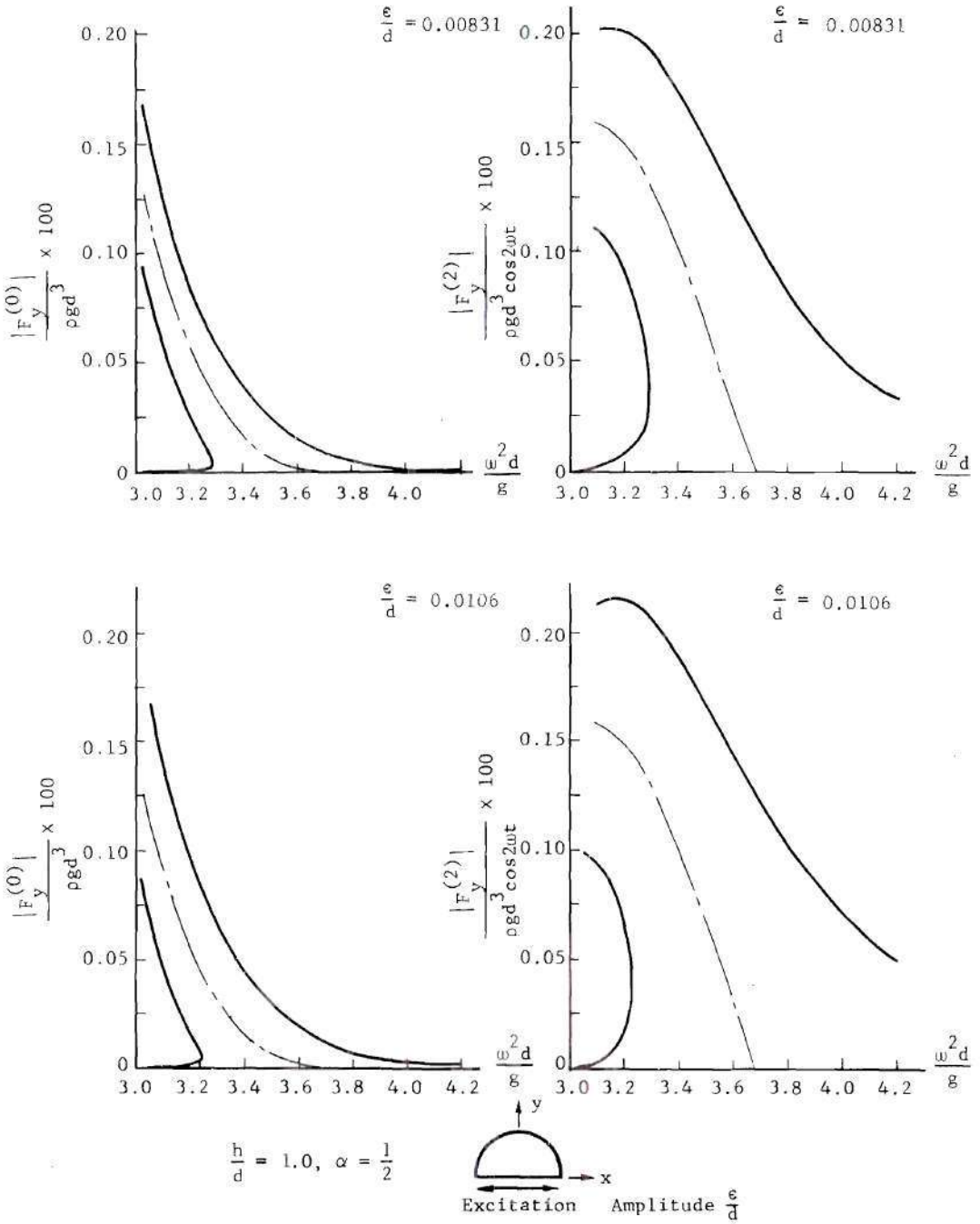

Figure 9. Semicircular Tank: Calculated Response Curves for Components of Crosswise Liquid Force (y-direction), II

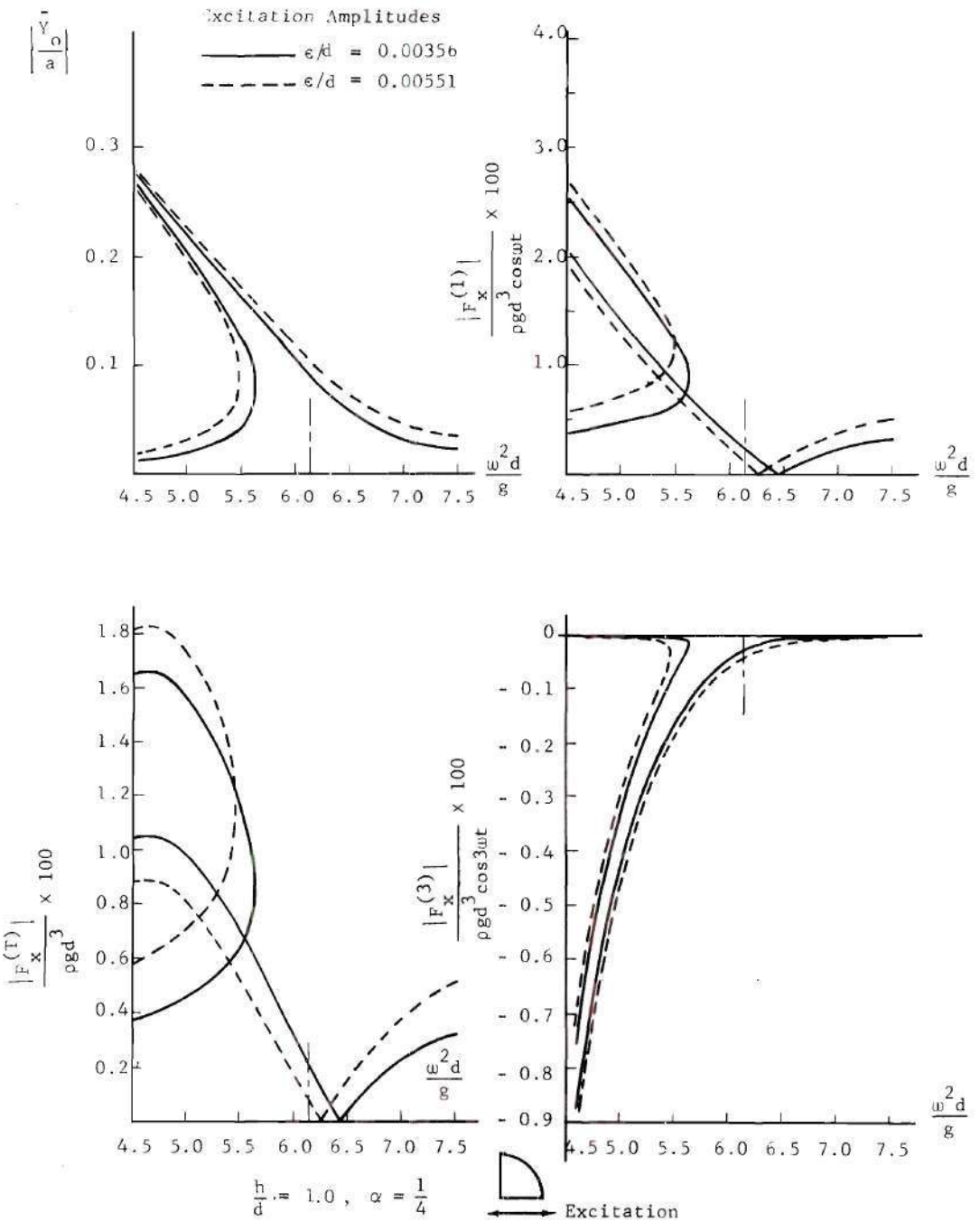

Figure 10. Quarter Sector Tank: Liquid Force and Surface Displacement Response Curves

CHAPTER VI

APPLICATION TO VIBRATION REDUCTION

In the foregoing investigation of lateral oscillation of a liquid in a rigid container, a characteristic depth is found for each tank configuration such that, at that depth, the liquid exhibits linear vibration characteristics.

Using this concept of a characteristic depth, we now explore, both theoretically and experimentally, the dynamic coupling of the liquid system to another dynamic system to investigate application of liquid lateral response as a dynamic vibration absorber. Let us first review briefly the description of liquid motion in a rigid container by a dynamically equivalent mechanical model.

Equivalent Mechanical Model for the Liquid Motion

The linearized ideal fluid theory for the small oscillation of a liquid in a rigid container is well established. The dynamically equivalent mechanical model for the linear oscillation of the liquid is also well studied. One of the advantages of introducing an equivalent mechanical model is that the equations of motion for a continuous medium such as liquid can be replaced by the equations of motion for lumped masses and rigid bodies so that they can be used more readily for the overall stability analysis of a spece vehicle or for other purposes. Another reason for using equivalent mechanical models to represent the sloshing behavior of a contained liquid is that the slight damping

normally present in sloshing can be treated by adding linear dashpots to the undamped model system.

When a container partially filled with liquid is excited, the liquid in the bottom of the tank is only slightly disturbed, i.e., it moves like a rigid body, whereas liquid near the free surface oscillates. This means that the sloshing mass corresponding to a vibration mode is performing a motion relative to the container wall. Analogously therefore, the model is composed of a fixed mass in the bottom of the container to represent the essentially rigid or non-sloshing part of the liquid and a movable mass near the top of the container to represent the sloshing part of the liquid. The sum of the fixed and movable masses are taken equal to the total mass of the liquid. According to the theoretical development of liquid sloshing, a complete mechanical analogy for transverse sloshing must include an infinite number of movable masses, one for each of the infinitely many normal sloshing modes. However, it can be shown that the size of each of these movable masses decreases rapidly with increasing mode number. Thus for a practical application, a simple mechanical model is generally acceptable, i.e., to include in the mechanical model only one movable mass, m_1, corresponding to the fundamental mode [25]. (In this case, the assumption has to be made that the sum of the fixed mass, m_o, and the only one movable mass, m_1, equals the total liquid mass, m_T.)

The size of the movable masses and their locations and the other model elements can be determined by comparing results of the analytical mechanical model with those of potential theory for the liquid. A detailed analysis and expressions for model elements, presented in a

tabulated form, for various types of mechanical models, can be found in References [5,27].

Several types of mechanical systems can be used to describe the linear liquid behavior in a rigid container. Examples would include a spring-mass model, a simple-pendulum model, a torsional-pendulum model, a torsional-spring-mass model, and a compound-double-pendulum model. However, the kind of movable mass to be used and its restraints depend on the type of excitation encountered. For example, a spring-mass or simple-pendulum model is widely used for translational and pitching excitations. For roll excitation, either a torsional-pendulum or torsional-spring-mass model could be used.

For the present application, a simple mechanical model using a spring-mass model without dashpot (undamped system, see Figure 11) will serve our purpose.

For the investigation of the coupled dynamic system which follows in the next section, the following information is presented from Reference [5], which is a summary of the results obtained by various investigators.

Circular Cylindrical Tank

$$\left.\begin{aligned} &\text{Natural Frequency:} && \omega_1^2 = \frac{g}{a}\,\epsilon_1 \tanh\left(\frac{\epsilon_1 h}{a}\right) \\ &\text{Slosh Mass:} && m_1 = \frac{2\tanh\left(\epsilon_1 \frac{h}{a}\right)}{\epsilon_1 \frac{h}{a}\left(\epsilon_1^2 - 1\right)} m_T \\ &\text{Non-Slosh Mass:} && m_0 = m_T - m_1 \end{aligned}\right\} \quad \text{(VI-1)}$$

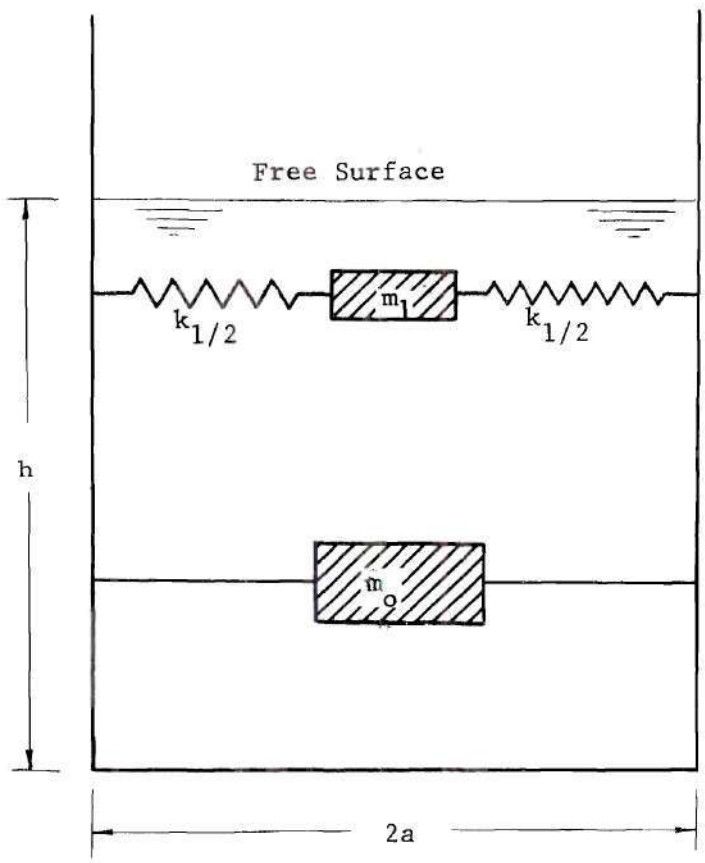

Figure 11. Spring-Mass Analogy for Simple Mechanical Model

where $\epsilon_1 = 1.84$; the first root of $J_1'(\epsilon_n) = 0$.

Rectangular Tank

$$\left.\begin{aligned} &\text{Natural Frequency:} && \omega_1^2 = \frac{\pi g}{c}\tanh\left(\frac{\pi h}{c}\right) \\ &\text{Slosh Mass:} && m_1 = \frac{8\tanh\left(\frac{\pi h}{c}\right)}{\frac{\pi^3 h}{c}} m_T \\ &\text{Non-Slosh Mass:} && m_0 = m_T - m_1 \end{aligned}\right\} \quad \text{(VI-2)}$$

where c = the length of the tank (parallel to the direction of excitation).

Mathematical Model for the Liquid Acting as a Vibration Absorber

One of the methods of reducing the effect of a resonance condition is the use of a dynamic vibration absorber. The principle of the dynamic vibration absorber was discovered by Frahm in 1909. The principle can be explained as follows:

Suppose we have an absorber with mass, m, and spring constant, k_2, attached to a main spring-mass system, k_1,M, with an external harmonic excitation applied on the main system. If the natural frequency, k_2/m, of the attached absorber is tuned to be equal to the frequency, ω, of the external excitation, then it can be shown that the main mass, M, does not vibrate at all. In this case, the absorber, k_2,m, vibrates in such a fashion that its spring force is at all instants equal and opposite to the external excitation force. Thus there is no net force acting

on the main system and therefore the mass, M, does not move at all.

The detailed analysis of this principle can be found from any standard vibration text book or can be illustrated by the present model to be discussed next.

A mathematical model which described the actual experimental arrangements (see Figure 14) is shown in Figure 12.

We note that the absorber considered here is the liquid in a rigid container filled to a characteristic depth H_{ch} where the absorber mass is the slosh mass of the liquid. Figure 12a shows the main system having spring constant, k_1, pendulum length, ℓ, and mass, M, which includes the non-slosh mass, mass of container, and mass of the supporting plate.

The equation of motion for the main system (Fig. 12a) is

$$M\ell^2\ddot{\bar{\theta}} + Mg\ell \sin\bar{\theta} + k_1\ell^2 \sin\bar{\theta} + k_e(\ell \sin\bar{\theta} - \epsilon \cos\omega t)\ell = 0$$

For small oscillation, $\sin\theta \simeq \theta$, thus we obtain

$$\ddot{\bar{\theta}} + \left(\frac{g}{\ell} + \frac{k_1 + k_e}{M}\right)\bar{\theta} = \frac{k_e \epsilon}{M\ell}\cos\omega t$$

or

$$\ddot{\bar{\theta}} + \Omega_n^2\,\bar{\theta} = \frac{k_e \epsilon}{M\ell}\cos\omega t \qquad \text{(VI-3)}$$

where $\Omega_n^2 = \frac{g}{\ell} + \frac{k_1 + k_e}{M}$ is the natural frequency of the main system.

The equations of motion for the coupled system (Fig. 12b) are obtained and simplified by considering small vibrations. They are

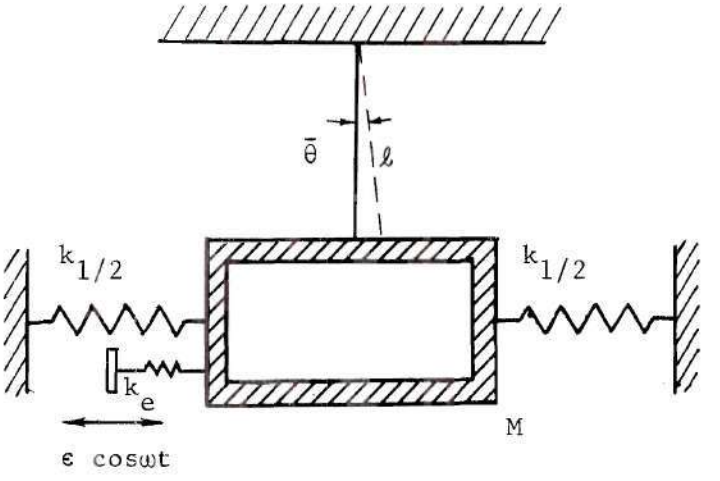

(a) Spring Mass Analogy - Main System Including Non-Sloshing Fluid Mass.

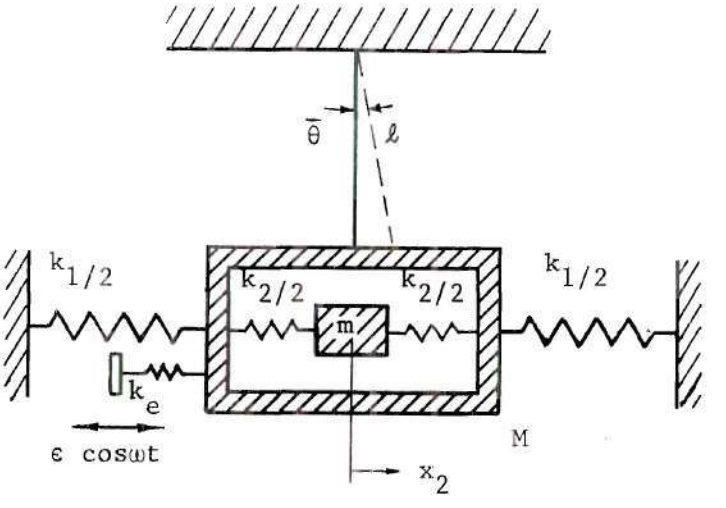

(b) Spring Mass Analogy - Main System Plus Vibration Absorber as Represented by Sloshing Fluid Mass.

Figure 12. Mechanical Model for Fluid as Vibration Absorber

$$\ddot{\bar{\theta}} + \Omega_n^2 \bar{\theta} + \frac{k_2}{M} \bar{\theta} - \frac{k_2}{Ml} x_2 = \frac{k_e \epsilon}{Ml} \cos \omega t \qquad \text{(IV-4)}$$

$$\ddot{x}_2 + \omega_a^2 x_2 - \omega_a^2 l \bar{\theta} = 0$$

where $\omega_a^2 = \frac{k_2}{m}$ and x_2 is the displacement of this absorber mass in the inertial system.

Assume a solution of the form

$$\bar{\theta} = \bar{\Theta} \cos \omega t$$

$$x_2 = X_2 \cos \omega t$$

which yields the expressions for amplitudes

$$\bar{\Theta} = \frac{\left(1 - \frac{\omega^2}{\omega_a^2}\right) \frac{k_e \epsilon}{M l \Omega_n^2}}{\left(1 + \mu \frac{\omega_a^2}{\Omega_n^2} - \frac{\omega^2}{\Omega_n^2}\right)\left(1 - \frac{\omega^2}{\omega_a^2}\right) - \frac{\omega_a^2 \mu}{\Omega_n^2}} \qquad \text{(VI-5)}$$

$$X_2 = \frac{\frac{k_e \epsilon}{M \Omega_n^2}}{\left(1 + \mu \frac{\omega_a^2}{\Omega_n^2} - \frac{\omega^2}{\Omega_n^2}\right)\left(1 - \frac{\omega^2}{\omega_a^2}\right) - \frac{\omega_a^2 \mu}{\Omega_n^2}} \qquad \text{(VI-6)}$$

where

where

$$\mu = \frac{m}{M}$$

From Eq. (VI-5), it is clear that, if $\omega = \omega_a$, i.e., the natural frequency of the absorber is chosen to be equal to the frequency of the external excitation, then the response amplitude of the main system θ is identically equal to zero, and the response amplitude of the absorber (i.e., the liquid) is finite as can be seen from Eq. (VI-6). That is, for $\omega = \omega_a$,

$$X_2 = \frac{k_e \epsilon}{-m\omega_a^2}$$

or

$$-m\omega_a^2 X_2 = k_e \epsilon \qquad \text{(VI-7)}$$

where the term on the right is the amplitude of the excitation force, and the term on the left is the absorber harmonic response representing the amplitude of slosh force. The negative sign on the left hand side means that the slosh force is exactly 180° out of phase with respect to the external excitation force. These imply that the sloshing liquid is acting as an undamped dynamic vibration absorber. The experiments to be discussed in the next chapter show that indeed the liquid system can be developed as a device for vibration reduction.

CHAPTER VII

THE EXPERIMENTS

Experimental Apparatus and Procedure

A photograph of the experimental apparatus used in the present investigation is shown in Fig. 13. The arrangement of the equipment is given in the diagram shown in Fig. 14. Two categories of experiments were conducted using the same apparatus with slight modifications. These two categories were: (1) tests of characteristic depth, and (2) tests of the liquid system as a vibration absorber. In the first category three types of containers were tested; namely, (i) a 12 inch long semicircular tank having a diameter of 7.78 inches, (ii) a 12 inch long annular semicircular tank having a radius ratio of $k = \frac{b}{a} = 0.306$ with a = 3.89 inches, and (iii) a rectangular tank of length 11.47 inches, width 7.7 inches, and height 6 inches. In the second category, tests were carried out using the same rectangular tank as in the first category, and in addition, a 12 inch long double-semicircular tank was used (actually a circular cylindrical tank with a vertical splitter plate parallel to the direction of excitation, diameter = 7.78 inches, so as to double the absorber mass and, at the same time, to suppress the liquid swirl motion which would appear in an uncompartmented circular cylindrical tank). All tanks were made of transparent acrylic plastic. Tank walls and bottoms had a thickness of one-fourth inch to ensure that these containers were essentially rigid in the operating frequency

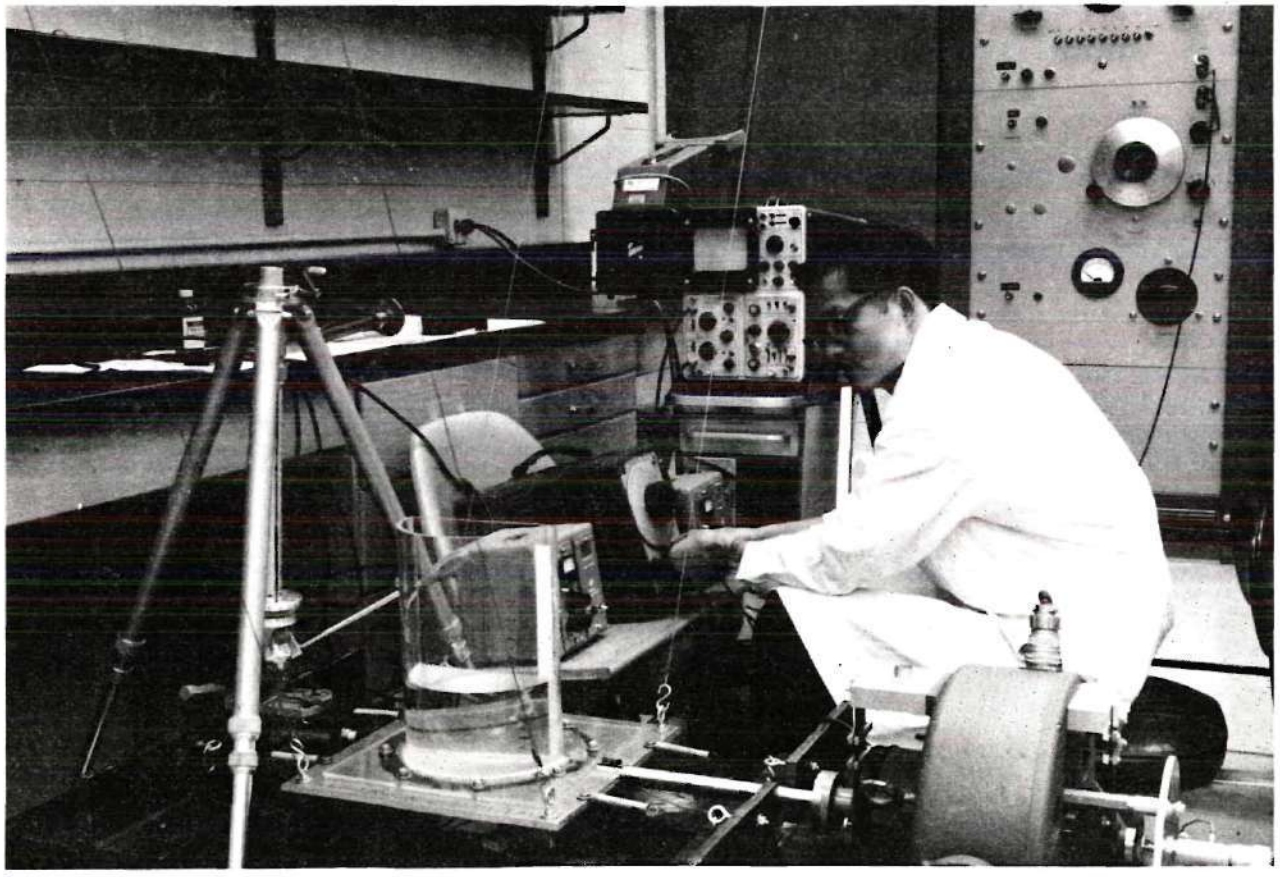

Figure 13. Experimental Apparatus

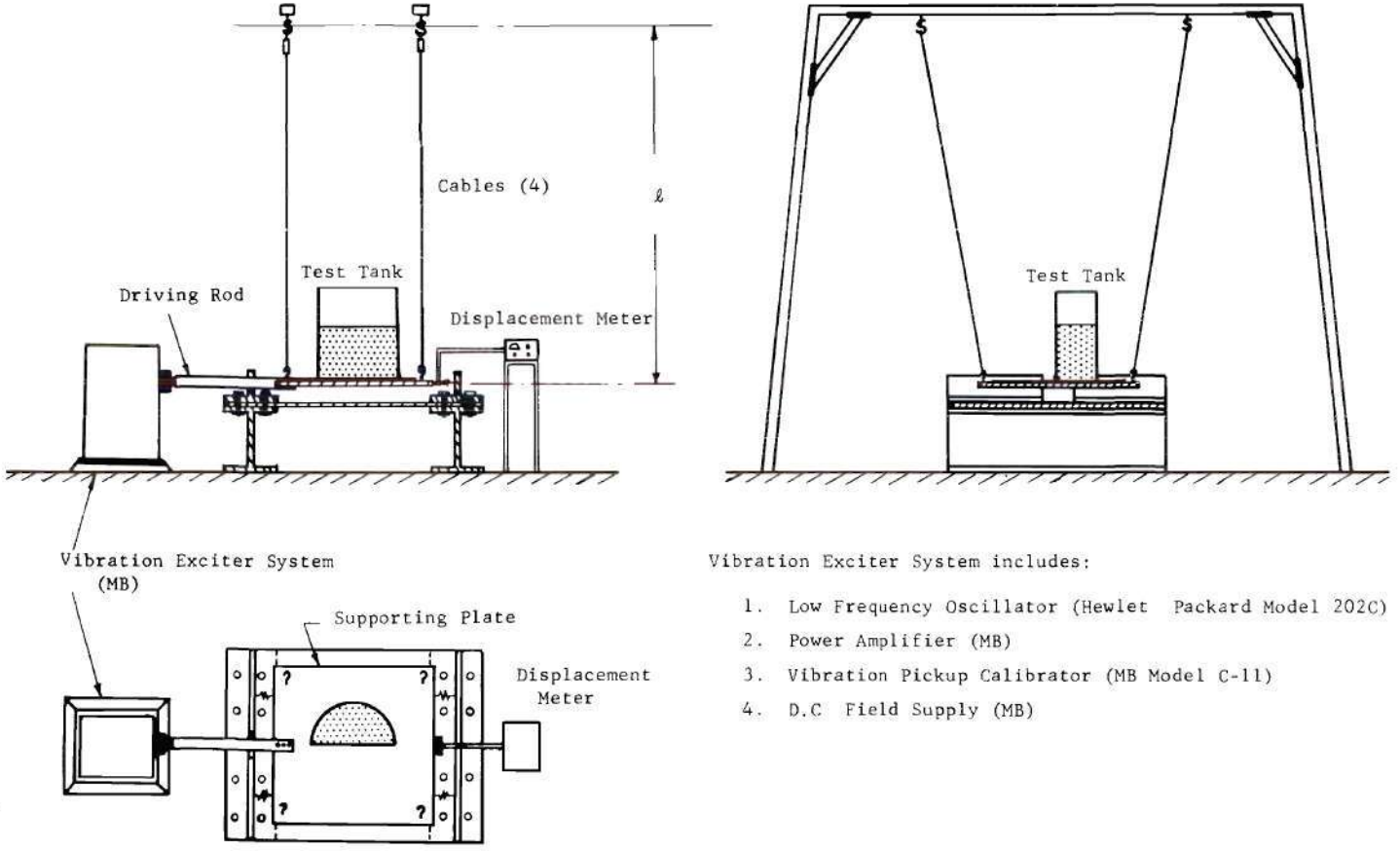

Figure 14. Diagrams of Experimental Apparatus

range of one to five cps.

As shown by Fig. 13, the apparatus consists of (a) an overhead frame with four cables to support an aluminum plate that carries the components of the system, (b) an electrodynamic vibration exciter system, (c) an instrumentation system, (d) a base frame used to attach four springs to the supporting plate when the apparatus was used for vibration absorber tests.

The length of the cables is adjustable and a level was used to check the horizontal position of the supporting plate before each test was started. The container was mounted on the supporting plate by bolts and nuts.

A 50 lb force output electrodynamic vibration exciter (MB Model C-11) was employed to provide a harmonic excitation. The original oscillator was replaced by an external low frequency oscillator (Hewlett-Packard Model 202C) in order to obtain a good control of the excitation frequency in the operating range of one to five cps. A proximity capacitance transducer (PT-5) was mounted at the bottom part of the shaker to form a capacitor with the end of the shaker armature. The variation of the capacitance due to the change in distance between the transducer probe and the end of the shaker armature creates a signal which was then fed into a dynagage (PS 605) and was displayed on the oscilloscope. In this way, a constant displacement input could be monitored. Another proximity capacitance transducer was employed to detect the displacement response of the supporting plate (the main system) when the tests of the liquid system as a vibration absorber were conducted.

A one inch diameter steel rod having a length of 12 inches was used as a driving rod for all the resonance tests. In preliminary tests of the absorber system, the same rod was used to drive the main system; however, the results were not desirable due to the fact that a complicated magnetic field was generated between the shaker armature and the field coil of the shaker such that the cancellation of the excitation force was not very effective when the vibration absorber was in action. Later a spring isolator coupling (see Fig. 15) was designed and inserted between the driving rod and the shaker armature. By this manner, the absorber action could be detected very clearly.

The liquid used in the experiments was tap water at room temperature (75-80°F). A tape with scale was fastened on the wall of each test tank at the location where maximum amplitude occurred. Then the maximum displacement of the free surface (double amplitude, i.e., the peak-to-peak amplitude) was measured visually. A scale of 0.05 inch could be read. A small amount of Webster Photocolors (No. 1A, green or orange) was added to improve readings.

The test procedure consisted of monitoring a constant displacement amplitude input excitation as frequency increased, then decreased, and measuring the maximum liquid responses directly from the tank wall. The procedure was repeated for different excitation amplitudes for a fixed liquid height. From the resulting response curves a backbone curve could be drawn that represented the liquid response at that liquid height. Various liquid heights were chosen for the experiments depending upon the liquid behavior in a container. By inspection of the backbone curves corresponding to various liquid heights, a characteristic

Figure 15. Components of Spring Isolator Coupling for Absorber Experiments

depth H_{ch} (vertical backbone curve) could be determined so as to assure a linear response.

After the characteristic depths had been determined for the semicircular tank and the rectangular tank, each tank was filled with liquid (water) to its individual characteristic depth and vibration absorber tests were conducted, measuring the displacement of the main system and that of the absorber.

Experimental Results

Tests of Characteristic Depth

Tank configurations investigated in this program were a semicircular tank, an annular semicircular tank, and a rectangular tank. The basic objective of the experiments was to determine experimentally the characteristic depth(s) for each container. These values were then compared with the theoretically predicted data. The results obtained for each container are described in the following. The amplitudes shown on the graphs are one half of the measured peak-to-peak values.

Semicircular Tank. The experimental response curves for various liquid heights in this container for several different excitation amplitudes are shown in Fig. 16. The resulting backbone curve shows the characteristics of the liquid motion at a particular depth. For $\frac{h}{a} = 0.3$, a nonlinear hardening effect is demonstrated. As liquid height increases, the liquid system exhibits less hardening effect and tends toward a nonlinear softening effect. No truly vertical backbone curve could be found in the experiments performed for this container to represent a perfectly linear response. The characteristic depth H_{ch}/a for this tank geometry was approximated by $H_{ch}/a = \frac{h}{a} = 0.52$, which is in good agreement

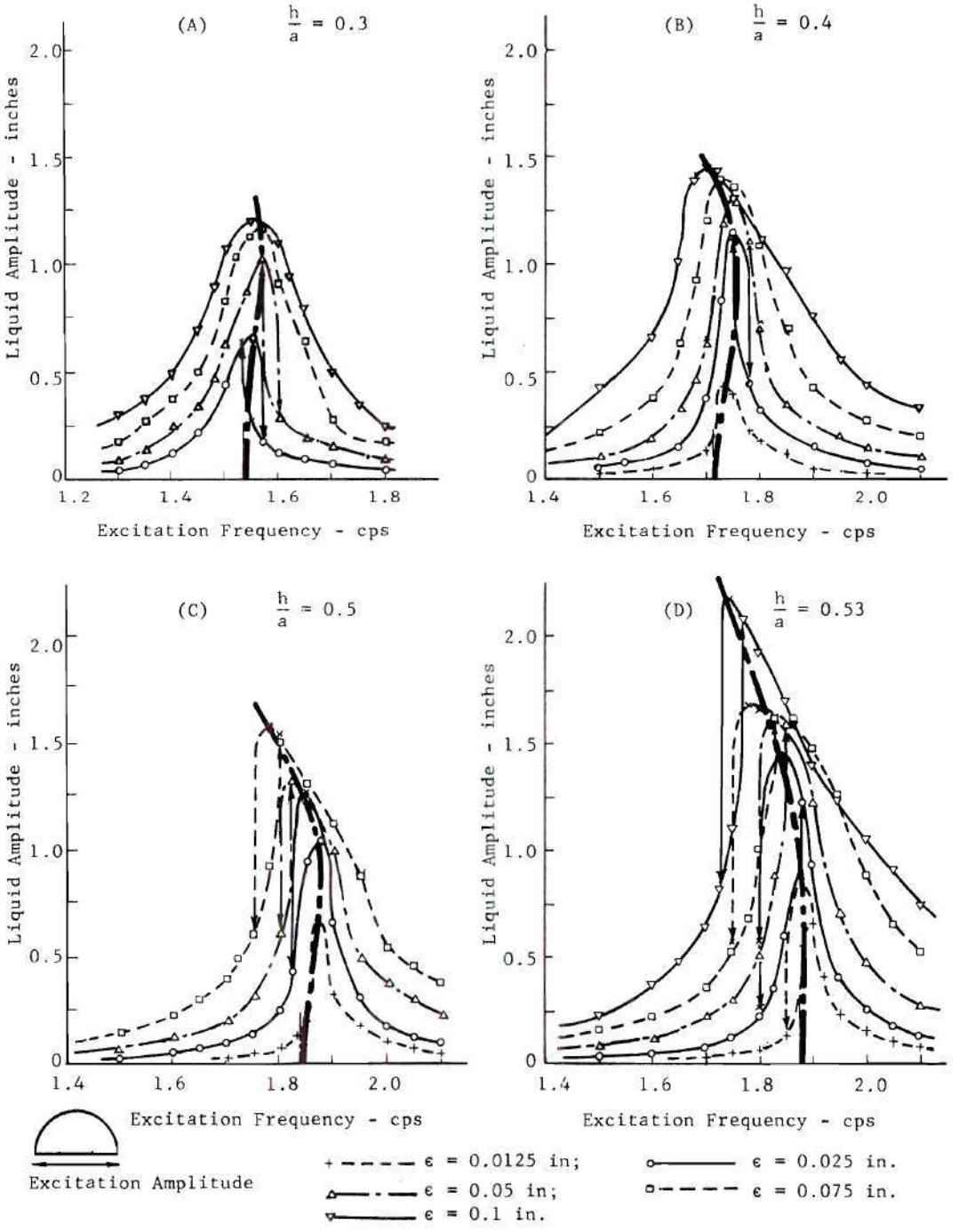

Figure 16. Semicircular Tank (a = 3.89 in.): Experimental Liquid Response for the First Antisymmetric Mode

with the theoretically calculated value $H_{ch}/a = 0.56$.

In Fig. 16 we observe in general that the liquid system exhibits hardening phenomena at low amplitudes, which tends to shift to softening for large amplitudes. Also, the response curves for larger excitation become wider and in the case of Figs. 16(A) and 16(B), no jump phenomenon was observed. It is suggested that these large amplitude effects are due to damping in the system and the contribution of higher order modes.

Annular Semicircular Tank. Previous theoretical analysis shows that there are two characteristic depths for the annular tank configuration where $k = \frac{b}{a} = 0.3$. In the experiments, a container with $k = 0.306$ was used and results are shown in Figure 17. For $\frac{h}{a} = 0.2$, the liquid acts as a hard spring while for $\frac{h}{a} = 0.38$, it exhibits a softening effect. The linear characteristic depth is approximated by $H_{ch}/a = 0.37$. It is interesting to note that the experiments showed, for liquid heights at around $\frac{h}{a} = 0.6$, a "sudden reversal" phenomenon (from a nonlinear softening effect to a nonlinear hardening effect without passing through the characteristic) as predicted by the present theoretical analysis (Chapter V). In fact, in the experiments, this phenomenon persisted for a liquid height of $\frac{h}{a} = 0.7$ also. The first symmetric mode surface wave at double the excitation frequency became strong and was seen very clearly at these liquid heights. As the liquid height continues to increase, the liquid system becomes less hard, then passes through the second characteristic depth and tends towards softening again. The second characteristic depth is approximated by $H_{ch}/a = 1.1$.

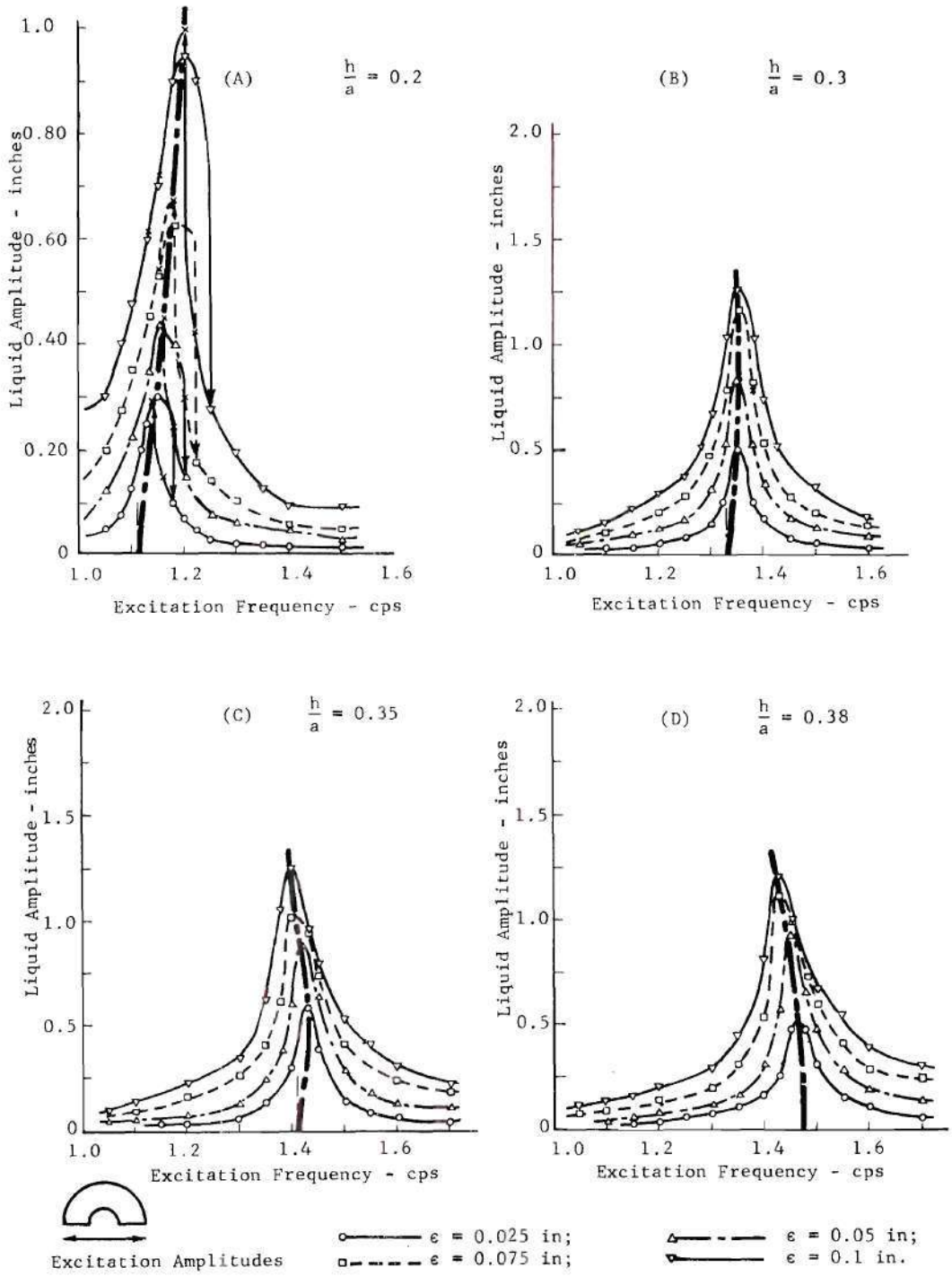

Figure 17a. Annular Semicircular Tank (b = 1.19 in., a = 3.89 in.): Experimental Liquid Response for the First Antisymmetric Mode

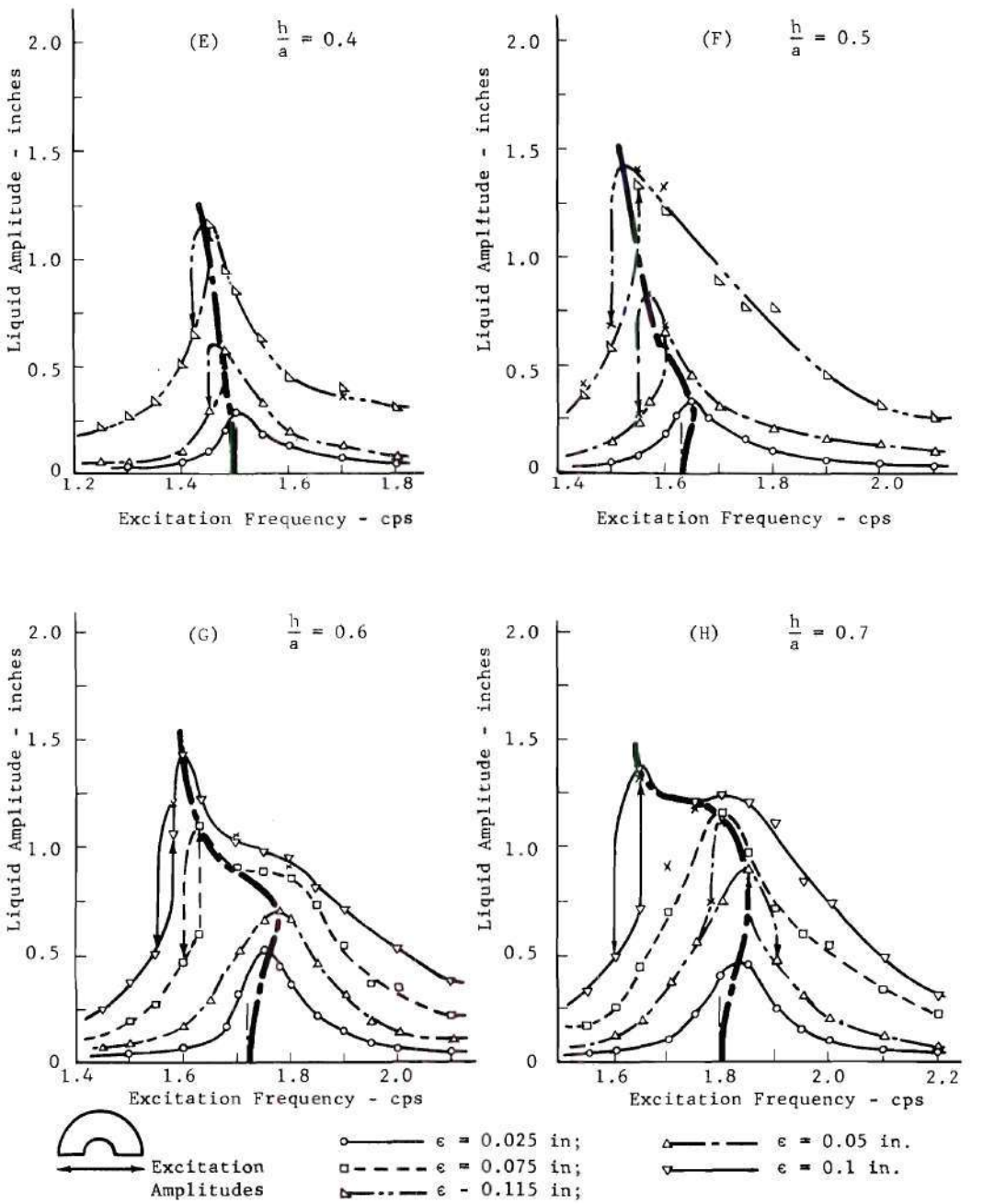

Figure 17b. Annular Semicircular Tank (b = 1.19 in., a = 3.89 in.): Experimental Liquid Response for the First Antisymmetric Mode

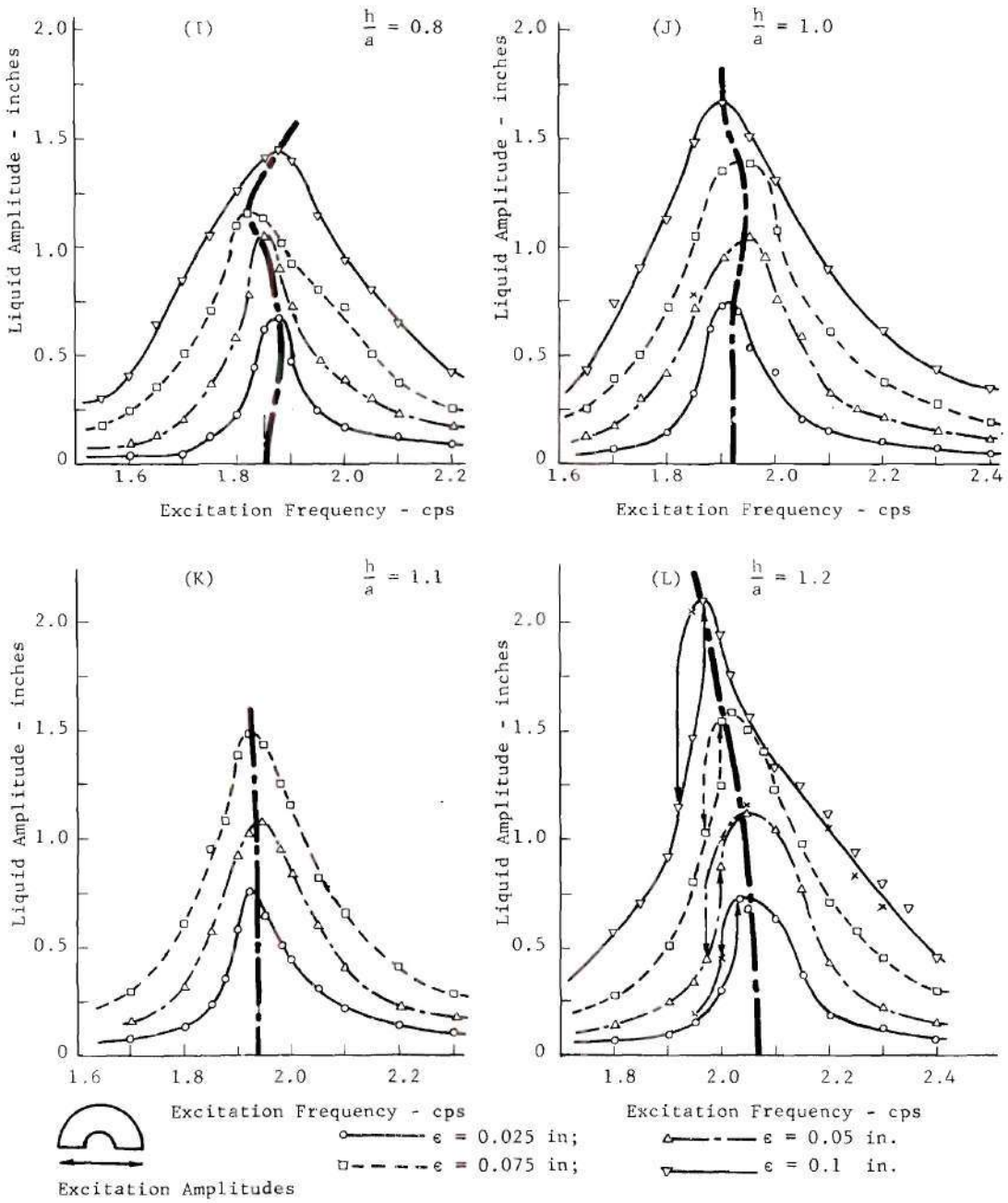

Figure 17c. Annular Semicircular Tank (b = 1.19 in., a = 3.89 in.): Experimental Liquid Response for the First Anticymmetric Mode

Rectangular Tank. Theoretical analysis for the first antisymmetric mode [20] predicted that the characteristic depth for the rectangular tank geometry would be $\frac{h}{c} = 0.204$, where c is the length of the rectangular tank. The experimental results for this tank configuration* are shown in Fig. 18. The characteristic depth is found to be $H_{ch}/c = 0.25$. The backbone curve corresponding to this liquid height is nearly vertical. This indicates that the liquid system behaves nicely as a linear spring-mass system and should act as a good vibration absorber (to be tested in the next section). For $\frac{h}{c} < 0.25$, the liquid exhibits nonlinear hardening characteristics while for $\frac{h}{c} > 0.25$, it acts as a nonlinear soft spring.

Test of Liquid System as a Vibration Absorber

Two containers were used to investigate the vibration absorber of the liquid; a double-semicircular tank and a rectangular tank. From previous tests it was found that the characteristic depth for a rectangular tank was $H_{ch}/c = 0.25$ and that for a semicircular tank, $H_{ch}/a = 0.52$; a double-semicircular tank instead of a single semicircular container was used to increase the absorber liquid mass for more effective absorber action. Experiments were then carried out based on these characteristics depths. Results were as follows.

Double-Semicircular Tank. The following data apply:

$k_1 = 3.2$ lb/in. ; $\Omega_n = \omega_a = 11.7$ rad/sec (1.86 cps)

---

*A rectangular tank with finite width (7.7 in.) was used for the experiment while in Reference [20] the analysis was based on a rectangular tank of infinite width.

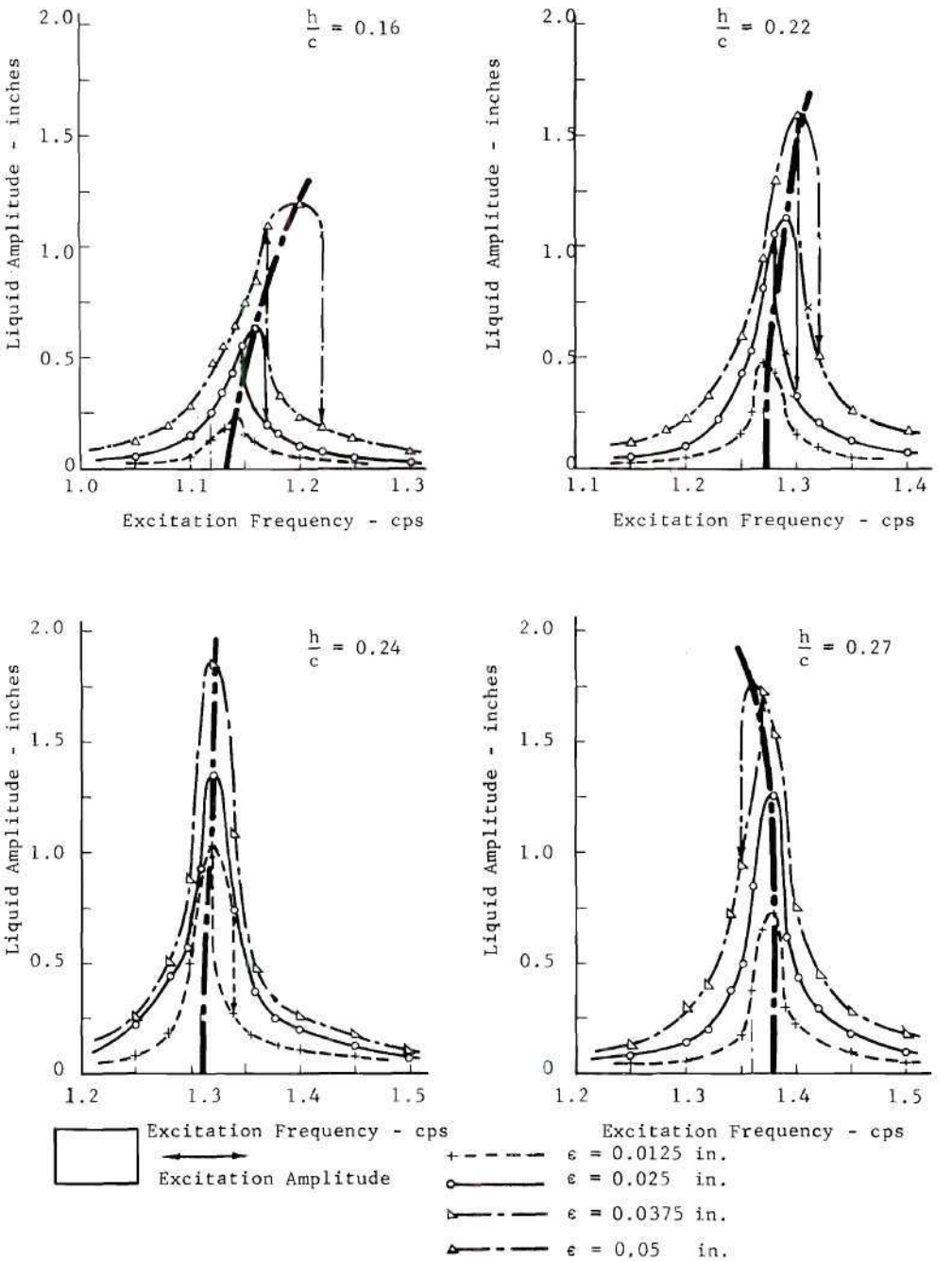

Figure 18a. Rectangular Tank (L = 11.47 in., W = 7.7 in., H = 6 in.): Experimental Liquid Response for the First Antisymmetric Mode

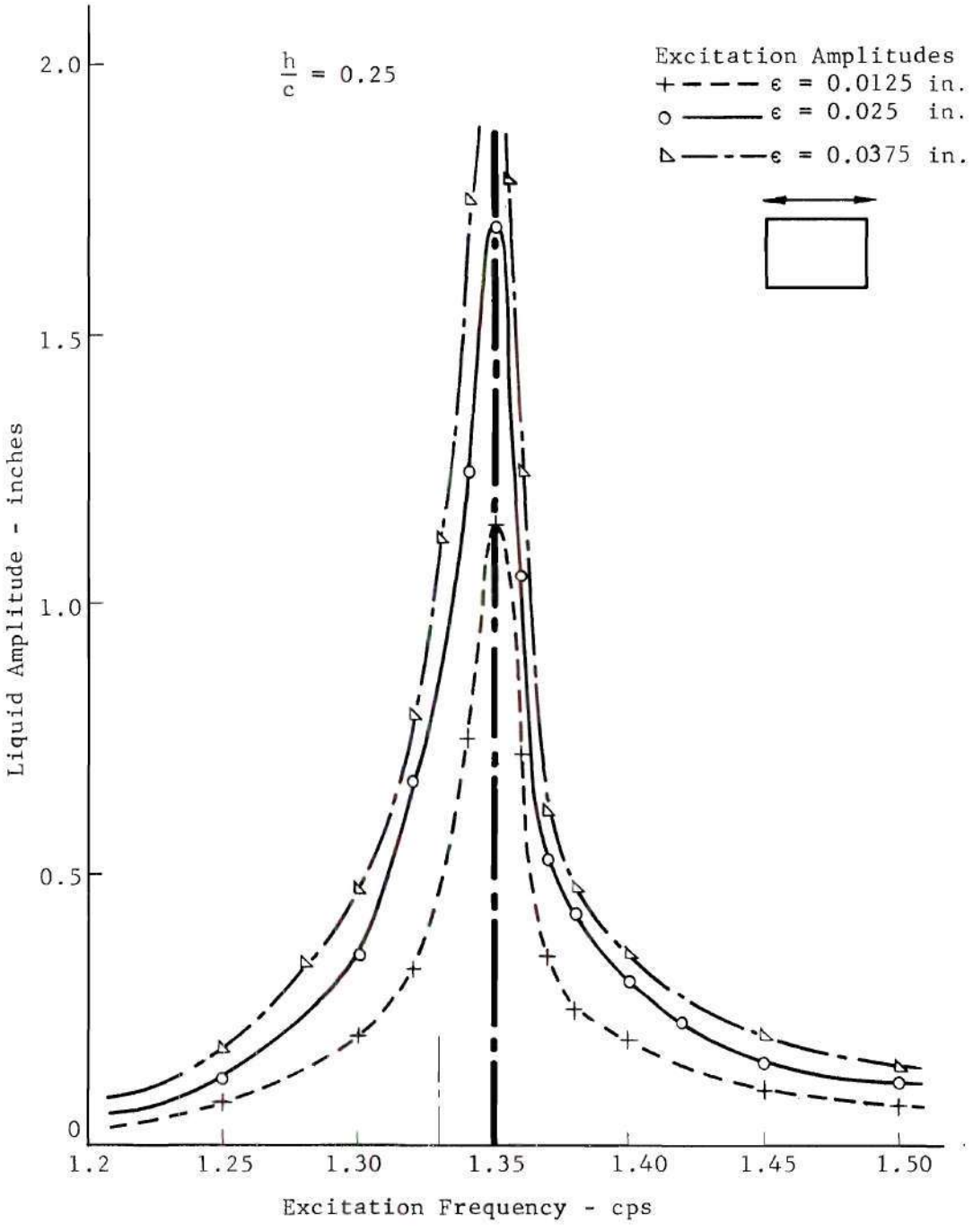

Figure 18b. Rectangular Tank (L = 11.47 in., W = 7.7 in., H = 6 in.): Experimental Liquid Response for the First Antisymmetric Mode

$$k_e = 8 \quad \text{lb/in} \quad ; \quad H_{ch}/a = \frac{h}{a} = 0.52$$

$$\ell = 6 \quad \text{ft} \quad ; \quad M = \frac{k_1 + k_e}{\Omega_n^2 - \frac{g}{\ell}}$$

$$\mu = \frac{m}{M} = \frac{2.31}{32.8} = 0.07.$$

The response of the platform to harmonic excitation near resonance is shown in Fig. 19, while response of the coupled platform-fluid system is presented in Fig. 20. From Fig. 20(a) it is clear that the liquid oscillating at the first antisymmetric mode dramatically reduces vibration of the platform, although it should be noted that a very small residual amplitude (4×10^{-3} inches) remains. This deviation of experimental results from the zero amplitude of theoretical predictions is not surprising since tests of the characteristic depth had shown that liquid at this height in this container did not have a completely linear response. Other factors which attribute to the difference between experimental results and theory might be the small mass ratio μ, the actual damping effect of the liquid, and friction in the spring coupling to the exciter.

Rectangular Tank. In this case:

$$k_1 = 3.2 \text{ lb/in.} \quad ; \quad \Omega_n = \omega_a = 8.48 \text{ rad/sec (1.35 cps)}$$

$$k_e = 2.6 \text{ lb/in.} \quad ; \quad H_{ch}/c = \frac{h}{c} = 0.25$$

$$\ell = 6 \quad \text{ft} \quad ; \quad M = \frac{k_1 + k_e}{\Omega_n^2 - \frac{g}{\ell}}$$

$$\mu = \frac{m}{M} = \frac{6.475}{34.04} = 0.19.$$

Experimental responses of the platform alone and those of the coupled platform-fluid system are shown in Figures 21 and 22, respectively.

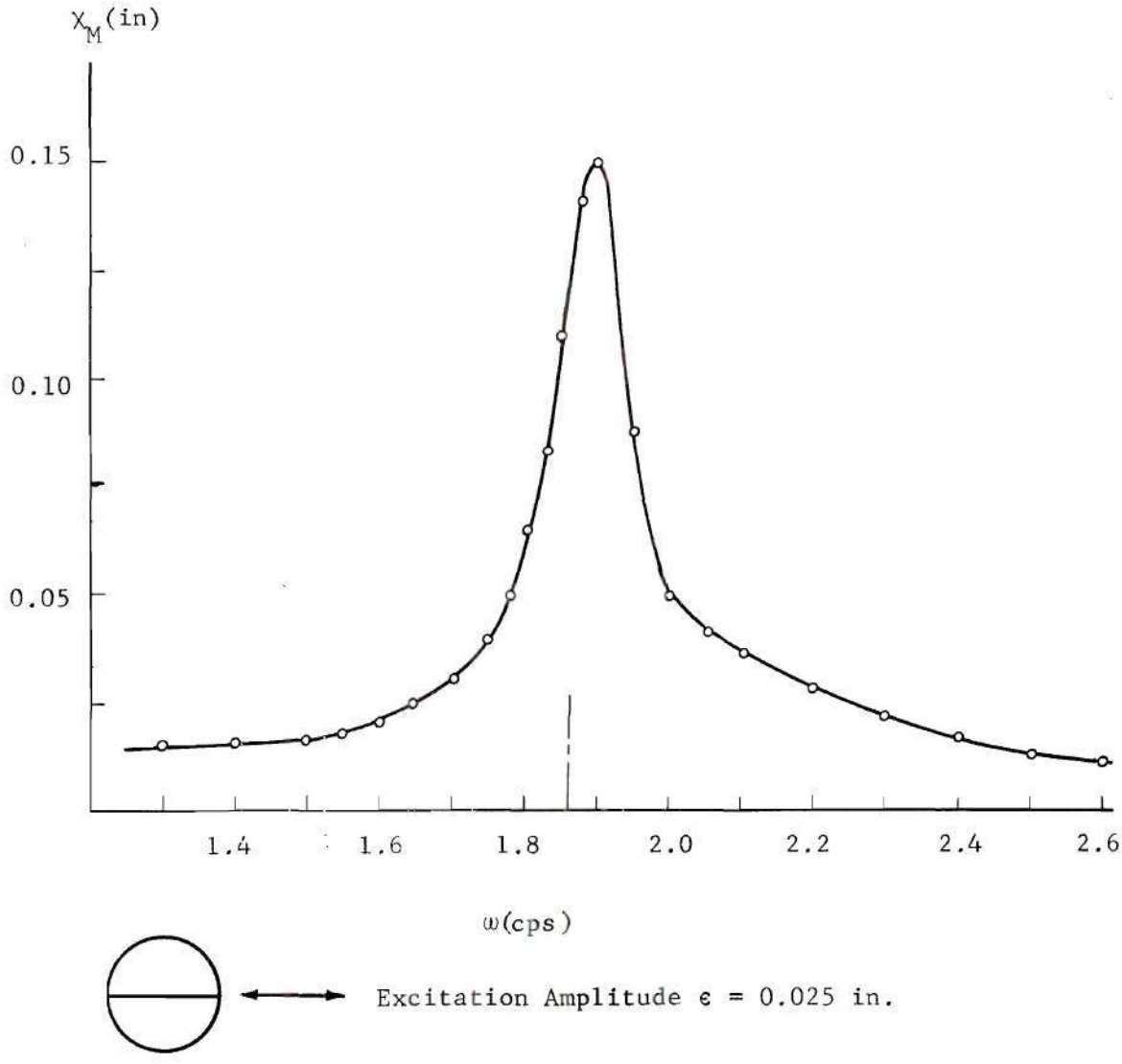

Figure 19. Double-Semicircular Tank (a = 3.89 in.): Amplitude vs. Frequency of Main System Including Non-sloshing Fluid Mass by Weights

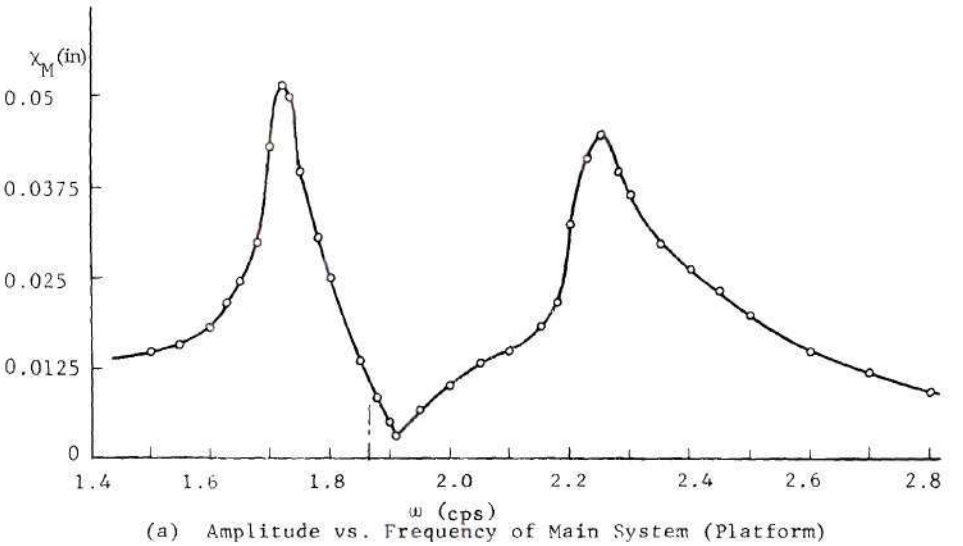

(a) Amplitude vs. Frequency of Main System (Platform)

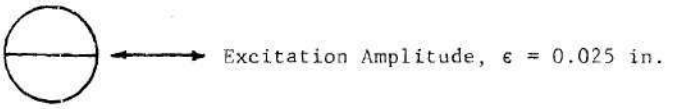

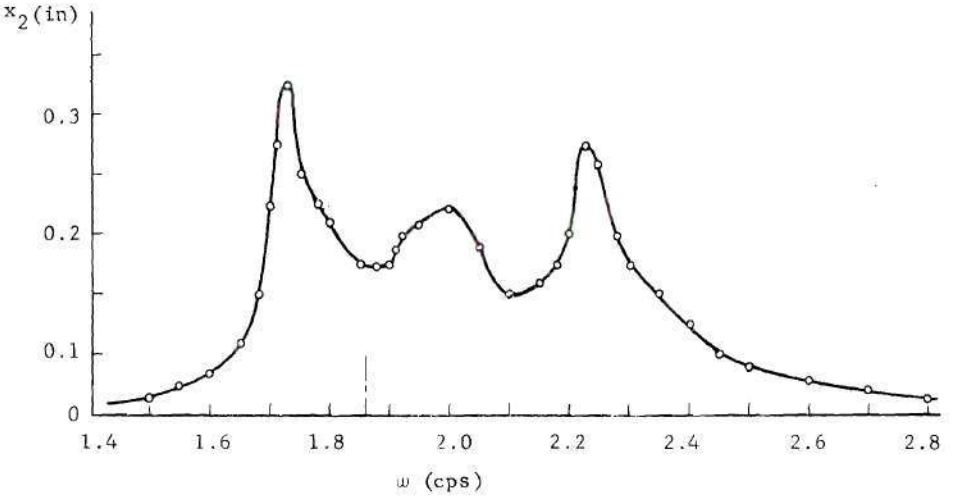

(b) Amplitude vs. Frequency of Liquid (absorber)

Figure 20. Double-Semicircular Tank (a = 3.89 in.): Amplitude vs. Frequency of the Coupled System

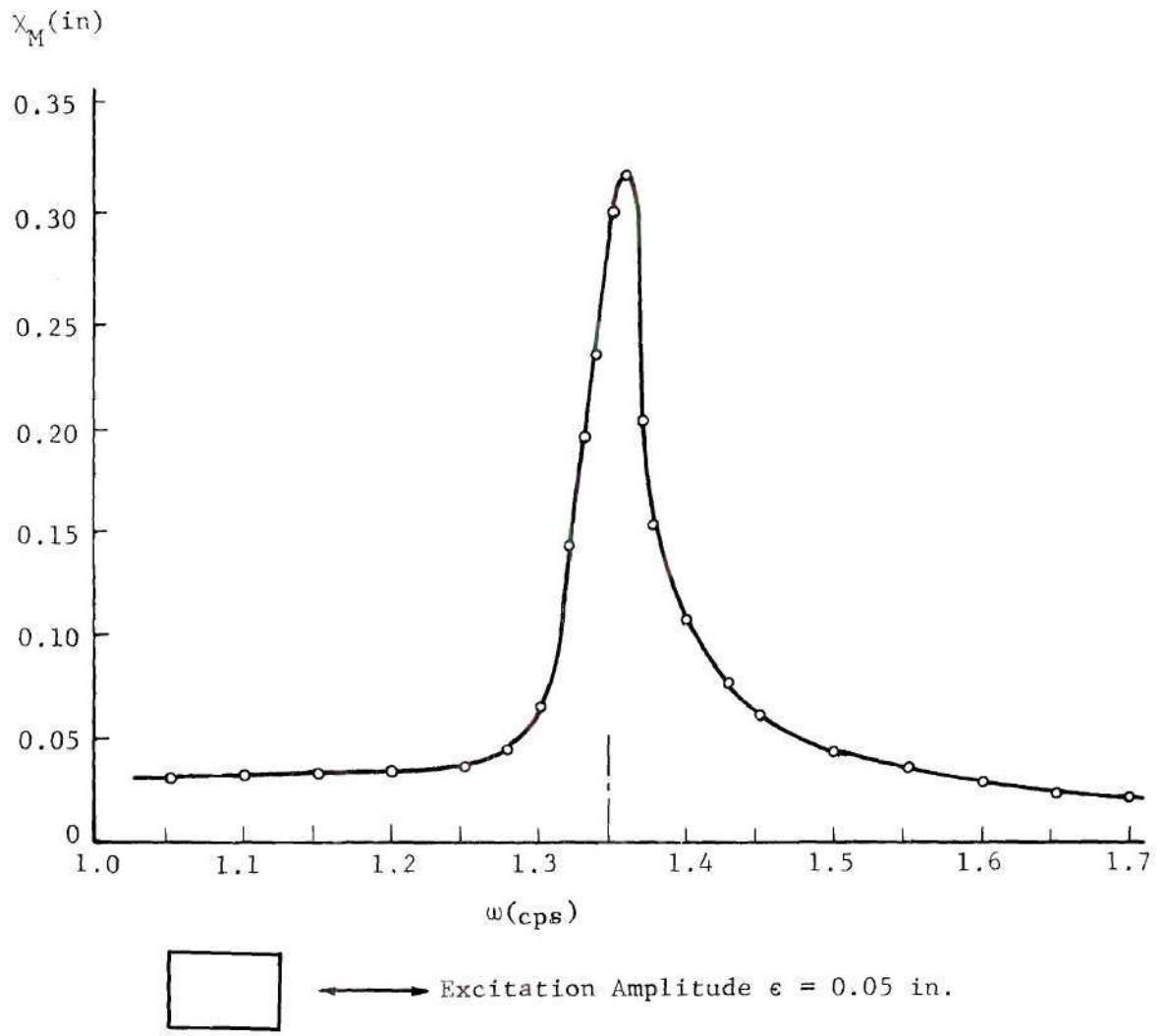

Figure 21. Rectangular Tank (L = 11.47 in., W = 7.7 in., H = 6 in.): Amplitude vs. Frequency of Main System Including Non-sloshing Fluid Mass by Weights

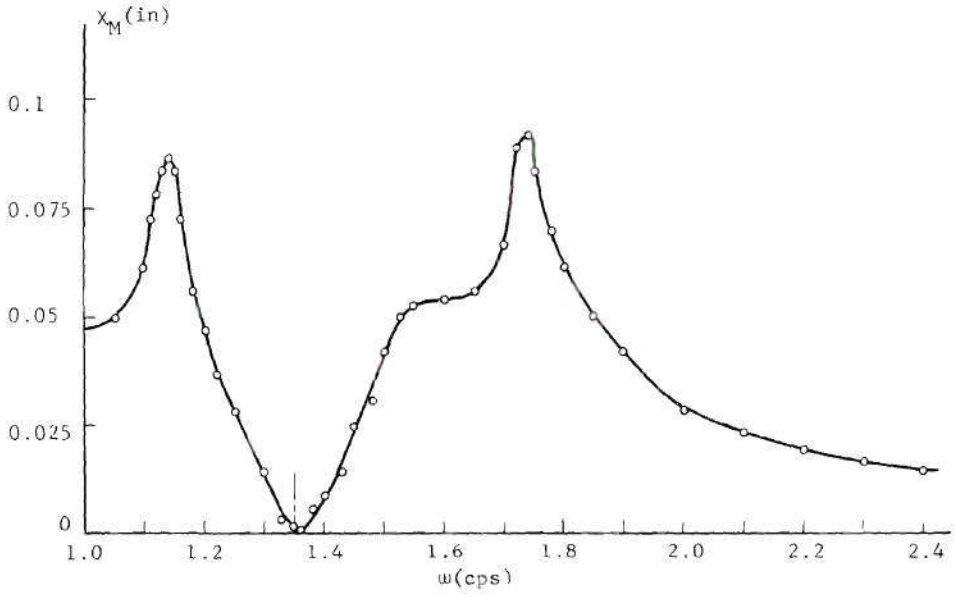

(a) Amplitude vs. Frequency of Main System (platform).

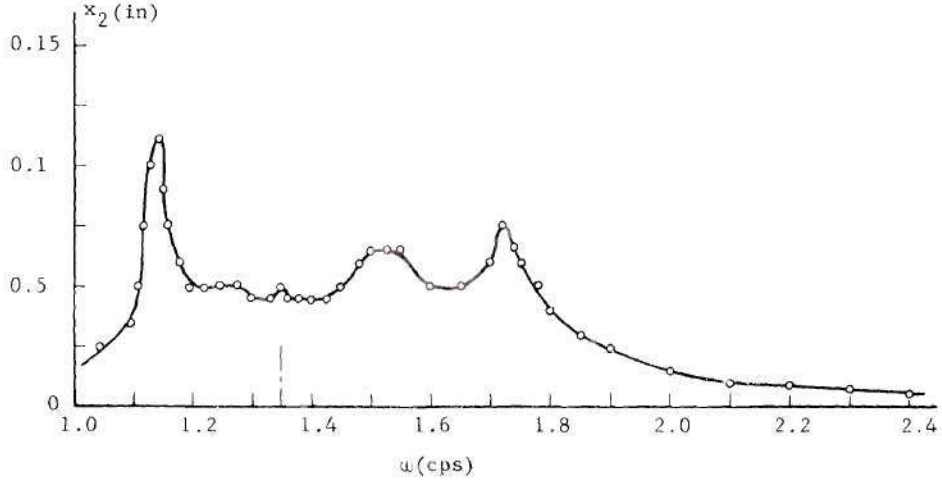

(b) Amplitude vs. Frequency of Liquid (absorber).

Figure 22. Rectangular Tank (L = 11.47 in., W = 7.7 in., H = 6 in.): Amplitude vs. Frequency of the Coupled System

Excellent vibration absorber action was obtained for this case as demonstrated in Fig. 22(a), where the displacement of the platform is essentially zero at the natural frequency of the liquid (absorber) as expected. In fact, this could be anticipated by observing the results of resonance tests where a nearly vertical backbone curve was obtained, indicating that liquid at this characteristic depth in a rectangular tank would behave as an essentially linear spring-mass system. Furthermore, the large mass ratio μ for this case ($\mu = 0.19$) contributed to the success of this test.

CHAPTER VIII

CONCLUSION

Both theoretical and experimental investigations have been made of a liquid oscillating in a rigid container. In the theoretical analysis, the nonlinear behavior of the liquid in a cylindrical tank of annular sectored cross section subjected to a lateral excitation has been studied. The tank configuration is very general; it can be re-generated to various annular or various sector containers. The analysis is carried out for a first-antisymmetric-mode standing wave; however, the same procedure may also be applied to any other mode of interest.

Nonlinear effects were accounted for by coupling free surface waves between the predominant mode (lowest antisymmetric mode) and secondary modes (first symmetric mode and first cos 2θ-mode) based on a third order theory. Thus the problem is simplified and is less complicated than that of other methods, e.g., the perturbation method or the Krylov-Bogoliubov method.

The analysis has been performed for both free and forced oscillations of the liquid. The procedures of the analysis can be outlined as follows:

(1) Formulate equation of motion and boundary conditions.

(2) Approximate the nonlinear free surface conditions.

(3) Find the eigenvalues and eigenvunctions for the problem.

(4) Introduce permissible assumptions based upon the order of magnitude considerations. A third order solution is considered.

(5) Employ the Boundary Galerkin Method to reduce nonlinear partial differential equations to nonlinear ordinary differential equations.

(6) Solve the nonlinear vibration problem described by a set of second order ordinary differential equations.

(7) Obtain the relationship between natural frequency and liquid amplitude (free oscillation).

(8) Calculate the free surface elevation, pressure distributions, liquid forces and moments exerting onto the container due to the liquid oscillation caused by a lateral harmonic excitation (forced oscillation).

(9) Apply the concept of a characteristic depth obtained from the free oscillation analysis with the principle of a dynamic vibration absorber to investigate the coupling of liquid systems with other dynamic systems.

The nonlinear vibration problem described by a set of second order ordinary differential equations in step (6) is solved by applying the Ritz Averaging Method. Thus the solution is applicable for both resonant and non-resonant cases. It is found that the character of the nonlinear behavior of the liquid is described by a generalized Duffing-type equation.

Numerical examples are carried out for both free and forced oscillations and are compared with available theoretical and experimental data. The relationship between natural frequency and liquid amplitude

for nonlinear oscillation, which yields the well-known "backbone curve," is determined theoretically for the first antisymmetric mode. For a given tank configuration, backbone curves are obtained for various liquid depths. From these, a characteristic depth, H_{ch}, is found for each of the several tanks studied such that at that depth the liquid would exhibit linear vibration characteristics. For a liquid height $h \neq H_{ch}$, the liquid system would behave as either a nonlinear soft spring or as a nonlinear hard spring. Results of this theoretical analysis are then compared with experimentally obtained values.

The characteristic depth for a semicircular tank calculated by the present analysis is found to be $H_{ch}/a = 0.56$, which is in good agreement with the result ($H_{ch}/a = 0.5$) obtained by DiMaggio and Rehm using the perturbation method. The experiments show that $H_{ch}/a = 0.52$. The characteristic depth for a quarter sector tank is found to be $H_{ch}/a = 0.27$, which agrees very well with the result ($H_{ch}/a = 0.29$) obtained by Baird using the Krylov-Bogoliubov method. For a 45° sector tank, $H_{ch}/a = 0.17$ is obtained. No experimental data were available for comparison for the other tank configurations investigated. These results indicate that a sector tank with decreasing apex angle results in a lower characteristic depth; this means that the liquid behaves as a nonlinear soft spring in a wider range of the liquid heights.

For an annular semicircular tank, an interesting result was obtained in which it was found that more than one characteristic depth can exist for certain tank configurations. For example, for an annular semicircular tank with $k = 0.3$, the analysis predicts two characteristic depths: one at $H_{ch}/a = 0.38$, the other at $H_{ch}/a = 1.12$. Experiments

(employing an annular semicircular tank of k = 0.306) confirmed that there were indeed two characteristic depths (H_{ch}), one at $H_{ch}/a = 0.37$, the other at $H_{ch}/a = 1.1$.

Another interesting result obtained from the present analysis was that (for certain tank configurations) there was a sudden reversal of the nonlinear character of the liquid at certain liquid heights without passing through a characteristic depth. This occurred at the liquid height $\frac{h}{a} = 0.6$ for the annular semicircular tank of k = 0.3, and at a height $\frac{h}{a} = 0.154$ for the semicircular tank. The experiments verified that such a "sudden reversal" phenomenon exists for the annular semicircular tank tested (k = 0.306). This phenomenon is demonstrated in Figure 17 for $\frac{h}{a} = 0.6$ and 0.7. It appears to be due to the superharmonic resonance of the first symmetric mode (secondary mode), which has the opposite nonlinear effect to the first antisymmetric mode.

A common characteristic of these results for nonlinear liquid oscillations for various tank geometries was that, up to a certain liquid height, the backbone curve remained almost the same, that is further increase in liquid height had little effect on the nonlinear response as can be seen from Figures 2, 3, 4, and 5.

For forced oscillation, numerical evaluations for liquid response due to harmonic excitation were carried out for a semicircular tank and for the quarter sector tank. Total force response in the x-direction for a semicircular tank was compared with experimental results obtained by Abramson, et al. [14]. Good agreement was obtained by including the higher harmonic components of response in the theory. The importance of including the triple harmonic component for forced response in the

x-direction is clearly shown in Figures 6 and 7. Forced responses for a quarter sector tank were similar in form to those of the semicircular tank and are given in Fig. 10.

In the experiments for the determination of characteristic depth, a rectangular tank was also studied. These results are shown in Fig. 18. The characteristic depth is found to be $\frac{h}{c} = 0.25$, where c is the length of the tank parallel to the direction of excitation.

The concept of a characteristic depth is then applied to investigate theoretically and experimentally the application of liquid lateral response as a tuned dynamic vibration absorber. It was shown theoretically in Chapter VI that the sloshing liquid with height at a characteristic depth in a rigid container should act as an undamped dynamic vibration absorber. The experiments confirmed that the liquid oscillating at the first antisymmetric mode did reduce the vibration of the main system in the manner of a vibration absorber, although not perfect amplitude reduction was obtained for the double-semicircular tank. However, excellent vibration absorber action was noted for the rectangular tank and this is shown in Fig. 22(a). Here, the displacement of the main system is essentially zero at the natural frequency of the liquid (absorber) as predicted.

Finally, it is said that a picture is worth a thousand words; a motion picture supplementing this dissertation has been taken. The contents of the movies can be summarized as follows:

(1) Present the experimental apparatus and operational procedures.

(2) Demonstrate the liquid nonlinear jump phenomena (resonance tests).

(3) Show that the oscillating liquid system can be developed as a device for vibration reduction.

APPENDIX I

DEFINITION OF VARIOUS CONSTANTS AND SYMBOLS

(A)

Define

$$I\left[rF(r)\right] = \int_b^a r\,F(r)\,dr$$

$$C_0 = C_0(\lambda_{01} r) \quad ; \quad C_{\nu_1} = C_{\nu_1}(\lambda_{11} r) \quad ; \quad C_{\nu_2} = C_{\nu_2}(\lambda_{21} r)$$

then

$$F_{11} = \frac{\lambda_{01}\lambda_{11}\, I\left[rC_0' C_{\nu_1}' C_{\nu_1}\right]}{I\left[rC_{\nu_1}^2\right]} \quad ; \quad F_{12} = \frac{I\left[rC_0 C_{\nu_1}^2\right]}{I\left[rC_{\nu_1}^2\right]}$$

$$F_{13} = \frac{\lambda_{21}\lambda_{11}\, I\left[rC_{\nu_1}' C_{\nu_2}' C_{\nu_1}\right] + \nu_1\nu_2\, I\left[\frac{1}{r} C_{\nu_1}^2 C_{\nu_2}\right]}{2\, I\left[rC_{\nu_1}^2\right]} \quad ; \quad F_{14} = \frac{I\left[rC_{\nu_1}^2 C_{\nu_2}\right]}{2\, I\left[rC_{\nu_1}^2\right]}$$

$$F_{15} = \frac{3\lambda_{11}^2\, I\left[rC_{\nu_1}^4\right]}{I\left[rC_{\nu_1}^2\right]} \quad ; \quad F_{01} = \frac{I\left[rC_0 C_{\nu_1}^2\right]}{I\left[rC_0^2\right]}$$

$$F_{02} = \frac{\lambda_{11}^2\, I\left[rC_{\nu_1}'^2 C_0\right] + \nu_1^2\, I\left[\frac{1}{r} C_{\nu_1}^2 C_0\right]}{4\, I\left[rC_0^2\right]} \quad ; \quad F_{03} = \frac{F_{01}}{2}$$

$$F_{21} = \frac{I\left[rC_{\nu_1}^2 C_{\nu_2}\right]}{2\, I\left[rC_{\nu_2}^2\right]} \quad ; \quad F_{22} = \frac{\lambda_{11}^2 I\left[rC_{\nu_1}'^2 C_{\nu_2}\right] - \nu_1^2 I\left[\frac{1}{r} C_{\nu_1}^2 C_{\nu_2}\right]}{4\, I\left[rC_{\nu_2}^2\right]}$$

$$F_{23} = \frac{F_{21}}{2} \quad ; \quad F_{16} = E_{15} + 3F_{15}$$

$$E_{11} = F_{11} - \lambda_{01}^2 F_{12} \quad ; \quad E_{12} = F_{11} - \lambda_{11}^2 F_{12}$$

$$E_{13} = F_{13} - \lambda_{11}^2 F_{14} \quad ; \quad E_{14} = F_{13} - \lambda_{21}^2 F_{14}$$

$$E_{01} = 2F_{02} - \lambda_{11}^2 F_{01} \quad ; \quad E_{21} = 2F_{22} - \lambda_{11}^2 F_{21}$$

$$E_{15} = \frac{3\lambda_{11}^2 I[r C_{\nu_1}'^2 C_{\nu_1}^2]}{4 I[r C_{\nu_1}^4]} + \frac{\nu_1^2 I[\frac{1}{r} C_{\nu_1}^4]}{4 I[r C_{\nu_1}^2]} - F_{15}$$

$$\chi_{11} = \frac{I[r^2 C_{\nu_1}]}{\pi I[r C_{\nu_1}^2]} \left(\frac{\sin(2\alpha-1)\pi}{2\alpha-1} + \frac{\sin(2\alpha+1)\pi}{2\alpha+1} \right)$$

$$\chi_{01} = \frac{I[r^2 C_0] \cdot \sin 2\pi\alpha}{I[r C_0^2] \cdot 2\pi\alpha}$$

$$\chi_{21} = \frac{I[r^2 C_{\nu_2}]}{\pi I[r C_{\nu_2}^2]} \left(\frac{\sin 2(\alpha-1)\pi}{2(\alpha-1)} + \frac{\sin 2(\alpha+1)\pi}{2(\alpha+1)} \right)$$

(B)

$$C_{11} = F_{16} + 2(E_{01}F_{12} + E_{21}F_{14}) + \frac{E_{01}g^2}{\omega_{01}^2\omega_{11}^2}(2E_{11} + F_{11}) + \frac{E_{21}g^2}{\omega_{21}^2\omega_{11}^2}(2E_{14} + F_{13}) + 2E_{15}$$

$$C_{12} = E_{15} + E_{01}F_{12} + E_{21}F_{14} + F_{15} + \frac{E_{01}E_{11}g^2}{\omega_{01}^2\omega_{11}^2} + \frac{E_{21}E_{14}g^2}{\omega_{21}^2\omega_{11}^2}$$

$$C_{13} = \frac{g}{\omega_{11}^2}E_{12} + \frac{\omega_{11}^2}{g}F_{12}$$

$$C_{14} = \frac{g}{\omega_{11}^2}E_{13} + \frac{\omega_{11}^2}{g}F_{14}$$

$$C_{15} = \frac{g}{\omega_{01}^2}(E_{11} + F_{11}) + \frac{g}{\omega_{11}^2}E_{12} + \frac{\omega_{11}^2}{g}F_{12}$$

$$C_{16} = \frac{g}{\omega_{01}^2}E_{11} + \frac{\omega_{11}^2}{g}F_{12}$$

$$C_{17} = \frac{g}{\omega_{21}^2}(E_{14} + F_{13}) + \frac{g}{\omega_{11}^2}E_{13} + \frac{\omega_{11}^2}{g}F_{14}$$

$$C_{18} = \frac{g}{\omega_{21}^2}E_{14} + \frac{\omega_{11}^2}{g}F_{14}$$

$$C_{01} = \frac{g}{\omega_{11}^2}E_{01} + \frac{\omega_{01}^2}{g}F_{01}$$

$$C_{02} = \frac{g}{\omega_{11}^2}E_{01} + \frac{\omega_{01}^2}{g}\left(\frac{g^2}{\omega_{11}^4}F_{02} + F_{03}\right)$$

$$c_{21} = \frac{g}{\omega_{11}^2} E_{21} + \frac{\omega_{21}^2}{g} F_{21}$$

$$c_{22} = \frac{g}{\omega_{11}^2} E_{21} + \frac{\omega_{21}^2}{g}\left(\frac{g^2}{\omega_{11}^4} F_{22} + F_{23}\right)$$

$$P_{11} = \frac{\omega_{11}^2}{g} x_{11}$$

$$P_{01} = \frac{\omega_{01}^2}{g} x_{01}$$

$$P_{21} = \frac{\omega_{21}^2}{g} x_{21}$$

(c)

$$K_1 = \frac{1}{4}(c_{11} - 3c_{12})$$

$$K_2 = -\frac{r_{01}^2}{4}(c_{13} - 2c_{15} + 4c_{16})(c_{01} + c_{02}) - \frac{r_{21}^2}{4}(c_{14} - 2c_{17} + 4c_{18})(c_{21} + c_{22})$$

$$- \frac{1}{2}\left[c_{13} r_{01}^2 (c_{01} - c_{02}) + c_{14} r_{21}^2 (c_{21} - c_{22})\right] + (c_{11} - 3c_{12})(r_{01}^2 + r_{21}^2)$$

$$K_3 = r_{01}^2 r_{21}^2 \left[4(c_{11} - 3c_{12}) + (c_{13} - 2c_{15} + 4c_{16})(c_{01} + c_{02}) + (c_{14} - 2c_{17} + 4c_{18})\right.$$

$$\left. \cdot (c_{21} + c_{22})\right] + 2(r_{01}^2 + r_{21}^2)\left[c_{13} r_{01}^2 (c_{01} - c_{02}) + c_{14} r_{21}^2 (c_{21} - c_{22})\right]$$

$$K_4 = -8 r_{01}^2 r_{21}^2 \left[c_{13} r_{01}^2 (c_{01} - c_{02}) + c_{14} r_{21}^2 (c_{21} - c_{22})\right]$$

$$K_5 = \frac{1}{4}(c_{11} + c_{12})$$

$$K_6 = -(\gamma_{01}^2 + \gamma_{21}^2)(C_{11} + C_{12}) + \frac{\gamma_{01}^2}{4}(C_{13} + 2C_{15} + 4C_{16})(C_{01} + C_{02}) + \frac{\gamma_{21}^2}{4}(C_{14} + 2C_{17} + 4C_{18})(C_{21} + C_{22})$$

$$K_7 = \gamma_{01}^2 \gamma_{21}^2 \left[4(C_{11} + C_{12}) - (C_{13} + 2C_{15} + 4C_{16})(C_{01} + C_{02}) - (C_{14} + 2C_{17} + 4C_{18})(C_{21} + C_{22})\right]$$

(D)

$$\delta_1 = -\frac{\omega g}{\omega_{11}^2}$$

$$\delta_2 = -\delta_1 \left[\frac{g}{\omega_{11}^2} E_{12}\left(\frac{\beta_3}{2} - \beta_2\right) + \frac{g}{\omega_{11}^2} E_{13}\left(\frac{\beta_3}{2} - \beta_4\right) - \frac{1}{4}\left(E_{15} + \frac{g^2}{\omega_{01}^2 \omega_{11}^2} E_{11} E_{01} + \frac{g^2}{\omega_{21}^2 \omega_{11}^2} E_{14} E_{21}\right) - \frac{g}{\omega_{21}^2} E_{14} \beta_5 - \frac{g}{\omega_{01}^2} E_{11} \beta_3\right]$$

$$\delta_3 = \delta_1 \left[3\beta_1 + \left(\frac{g}{\omega_{01}^2} E_{11} + \frac{g E_{12}}{2\omega_{11}^2}\right)\beta_3 + \left(\frac{g}{\omega_{21}^2} E_{14} + \frac{g}{2\omega_{11}^2} E_{13}\right)\beta_5 + \frac{1}{4}\left(E_{15} + \frac{g^2}{\omega_{01}^2 \omega_{11}^2} E_{01} E_{11} + \frac{g^2}{\omega_{21}^2 \omega_{11}^2} E_{14} E_{21}\right)\right]$$

$$\delta_4 = \frac{g}{\omega_{01}^2}\left(\frac{E_{01}}{2}\delta_1 - 2\beta_3 \omega\right)$$

$$\delta_5 = \frac{g}{\omega_{21}^2}\left(\frac{E_{21}}{2}\delta_1 - 2\beta_5 \omega\right)$$

$$\delta_6 = \frac{-\delta_1^2}{2(a^2 - b^2)}\left\{\lambda_{11}^2 I[r C_{\lambda_1}'^2] + \nu_1^2 I\left[\frac{1}{r} C_{\lambda_1}^2\right] + \frac{\omega_{11}^4}{g^2} I[r C_{\lambda_1}^2]\right\}$$

$$\delta_7 = -\frac{\omega_{11}^2 \delta_1}{g(a^2 - b^2)} I[r C_{\lambda_1}^2]$$

$$\delta_8 = \frac{2\omega^2(a^2 + ab + b^2)}{3(a+b)} \cdot \frac{\sin 2\pi\alpha}{2\pi\alpha}$$

APPENDIX II

EVALUATIONS OF FORCES AND MOMENTS

Forces

In view of Eqs. (IV-13) and (IV-14), the force in the x-direction (Eq. (IV-12)) can be written as

$$F_x = F_{x1} + F_{x2} + F_{x3} + F_{x4} \qquad \text{(APII-1)}$$

where

$$F_{x1} = \int_0^{2\pi\alpha} \cos\theta \int_{-h}^{0} \left[a\, p(a,\theta,z,t) - b\, p(b,\theta,z,t) \right] dz\, d\theta$$

$$F_{x2} = \int_0^{2\pi\alpha} \cos\theta \left\{ a \left[\eta\right]_{r=a} p(a,\theta,0,t) - b \left[\eta\right]_{r=b} p(b,\theta,0,t) \right.$$

$$\left. + \frac{1}{2} \left[a \left[\eta^2\right]_{r=a} p_z(a,\theta,0,t) - b \left[\eta^2\right]_{r=b} p_z(b,\theta,0,t) \right] \right\} d\theta$$

$$F_{x3} = -\sin 2\pi\alpha \int_a^b \int_{-h}^{0} p(r, 2\pi\alpha, z, t)\, dz\, dr$$

$$F_{x4} = -\sin 2\pi\alpha \int_b^a \left[\eta\, p(r, 2\pi\alpha, 0, t) + \frac{\eta^2}{2} p_z(r, 2\pi\alpha, 0, t) \right]_{\theta = 2\pi\alpha} dr$$

in which the appropriate pressure distributions p can be found from Eq. (IV-2), η from Eq. (III-29), and p_z from Eq. (IV-11).

Similarly, the force in the y-direction (Eq. (IV-4)) is found to be

$$\overline{F_y} = \overline{F_{y1}} + \overline{F_{y2}} + \overline{F_{y3}} + \overline{F_{y4}} \qquad \text{(APII-2)}$$

where

$$\overline{F_{y1}} = \int_0^{2\pi\alpha} \sin\theta \left\{ \int_{-h}^{0} \left[a\, p(a,\theta,z,t) - b\, p(b,\theta,z,t) \right] dz \right\} d\theta$$

$$\overline{F_{y2}} = \int_0^{2\pi\alpha} \sin\theta \left\{ a\,[\eta]_{r=a}\, p(a,\theta,0,t) - b\,[\eta]_{r=b}\, p(b,\theta,0,t) \right.$$

$$\left. + \frac{1}{2}\left[a\,[\eta^2]_{r=a}\, p_z(a,\theta,0,t) - b\,[\eta^2]_{r=b}\, p_z(b,\theta,0,t) \right] \right\} d\theta$$

$$\overline{F_{y3}} = \int_b^a \int_{-h}^{0} \left\{ \cos 2\pi\alpha\, [p]_{\theta=2\pi\alpha} - [p]_{\theta=0} \right\} dz\, dr$$

$$\overline{F_{y4}} = \int_b^a \left\{ \cos 2\pi\alpha\, [\eta]_{\theta=2\pi\alpha}\, p(r,2\pi\alpha,0,t) - [\eta]_{\theta=0}\, p(r,0,0,t) \right\} dr$$

$$+ \frac{1}{2} \int_b^a \left\{ \cos 2\pi\alpha\, [\eta^2]_{\theta=2\pi\alpha}\, p_z(r,2\pi\alpha,0,t) - [\eta^2]_{\theta=0}\, p_z(r,0,0,t) \right\} dr$$

Moments

In calculating moments, we have to expand the function "z p(r,θ,z,t)" into Taylor series. It is to be noted that

$$\frac{\partial}{\partial z}(z\,p) = p + z\,p_z$$

$$\frac{\partial^2}{\partial z^2}(z\,p) = p_z + p_z + z\,p_{zz} = 2\,p_z + z\,p_{zz}$$

hence

$$z\,p(r,\theta,z,t) = z\,p(r,\theta,0,t) + z^2\,p_z(r,\theta,0,t) + \cdots$$

and

$$\int_0^{\eta} z\,p\,dz = \frac{\eta^2}{2}\,p(r,\theta,0,t) + \frac{\eta^3}{3}\,p_z(r,\theta,0,t) + O(\eta^4) \qquad \text{(APII-3)}$$

Thus the moment in x-direction (Eq. (IV-6)) is found to be

$$M_x = M_{x1} + M_{x2} + M_{x3} + M_{x4} + M_{x5} \qquad \text{(APII-4)}$$

where

$$M_{x1} = -\int_0^{2\pi\alpha} \sin\theta \left\{ \int_{-h}^{0} \left[a\,p(a,\theta,z,t) - b\,p(b,\theta,z,t) \right] \left(\frac{h}{2} + z\right) dz \right\} d\theta$$

$$M_{x2} = -\frac{h}{2}\overline{F}_{y2} - \frac{1}{2}\int_0^{2\pi\alpha} \sin\theta \left\{ a\left[\eta^2\right]_{r=a} p(a,\theta,0,t) - b\left[\eta^2\right]_{r=b} p(b,\theta,0,t) \right\} d\theta$$

$$- \frac{1}{3}\int_0^{2\pi\alpha} \sin\theta \left\{ a\left[\eta^3\right]_{r=a} p_z(a,\theta,0,t) - b\left[\eta^3\right]_{r=b} p_z(b,\theta,0,t) \right\} d\theta$$

$$M_{x3} = -\int_b^a \int_{-h}^{0} \left(\frac{h}{2} + z\right) \left[\cos 2\pi\alpha \cdot p(r,2\pi\alpha,z,t) - p(r,0,z,t) \right] dz\,dr$$

$$M_{x4} = -\frac{h}{2}\overline{F}_{y4} - \frac{1}{2}\int_b^a \left\{ \cos 2\pi\alpha \left[\eta^2\right]_{\theta=2\pi\alpha} p(r,2\pi\alpha,\theta,t) - \left[\eta^2\right]_{\theta=0} p(r,0,0,t) \right\} dr$$

$$- \frac{1}{3}\int_b^a \left\{ \cos 2\pi\alpha \left[\eta^3\right]_{\theta=2\pi\alpha} p_z(r,2\pi\alpha,0,t) - \left[\eta^3\right]_{\theta=0} p_z(r,0,0,t) \right\} dr$$

$$M_{x5} = -\int_0^{2\pi\alpha} \int_b^a p(r,\theta,-h,t) \cdot r^2 \sin\theta\, dr\, d\theta$$

In a similar way, the moment in y-direction (Eq. (IV-7)) is found to be

$$M_y = M_{y1} + M_{y2} + M_{y3} + M_{y4} + M_{y5} \qquad \text{(APII-5)}$$

where

$$M_{y1} = \int_0^{2\pi\alpha} \cos\theta \left\{ \int_{-h}^{0} \left(\frac{h}{2}+z\right)\left[a\,p(a,\theta,z,t) - b\,p(b,\theta,z,t)\right]dz \right\} d\theta$$

$$M_{y2} = \frac{h}{2}\cdot F_{x2} + \frac{1}{2}\int_0^{2\pi\alpha} \cos\theta \left\{ a\left[\eta^2\right]_{r=a} p(a,\theta,0,t) - b\left[\eta^2\right]_{r=b} p(b,\theta,0,t) \right\} d\theta + \frac{1}{3}\int_0^{2\pi\alpha} \cos\theta \left\{ a\left[\eta^3\right]_{r=a} p_z(a,\theta,0,t) - b\left[\eta^3\right]_{r=b} p_z(b,\theta,0,t) \right\} d\theta$$

$$M_{y3} = -\sin 2\pi\alpha \int_b^a \int_{-h}^{0} \left(\frac{h}{2}+z\right) p(r, 2\pi\alpha, z, t)\, dz\, dr$$

$$M_{y4} = \frac{h}{2}\cdot F_{x4} - \frac{1}{2}\sin 2\pi\alpha \int_b^a \left[\eta^2\right]_{\theta=2\pi\alpha} p(r, 2\pi\alpha, 0, t)\, dr - \frac{1}{3}\sin 2\pi\alpha \int_b^a \left[\eta^3\right]_{\theta=2\pi\alpha} p_z(r, 2\pi\alpha, 0, t)\, dr$$

$$M_{y5} = \int_0^{2\pi\alpha}\int_b^a p(r,\theta,-h,t)\, r^2 \cos\theta\, dr\, d\theta$$

LITERATURE CITED

1. Lamb, H., Hydrodynamics, Dover Publications, New York, 1945, sixth edition.

2. Rayleigh, Lord, "On Waves," Philosophical Magazine, Series 5, Vol. 1, 1876, pp. 257-279.

3. Cooper, R. M., "Dynamics of Liquids in Moving Containers," American Rocket Society Journal, Vol. 30, August 1960, p. 725.

4. Abramson, H. N., "Dynamic Behavior of Liquids in Moving Containers," Applied Mechanics Review, Vol. 16, No. 7, July 1963, pp. 501-506.

5. Roberts, J. R., Basurto, E. R., and Chen, P. Y., "Slosh Design Handbook I," NASA CR-406, May 1966.

6. Gutherie, F., "On Stationary Liquid Waves," Phil. Mag., Series 4, Vol. 50, 1875, pp. 290-337.

7. Verma, G., and Keller, J. B., "Three-Dimensional Standing Surface Waves of Finite Amplitude," Physics of Fluids, 5 (1962) pp. 52-56.

8. Lin, J. D., and Howard, L. N., "Non-linear Standing Waves in a Rectangular Tank Due to Forced Oscillation," M.I.T. Hydrodynamics Laboratory, Dept. Civil and Sanitary Engineering, TR No. 44 (1960).

9. Dodge, F. T., Kana, D. D., and Abramson, H. N., "Liquid Surface Oscillations in Longitudinally Excited Rigid Cylindrical Containers," Southwest Research Institute TR2, Contract NAS8-11045 (April 1964).

10. Baird, J. A., Jr., "Nonlinear Fluid Oscillations in a Partially Filled Cylindrical Sector Container," Research Laboratories, Brown Engineering Company, Inc., Huntsville, Alabama, 1966.

11. Stakgold, Ivar, Boundary Value Problems of Mathematical Physics, Volume I, The Macmillan Company, New York, 1967.

12. Abramson, H. N., Chu, W. H., and Garza, L. R., "Liquid Sloshing in 45° Sector Compartmented Cylindrical Tanks," Technical Report No. 3, Contract NAS8-1555, S_wRI, November 1962.

LITERATURE CITED (Continued)

13. Abramson, H. N., and Garza, L. R., "Some Measurements of Liquid Frequencies and Damping in Compartmented Cylindrical Tanks," AIAA Journal of Spacecraft and Rockets, Vol. 2, No. 3, May-June 1965, pp. 453-455.

14. Abramson, H. N., Chu, W. H., and Kana, D. D., "Some Studies of Nonlinear Lateral Sloshing in Rigid Containers," Journal of Applied Mechanics, December 1966.

15. Moiseyev, N. N., "On the Theory of Nonlinear Vibrations of a Liquid of Finite Volume," Journal of Applied Mathematics and Mechanics (PMM), Vol. 22, No. 5, 1958, pp. 860-870.

16. Penney, W. G., and Price, A. T., "Some Gravity Wave Problems in the Motion of Perfect Liquids," Philosophical Transactions of Royal Society (London), Vol. A244, No. 254, 1952.

17. Taylor, G. I., "An Experimental Study of Standing Waves," Proceedings of Royal Society (London), Vol. A218, 1952, pp. 44-59.

18. Tadjbakhsh, I., and Keller, J. B., "Standing Waves of Finite Amplitude," Journal of Fluid Mechanics, Vol. 8, No. 3, July 1960, pp. 433-451.

19. Fultz, D., "An Experimental Note on Finite Amplitude Standing Gravity Waves," J. Fluid Mech., Vol. 13, No. 2, June 1962, pp. 193-213.

20. Bauer, H. F., "Nonlinear Propellant Sloshing in a Rectangular Container of Infinite Length," North American Aviation, Inc., S and ID Report, SID 64-1593, 1964; also, Proceedings of the SECTAM, Volume 3, 1966.

21. Hutton, R. E., "An Investigation of Resonant, Nonlinear Non-planer Free Surface Oscillations of a Fluid," NASA TND-1870, 1963.

22. Mack, L. R., "Periodic, Finite-Amplitude Axisymmetric Gravity Waves," Journal of Geophysical Research, 67, pp. 829-843 (1962).

23. DiMaggio, O. D., and Rehm, A., "Finite Amplitude Liquid Oscillations, I. Free Oscillations, II. Forced Resonant Oscillations," North American Aviation, SID 65-853 (1965).

LITERATURE CITED (Concluded)

24. Merian, J. R., "Über die bewegung tropfbarer Flüssigkeiten in Gefässen," 1828, Basel.

25. Bauer, H. F., "Fluid Oscillations in the Containers of a Space Vehicle and Their Influence Upon Stability," NASA TR R-187, 1964.

26. Bauer, H. F., "Tables and Graphs of Zeroes of Cross Product Bessel Functions $J'_p(\xi)\ Y'_p(k\xi) - J'_p(k\xi)\ Y'_p(\xi) = 0$," MSFC, MTP-AERO-63-50, 1963; also, Journal of Mathematical Computation (January 1964).

27. Abramson, H. N., "The Dynamic Behavior of Liquid in Moving Containers," NASA SP-106, Office of Scientific and Technical Information, Washington, D. C., 1966.

28. Lebedev, N. N., Skalskaya, I. P., and Uflyand, Y. S., Problems of Mathematical Physics, translated by R. A. Silverman, Prentice-Hall, Inc., New Jersey, 1965.

VITA

Pei-Ying Chen was born on December 27, 1936, in Chia-Yi, Taiwan, China. In 1955, he graduated from Provincial Chia-Yi High School with honor and was therefore permitted to enter the National Taiwan University without taking the otherwise required entrance examination. From this university he received the degree of Bachelor of Science in Mechanical Engineering in 1959. He was qualified as a Registered Professional Mechanical Engineer in Taiwan in 1960 by passing an examination. From April, 1961 to September, 1962, he worked as a mechanical engineer for the Chinese Petroleum Corporation in Chia-Yi, Taiwan.

In September, 1962, he was awarded a teaching assistantship for pursuing graduate study at the University of Houston, in Houston, Texas, and completed the requirements for the Master of Science in Mechanical Engineering in June, 1964. He was then employed as a research engineer by the Northrop Space Laboratories in Huntsville, Alabama, where he was a member of the "slosh team."

In September, 1965, on an educational leave of absence from Northrop Corporation, he entered the Georgia Institute of Technology as a graduate student and also as a research assistant in the School of Engineering Science and Mechanics. In 1967, he received the degree of Master of Science in Engineering Mechanics and continued to study for the doctoral degree. During this period he had constant contact with Northrop and was employed by them during the summer and part time at

their request.

He is a member of Tau Beta Pi and Sigma Xi honorary societies.

In 1965, he was married to the former Miss Diana Chew-Mei Hung of Nan-Tou, Taiwan, and they have a son, Theodore (Teddy) Anthony Chen.